Performance Modelling and Resource Allocation of the Emerging Network Architectures for Future Internet

Wang Miao

A dissertation submitted for the degree of

Doctor of Philosophy

in

Computer Science

College of Engineering, Mathematics and Physical Sciences

University of Exeter

January 2017

I, Wang Miao, confirm that the work presented in this thesis is my own. Where information has been derived from other sources, I confirm that this has been indicated in the work.

Abstract

With the rapid development of information and communications technologies, the traditional network architecture has approached to its performance limit, and thus is unable to meet the requirements of various resource-hungry applications. Significant infrastructure improvements to the network domain are urgently needed to guarantee the continuous network evolution and innovation. To address this important challenge, tremendous research efforts have been made to foster the evolution to Future Internet. Long-term Evolution Advanced (LTE-A), Software Defined Networking (SDN) and Network Function Virtualisation (NFV) have been proposed as the key promising network architectures for Future Internet and attract significant attentions in the network and telecom community. This research mainly focuses on the performance modelling and resource allocations of these three architectures. The major contributions are three-fold:

1) LTE-A has been proposed by the 3rd Generation Partnership Project (3GPP) as a promising candidate for the evolution of LTE wireless communication. One of the major features of LTE-A is the concept of Carrier Aggregation (CA). CA enables the network operators to exploit the fragmented spectrum and increase the peak transmission data rate, however, this technical innovation introduces serious unbalanced loads among in the radio resource allocation of LTE-A. To alleviate this problem, a novel QoS-aware resource allocation scheme, termed as Cross-CC User Migration (CUM) scheme, is proposed in this research to support real-time services, taking into consideration the system throughput,

user fairness and QoS constraints.

2) SDN is an emerging technology towards next-generation Internet. In order to improve the performance of the SDN network, a preemption-based packet-scheduling scheme is firstly proposed in this research to improve the global fairness and reduce the packet loss rate in SDN data plane. Furthermore, in order to achieve a comprehensive and deeper understanding of the performance behaviour of SDN network, this work develops two analytical models to investigate the performance of SDN in the presence of Poisson Process and Markov Modulated Poisson Process (MMPP) respectively.

3) NFV is regarded as a disruptive technology for telecommunication service providers to reduce the Capital Expenditure (CAPEX) and Operational Expenditure (OPEX) through decoupling individual network functions from the underlying hardware devices. While NFV faces a significant challenging problem of Service-Level-Agreement (SLA) guarantee during service provisioning. In order to bridge this gap, a novel comprehensive analytical model based on stochastic network calculus is proposed in this research to investigate end-to-end performance of NFV network.

The resource allocation strategies proposed in this study significantly improve the network performance in terms of packet loss probability, global allocation fairness and throughput per user in LTE-A and SDN networks; the analytical models designed in this study can accurately predict the network performances of SDN and NFV networks. Both theoretical analysis and simulation experiments are conducted to demonstrate the effectiveness of the proposed algorithms and the accuracy of the designed models. In addition, the models are used as practical and cost-effective tools to pinpoint the performance bottlenecks of SDN and NFV networks under various network conditions.

Acknowledgements

I would like to express my deepest appreciate to my PhD supervisor, Prof. Geyong Min, who guided me in the research path, taught me how to be a good, optimistic, and responsible researcher. Thank you so much for providing special funding and encouraging me to attend industry events held in the UK and EU, which make my research much closer to the industry development. I really appreciate what he did for my study.

I would like to thank Dr. Yulei Wu, my second PhD supervisor, for numerous meetings to discuss my research progress and hard work to polish my research papers. Without his guidance, mentoring and knowledge, this study would not have been completed.

In addition, I would like to thank, Dr. Jia Hu, Dr. Chunbo Luo, Mr. Haozhe Wang, Mrs. Noushin Najjari, Mr. Chengqiang Huang, Mr. Yuan Zuo, Mr. Xiangle Chen, Dr. Lejun Chen and so on, who provided a lot of help during my PhD study.

Finally, special thanks to my parents and my wife. They encouraged me when I was frustrated. My wife sacrifices a lot for our family. Especially during the final year of my study, when our little baby, Joyce, arrived at this world, I was very busy with my research and did not provide enough support for her and baby. Thank you so much and I really really love you and Joyce.

Table of Contents

List of Figures

List of Tables

List of Abbreviations

4G Fourth Generation of Mobile Communication

5G Fifth Generation of Mobile Communication

ACL Access Control List

AMBR Aggregated Maximum Bit Rate

APC antigeen-presenterende cel

CA Component Aggregation

CAPEX Capital Expenditures

CC Component Carrier

CDMA Code Division Multiple Access

CoMP Coordinated Multi-Point

DC Downlink Channel

DPDK Data Plane Development Kit

DPI Deep Packet Inspection

EBA Empty Buffer Approximation

EBB Exponentially Bounded Burstiness

ETSI European Telecommunication Standards Institute

FBM Fractional Brownian Motion

FIFO First In First Out

GBR Guaranteed Bit Rate

GSM Global System for Mobile Communications

HoL Head of Line

LTE-A Long-Term-Evolution Advanced

LTP Long Term Perspective

MANO Management and Orchestration

MGF Moment Generation Function

MIMO Multiple-Input and Multiple-Output

MME Mobility Management Entity

MMPP Markov Modulated Poisson Process

MPLS Multi-protocol Label Switch

NAT Network Address Translation

NFV Network Function Virtualisation

OFDMA Orthogonal Frequency Division Multiple Access

OMNeT++ Objective Modular Network Testbed in C++

ONF Open Networking Foundation

OPEX Operational Expenditures

PCRF Policy and Charging Rules Function

PE Provider Edge

PF Proportional Fair

PQ Priority Queue

PRB Physical Resource Block

QCI QoS Class Identifier

List of Publications

- Wang Miao, Geyong Min, Yulei, Wu, Haozhe Wang, Jia Hu, "Stochastic Performance Analysis of Network Function Virtualisation with Random Service Model", to be submitted to *IEEE Transactions on Wireless Communications*.

- Wang Miao, Geyong Min, Yulei Wu, Haozhe Wang, Jia Hu, "Performance Modelling and Analysis of Software Defined Networking with Bursty Traffic", *ACM Transaction on Multimedia Computing, Communications, and Applications (TOMM)*, Volume 12, Issue 5s, pp.77:1-19, 2016.

- Haozhe Wang, Geyong Min, Jia Hu, Wang Miao, "Performance Evaluation of Information-Centric Networking for Multimedia Service", in *Proceedings of Symposium on Service-Oriented System Engineering (SOSE-2016)*, pp.174-179, 2016.

- Wang Miao, Geyong, Min, Yulei Wu, Haozhe Wang, "Performance Modelling of a New Preemption-based Packet Scheduling (P^2S) for Data Plane in SDN Networks", in *Proceedings of IEEE International Conference on Smart City (Smartcity-2015)*, pp. 60-65, 2015.

- Wang Miao, Geyong Min,Yuming Jiang,Xiaolong Jin,Haozhe Wang, "QoS-aware Resource Allocation for LTE-A Systems with Carrier Aggregation", in *Proceedings of IEEE Wireless Communications and Networking Conference (WCNC-2014)*, pp. 1403-1408, 2014.

- Haozhe Wang, Geyong Min, Jia Hu,Hao Yin, Wang Miao, "Caching of Content-Centric Networking under Bursty Content Requests", in *Proceedings of IEEE Wireless Communications and Networking Conference (WCNC-2014)*, pp. 2522-2527, 2014.

QoE Quality of Experience

QoS Quality of Service

RB Resource Block

SAC Stochastic Arrival Curve

SC-FDMA Single Carrier Frequency Division Multiple Access

SDN Software Defined Networking

SLA Service Level Agreement

SSC Stochastic Service Curve

SSSQ Single Server Single Queue

TD-PSS Time Domain Priority Set Priority

TLDS Two Level Downlink Scheduling

TOC Cost Of Ownership

TTI Transmit Time Interval

UC Uplink Channel

VIM Virtual Infrastructure Manager

VNF Virtual Network Function

Chapter 1

Introduction

With the rapid development of information and communication technologies, such as Cloud Computing, Social Networks, Network Virtualisation and Content Distribution Networks, the traditional network architecture has approached to its performance limit, and thus is unable to meet the requirements of various resource-hungry applications driven by streaming media, Ultra High Definition Video, enhanced reality, and Internet-of-Things. Significant infrastructure improvements to the network domain are urgently needed to guarantee the continuous network evolution and innovation. To address this important challenge, tremendous research efforts have been made from both academia and industry to foster the evolution to Future Internet. Recently, Long-Term-Evolution Advanced (LTE-A), Software Defined Networking (SDN), and Network Function Virtualisation (NFV) have been proposed as promising network architectures for Future Internet and attracted significant research efforts. This research focuses on the performance improvement of LTE-A, SDN and NFV through deriving the key performance metrics and optimising the network resources.

This chapter is organised as follows: Section 1.1 points out the motivations and challenges in this research; The research aims and major contributions of this thesis are presented in Section 1.2. Finally, the overall organisation of this thesis is introduced in

Section 1.3.

1.1 Motivations and Challenges

Analytical modelling and resource allocation, as efficient approaches to optimise the performance of the network system, have been attracted significant interests. Numerous research results have been reported in the literature to investigate the analytical modelling and resource allocation in LTE-A [1] [2] [3] [4], SDN [5] [6] [7] [8], and NFV [9] [10] [11]. However, there are still some practical and open research issues related to resource optimisation and performance modelling that need to be further tackled. For example,

(1) Carrier Aggregation (CA) is a primary feature for LTE-A architecture to achieve large virtual carrier bandwidth. By combining multiple separate spectrums through CA, telecommunication providers are capable of meeting the growing demands for the higher transmission rate and the lower latency and jitter. While, due to the unique transmission features such as interference and fading in wireless communication channels [12], CA poses significant challenges for resource allocation and optimisation in LTE-A networks. In addition, Quality-of-Service (QoS) is of critical importance for service provisioning in wireless communication networks [13]. Therefore, how to optimise wireless network resources to meet the strict user QoS in LTE-A networks with CA is a challenging and timing issue [14]. There have been some research results appeared in the literature [15] [16] [17], however, the majority of them mainly focused on independent Carrier Component (CC) and did not exploit the statistic multiplexing gain among multiple CCs. This problem becomes even more challenging in the presence of mobile users with different requirements in terms of bandwidth, tolerance to delay, and reliability.

(2) Through decoupling the network control from the underlying network infrastructure in forwarding plane, SDN provides unprecedented network programmability and con-

trol. A lot of research efforts have been made to leveraging these benefits provided by SDN to improve the network innovation and performance of Future Internet. However, most of the existing research sets simple assumption in their study, adopting First-In-First-Out (FIFO) packet scheduling as the primary approach to process arrival packets. Although, FIFO has been widely considered as an effective approach in the literatures [18], it incurs serious issues of low global fairness and performance degradation in SDN paradigm due to the inherent feature of SDN-feedback control loop between data plane and control plane. In order to fully release the potential of the SDN architecture, there is a need to design a more effective packet scheduling algorithm in the SDN network to improve the overall performance of data forwarding.

(3) Analytical modelling is an efficient approach to quantitatively investigate the performance of network systems [19] [20] [21] [22] [23] [24]. For SDN networks, several research results of analytical modelling have been recently reported in the literature [5] [6] [7]. Among those studies, analytical modelling has demonstrated its superiority in terms of cost-effectiveness in the evaluation of large-scale networks. However, for analytical tractability and simplification, existing analytical models are derived based on the assumptions that the network traffic follows the Poisson process which is suitable to model non-bursty text data and the data plane is modelled by one simplified Single Server Single Queue (SSSQ) system [25] [5] [26]. Recent measurement studies have shown that, due to the features of heavy volume and high velocity, the multimedia big data generated by real-world multimedia applications reveals the bursty and correlated nature in the network transmission [27] [28] [29] [30] [31]. Therefore, in order to achieve a deep understanding of SDN architecture, there is an urgent need to develop a comprehensive analytical model to capture the bursty and correlated feature of network traffic.

(4) Through decoupling the network functions from dedicated network devices, NFV

brings network operators the significant reduction of Operational Expense (OPEX) and Capital Expense (CAPEX) and the increased flexibility of service design, deployment and management. There have been research efforts to investigate the performance of service provisioning [9] [10] [11]. However, the existing work did not fully consider the dynamic and on-demand features of the NFV service provision. Especially, the service capabilities of VNFs are different due to their different network functions and also may change over the whole life-cycle in the manner of on-demand [32]. Furthermore, the network functions in NFV chain may be added, removed or modified, which form new NFV chain [33] to continuously offer the satisfied performance. To the best of our knowledge, analytical modelling and analysis of NFV network with the features of dynamic service and scalable resource has not been reported in the existing literature. In order to fully harvest the merits of NFV for network operators, there is a need and opportunity to use the probabilistic features of stochastic network function to investigate the dynamic features of NFV.

1.2 Research Aims and Contributions

This research focuses on the performance improvement of SDN, NFV and LTE-A systems through mathematics modelling and resource allocation. The main objectives of this research are:

- To propose a new resource allocation scheme for LTE-A system with CA with the aim of providing the QoS guaranteed network service.
- To propose an efficient resource allocation scheme for SDN network to improve the global fairness and reduce the packet loss probability in SDN data plane.
- To develop a comprehensive analytical model to quantitatively investigate the performance limits of SDN networks under the bursty and correlated network traffic.

- To develop a new stochastic analytical tool to capture the dynamic and on-demand features of NFV networks and achieve the end-to-end performance of NFV service chain.

To achieve the above objectives, this research develops new analytical models and resource allocation strategies. The effectiveness and accuracy of the proposed models and algorithms are demonstrated by extensive experimental results with various network conditions. The original contributions of this research are summarised as follows:

- A novel QoS-aware resource allocation scheme, termed as Cross-CC User Migration (CUM) scheme, is proposed to support real-time services in LTE-A downlink transmission with CA by jointly considering the system throughput, QoS constraints, and user fairness.

- A Peemption-based packet-scheduling scheme (P^2S) is proposed to improve the global fairness and reduce the packet loss rate in the SDN data plane. Comprehensive simulation experiments are conducted to demonstrate that P^2S can achieve better system performance compared to the traditional data plane packet scheduling in terms of global fairness index and packet loss probability.

- An analytical model is developed to quantitatively evaluate the performance of P^2S scheduling scheme. The developed model can capture the loop control, limited buffer resource, and preemption features of the P^2S scheme. The developed model is further leveraged to analyse and pinpoint the performance bottleneck of the SDN architecture.

- A novel analytical model is designed for SDN networks subject to the input of bursty multimedia traffic. The bursty and correlated nature of the traffic character-

istics on each link and component of SDN network is captured. The QoS performance metrics in terms of the average latency and average network throughput are derived based on the developed analytical model.

- A versatile method is proposed by extending the Empty Buffer Approximation (EBA) method to facilitate the decomposition of a Priority Queue (PQ) system to two Single-Server-Single-Queue (SSSQ) systems. Compared with the EBA, the proposed method takes the effects of higher priority queue into account and achieves better analytical performance.

- A new stochastic analytical model based on stochastic network calculus is developed to investigate the end-to-end performance of NFV networks. Through jointly exploiting leftover service and stochastic multiplexing technologies, the proposed analytical model provides an efficient and effective approach to capture the dynamic and on-demand features of NFV networks with the strict Service Level Agreement (SLA) requirements.

1.3 Outline of the Thesis

The rest of this thesis is organised as follows.

- Chapter 2 introduces the background knowledge of this thesis, including the architectures of SDN, NFV and LTE-A, CA, traffic models and analytical tool. A detailed literature review on the analytical model and resource allocation of SDN, NFV, and LTE-A is also presented.

- Chapter 3 designs a QoS-aware resource allocation scheme to support real-time services in LTE-A downlink transmission by jointly considering the system throughput, QoS constraints, and user fairness.

- Chapter 4 proposes a new packet-forwarding scheme in the SDN data plane and develops a new analytical model to investigate the performance of the proposal scheme. The bottleneck of the SDN network is analysed and feasible solutions are provided based on the developed model.

- Chapter 5 develops an analytical model for SDN networks with priority queue under bursty traffic. The analytical model is used to investigate the effects of the flow-table hit probability and resource allocations.

- Chapter 6 develops an analytical model for NFV networks based on stochastic network calculus to investigate the end-to-end performance of NFV networks.

- Finally, Chapter 7 concludes the thesis and presents the future research work.

Chapter 2

Background and Literature Review

LTE-A, SDN and NFV, as the promising network architectures for Future Internet, have been attracted significant research interests. This chapter presents the background knowledge and related work of LTE-A, SDN and NFV, with the focuses on the resource allocation and performance modelling. Firstly, the network architectures of LTE-A, SDN and NFV will be presented in Sections 2.1. Then, Sections 2.2 and Section 2.3 will introduce the fundamental knowledge and basic ideas of traffic models and analytical tools. A detailed literature review in the area of resource allocation and analytical modelling of LTE-A, SDN and NFV will be presented in Section 2.4. Finally, section 2.5 summaries this chapter.

2.1 Emerging Network Architectures and Technologies

2.1.1 LTE-A Architecture

LTE-A is a promising technology that offers high-data-rate transmission for the fourth-generation (4G) mobile communication systems [34] [35]. In order to satisfy the strict technique requirements of International Mobile Telecommunications (IMT), LTE-A inherits all the characteristics of LTE, such as Orthogonal Frequency Division Multiple Access (OFDMA) [36] for the downlink transmission to enable cost-efficient solutions

for high peak rates and Single-Carrier FDMA (SC-FDMA) for the uplink transmission to conserve power. Furthermore, several new technologies are proposed for LTE-A, including Carrier Aggregation (CA), enhanced Multiple-input and Multiple-output (MIMO) [37] and Coordinated Multi-Point (CoMP) transmission [38]. For supporting up to 100 MHz bandwidth, 5 Component Carriers (CCs) of 20 MHz are aggregated. The bandwidth of each CC follows the configurations of LTE systems, including 1.4, 3, 5, 10, 15, and 20 MHz [39]. In addition, the support for CCs with various bandwidths offers significant flexibility for efficient spectrum utilisation, and gradual re-farming of frequencies previously being used by other systems such as Global System for Mobile Communications (GSM) [40] or Code Division Multiple Access (CDMA) [41].

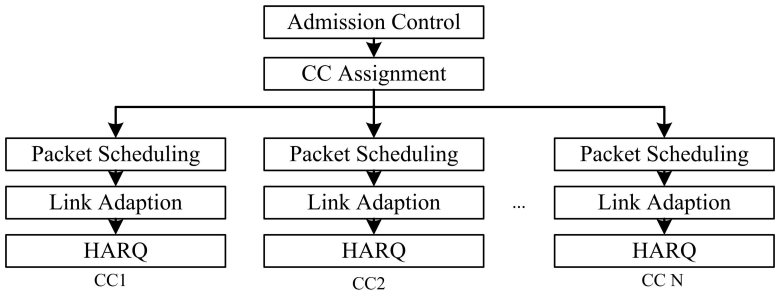

Figure 2.1: LTE-A Systems with Carrier Aggregation Standardised by 3GPP

The structure for allocation of radio resource in LTE-A systems is described in Fig. 2.1 [14]. The eNB firstly carries out the admission control process, and then employs CC assignment to allocate the users on different CCs [2]. Once all users are allocated by the CC assignment, the packet scheduling is performed to assign time/frequency resources for each of users allocated on different CCs, taking into account QoS requirements, system efficiency and user fairness. According to the LTE specification in [42], radio resources are divided into Resource Blocks (RBs) spanning over one-time-slot (1ms) in the time domain and over one sub-channel (180kHz) in the frequency domain, which is the smallest radio resource that can be assigned to a User Equipment (UE) for data transmission during resource allocation.

2.1.2 SDN Architecture

SDN is an approach to allow network administrators to manage network services through the centralised controller. It was proposed to accelerate network innovation and flexible deployment by decoupling the logic of the network control from the forwarding plane, enabling network operators to gain unprecedented programmability, automation, and network control [43] [44]. In order to advance the concept of SDN technology, Open Networking Foundation (ONF) published the white-paper for SDN and proposed a practical network architecture for SDN as shown in Fig. 2.2 [45].

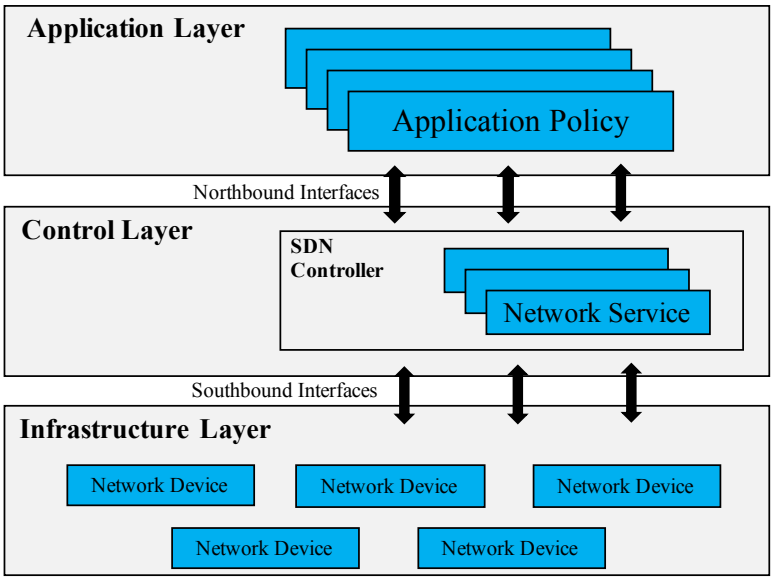

Figure 2.2: Three Layer SDN Architecture Proposed by Open Network Foundation

SDN architecture has three cooperative layers: infrastructure layer, control layer and application layer [46]: the infrastructure layer provides network forwarding services under the instructions of the control layer. The control layer maintains the network-wide information to manage and optimise the overall network performance. SDN controller uses southbound interfaces such as OpenFlow [47], Open vSwitch Database Management Protocol (OVSDB) [48] and OpFlex [49] to communicate with the infrastructure layer, and leverages northbound interfaces, for instance Restful APIs [50] to interact with the application layer. The application layer creates various services, e.g., network topol-

ogy discovery, virtual private network provisioning, and path reservations, based on the received network information from the control layer. With the logically centralised control of the network infrastructure, SDN enables the software intelligence to program networks via the well-defined programmatic interfaces, which are highly customisable, scalable, and agile to meet the requirements of transmission QoS.

OpenFlow is the first standard southbound communication protocol between the SDN controller and network forwarding devices [51] and has been implemented in various industry products [43]. In order to identify the network traffic and conduct various network functions, OpenFlow protocol defines three domains in the flow table of network devices, including match field, action field and statistic filed. The match field uses IP 5-tuple (source IP, source port ID, destination IP, destination port ID and protocol in use) to match the arrival packets based on the pre-defined rules. The action field stores the forwarding and routing information for the arrival packets. The statistics field is used to count the number of the packets that hit the match field. The statistical data would be used by the up-level application and service to detect or implement certain security processing. With OpenFlow, SDN controller is capable of accessing the flow table, collecting the statistics data and modifying the flow table to realise the intelligent network management and service deployment.

2.1.3 NFV Architecture

NFV is an architectural approach that focuses on decoupling network functions such as Network Address Translation (NAT) [52], Access Control Lists (ACL) [53], Layer 3 routing [54], Intrusion Prevention and Intrusion Detection Systems (IPS and IDS) [55], and more from the underlying hardware platform [56]. Allowing such functions to run inside virtual machines, on top of standard x86 servers, increases the deployment flexibility

in the network. With the help of NFV, network functions are released from the specific underlying network devices and can be installed or re-installed on any general network servers. This kind of network function migration brings significant benefits for network operation and maintenance. For instance, in the era of 5G, the condition that services and applications become more complex, dynamic and resource hungry, poses a huge challenge for the network service provisioning. NFV provides higher flexibility and programmability and faster innovation and enables new opportunity for network operator to enhance network management. Furthermore, NFV helps network service providers address a critical issue for their business: high Total Cost of Ownership (TCO) and low revenue. For instance, in order to continuously meet the user requirements for more resource-hungry and diverse applications, network service providers have to purchase expensive and dedicated physical network equipment, and train high skilled engineers to operate and manage these devices, which involve a huge amount of TCO for service provisioning. However, for the network service providers, these higher CAPEX and OPEX cannot be easily translated into high subscription fees, as they have learned that due to the high competition, both among themselves and from services being provided over-the-top on their data channels, increasing prices only leads to customer losses. Through deploying the network functions on common services rather than purchasing new dedicated devices, NFV provides a good solution for network service providers to reduce their CAPEX and OPEX [57], as the common server and network functions can be dynamically re-used in the manner of on-demand.

In order to realise the ambition of NFV technology, European Telecommunication Standards Institute (ETSI) proposed an NFV architecture [58] to guide the implementation and management of NFV, which consists of three main components, NFV Infrastructure (NFVI), Virtual Network Functions (VNFs) and NFV Management and Orchestration

(MANO) as shown in Fig. 2.3.

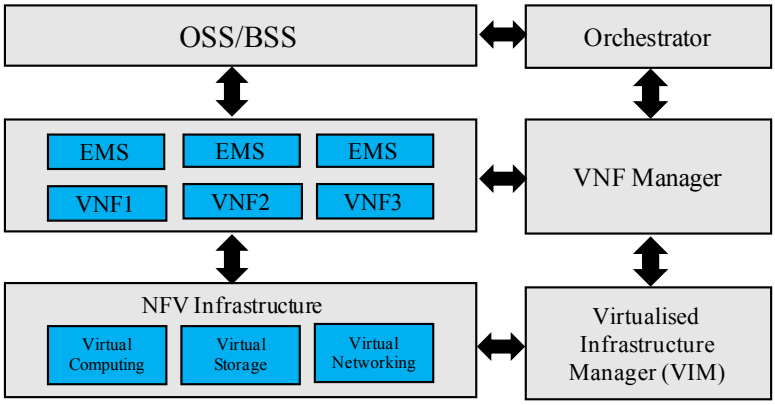

Figure 2.3: MANO NFV Architecture Proposed by European Telecommunications Standards Institute

NFVI in the bottom of Fig. 2.3 is the combination of the various virtual and hardware resources, including network, storage and computing resources. It is responsible for preparing, deploying and adjusting virtual resources to satisfy the operating requirements of the VNFs [59]. VNFs in the middle of Fig. 2.3 are the software modules of network functions that can be deployed on the virtual resources provided by NFVI. NFV MANO in the right side of Fig. 2.3 is the management and orchestration platform for VNFs and NFVI, consisting of Virtualised Infrastructure Manager (VIM), VNF Manager and Orchestrator. NFV MANO interacts with the right side of NFV architecture through reference points for the purpose of managing and orchestrating NFVI and VNFs. Different interfaces are defined to exchange the information among function blocks. Within NFV MANO, Orchestrator is responsible for the communication with the OSS/BSS to achieve the service and SLA information. Orchestrator analyses the received information from two areas: what kind of VNFs are needed to build the service chain to deploy the network service, and which kind of resource are needed to support the selected VNFs. Orchestrator sends the analysed information to VNF Manager and Virtual Infrastructure Manager (VIM). VNF Manager is charging for the VNF configuration to deploy NFV chains, including building, maintaining and tearing down the NFV chain; and VIM implements the

resource virtualisation and allocation to guarantee the Service Level Agreement (SLA) of NFV chain.

2.2 Traffic Models

In order to comprehensively investigate the performance of future network architecture under various multimedia traffic, the network traffic entering the network devices will be modelled by Poisson process and Markov Modulated Poisson Process (MMPP).

2.2.1 Poisson Process

Poisson process is one of the most well-known model to characterise the traffic in network system [60]. It has been widely used to analyse the system performance with the input of the non-bursty traffic, such as message and email data [61]. For Poisson process, the inter-arrival time follows the exponential distribution with arrival rate, λ, denoted as $P(T_a \leq t) = 1 - e^{-\lambda t}$ with $t \geq 0$. Poisson traffic exhibits a number of important and convenient properties, for instance, the superposition of multiple independent Poisson process with arrival rate, λ_i and $1 \leq i \leq N$, results in a new Poisson process characterised by λ_t, calculated as $\lambda_t = \prod_{i=1}^{N} \lambda_i$; the number of arrivals in disjoint intervals is statistically independent, which is known as independent increment property [60]. Given a time interval, t, the number of arrivals, $N(t)$, of Poisson process follows the distribution of $P(N(t) = n) = \frac{(\lambda t)^n}{n!} e^{-\lambda}$.

2.2.2 Markov Modulated Poisson Process (MMPP)

In order to capture the bursty and correlated feature of network traffic, the traffic entering SDN switch will be modelled as MMPP in this research, which is a doubly stochastic Poisson process with the arrival rate varying according to an irreducible continuous-time Markov chain [62] [63]. Due to the capability of capturing the time-varying arrival rate,

MMPP is an effective tool for modelling bursty and correlated traffic [64] [65]. In addition, the superposition and splitting operations of MMMPs generate a new MMPP [66] [67], facilitating the derivation of the analytical model in the complex network environment. A two-state MMPP has been widely used to investigate the performance of the network [68] [69] and is parameterised by an infinitesimal generator matrix of the Markov chain and an arrival rate matrix as follows

$$Q_i = \begin{bmatrix} -\varphi_{1i} & \varphi_{1i} \\ \varphi_{2i} & -\varphi_{2i} \end{bmatrix} \qquad \Lambda_i = \begin{bmatrix} -\lambda_{1i} & 0 \\ 0 & -\lambda_{2i} \end{bmatrix} \tag{2.1}$$

where φ_{1i} is the transition rate from state 1 to 2, and φ_{2i} is the rate out of state 2 to 1. λ_{1i} and λ_{2i} are the traffic rates when the Markov chain is in states 1 and 2, respectively. The subscript, i, denotes the type of the queue where the traffic arrives within the SDN architecture, e.g., low priority queue, high priority queue, Uplink Channel (UC) and Downlink Channel (DC) queues and the controller queue in SDN networks. Then, the mean arrival rate, λ_i^m, of $MMPP_i$ can be given by

$$\lambda_i^m = \frac{\lambda_{1i}\varphi_{2i} + \lambda_{2i}\varphi_{1i}}{\varphi_{1i} + \varphi_{2i}} \tag{2.2}$$

2.3 Stochastic Network Calculus

The traditional queuing theory focuses on the steady state of the network behaviour, and is dedicated to achieving the end-to-end average network performance [70]. While, compared with the queueing theory, the stochastic network calculus focuses on achieving the end-to-end performance bounds and conducting the QoS analysis from the worst case perspective. The aim of the stochastic network calculus is to probabilistically investigate the capability of providing a QoS-guaranteed service of the network infrastructure with

the constraints of network resources [71]. For instance, the QoS guarantee requirements for a network infrastructure have the following form,

$$P(Delay > x) \leq \varepsilon \quad or \quad P(Loss > x) \leq \varepsilon \tag{2.3}$$

where x is the targeted delay and loss; ε is the permissible violation probability. The aim of stochastic network calculus is to give the relationship between x and ε.

In stochastic network calculus, the time is discrete [72] [73] and τ, ν, and t are used to denote the discrete time. During the time interval $[0,t]$, the cumulative traffic generated by the end user is denoted as A(t); the service available at the system is $S(t)$, and the cumulative departures from the system is $D(t)$. Assume that the server is a lossless and work-conserving server, which means there is no packet loss during the service and the server would not stop until the buffer is empty. It is easy to get that $A(t)$, $S(t)$ and $D(t)$ are non-negative and non-decreasing functions. At the start of the time 0, $A(t)$, $S(t)$ and $D(t)$ are assumed to be 0. Further, the notation $A(\tau,t)$ denotes the cumulative traffic arriving at time interval $[\tau,t]$ and is equal to $A(t)-A(\tau)$. $S(t)$ and $D(t)$ have the similar notations as $S(\tau,t)$ and $D(\tau,t)$. According to dynamic server in [72], the relationship between $A(t)$, $S(t)$ and $D(t)$ can be expressed as

$$D(t) \geq \min_{\tau \in [0,t]} \{A(\tau) + S(\tau,t)\} \tag{2.4}$$

The right side of the above inequality achieves its minimum when τ is equal to the beginning time, τ^*, of the last busy period before t. At time τ^*, the queueing buffer is empty and $A(\tau^*) = D(\tau^*)$. The backlog at time t can be defined as $B(t) = A(t) - D(t)$, which comprises both the bits in the buffer and in the service. From Eq. (2.4), $B(t)$ can be described as follows,

$$B(t) \leq \max_{\tau \in [0,t]} A(\tau) + S(\tau, t) \tag{2.5}$$

In [74], the system delay at time t is defined as

$$W(t) = \min\{v \geq 0, A(t) \leq D(t+v)\} \tag{2.6}$$

which defines the time slot between the arrival and departures for bits that arrive at the system at time t. In network calculus theory, min-plus convolution denoted as operator $\bigotimes$ is introduced to simplify the complex equation derivation.

$$(A \otimes S)(t) = \max_{\tau \in [0,t]} \{A(\tau) + S(\tau, t)\} \tag{2.7}$$

Then Eq. (2.4) can be simplified as $D(t) \geq (A \otimes S)(t)$. Min-plus convolution is very useful for deriving the end-to-end network performance, as it inherits some useful properties from the classic convolution, such as associativity with the condition of independence.

2.4 Literature Review

There has been a significant amount of work on LTE-A, SDN, and NFV. In this section, the existing work related to resource allocation and performance modelling of LTE-A, SDN, and NFV will be surveyed. The contributions of this research will also be discussed.

2.4.1 Resource Allocation in LTE-A

Resource allocation is of utmost importance for LTE-A networks, as the optimal processing of the resource allocation can bring great system performance improvement [1] [3]. Therefore, a lot of research results [75] [76] [77] [78] [79] [80] [81] have been reported in the literature to find the low complexity, high utilisation and QoS guaranteed resource

allocation approaches. Within wireless 4G communication networks, such algorithms should consider the transmission quality of the wireless channel, user mobility, expected QoS requirements and overall system utilisation.

In [75], a decoupled time and frequency domain packet scheduling algorithm was proposed to study the performance of the dynamic packet scheduling of 3GPP Universal Terrestrial Radio Access Network (UTRAN) downlink. The simulation results were collected with different 3GPP macro scenarios and showed that the fairness of the resource allocation can be improved by adopting the time-frequency resource allocation strategy. Following [75], Monghal et al. [76] extended the decoupled time and frequency domain packet scheduling approach by introducing frequency domain metric weighting and Time Domain Priority Set Priority (TD-PSS) to investigate the throughput fairness of OFDMA downlink transmission. In [77], a multiuser scheduler with Proportional Fairness (PF) was proposed for the downlink of LTE cellar communication network with the fairness among users considered. The simulation results showed that compared with the well-known maximum rate algorithm [78], the proposed algorithm achieved the better fairness performance with a slight loss in terms of transmission throughput.

The above research work studied the improvement of throughput and the user fairness in packet scheduling, however, did not pay attention to the QoS requirement of the packet loss probability and delay. In this context, there have been many studies focusing on ensuring timely transmission for real-time traffic, providing guarantees on the packet transmission delay. For instance, for supporting the real-time traffic with multi-level delay constraints, a dynamic packet scheduling scheme was proposed in [79] for OFDMA system. According to users$'$ delay constraint level, a mathematical model was developed in the proposed scheduling scheme to make the resource allocation decision, which determines whether the head-of-the-line packets should be transmitted within the current

OFMDA Transmit Time Interval (TTI) or the next TTI. Numerical results showed that the proposed algorithm outperforms the round robin scheme, exponential scheduling scheme as well as the Modified Largest Weighted Delay First (M-LWDF). To provide the real-time services, M. Assaad in [82] investigates the similar problem to [79] by deriving the differentiated behaviours of the diverse average delay constraints. Furthermore, the resource allocation with the aim of maximising the total achievable throughput for multiple users with diverse QoS requirements was investigated in [80] as an optimisation problem. By intelligently assigning the priorities of different users with multimedia traffic, Chung et al. [16] studied the problem of enhancing system throughput while guaranteeing the QoS requirements in terms of average packet delay. Simulation results demonstrated that compared with the traditional resource allocation schemes, the proposed algorithm provided the better system performance in terms of throughput and fairness and achieved the guarantee of QoS requirements with heavy traffic load. Based on the information of channel state and queue length, a sub-optimal resource allocation algorithm for providing delay guarantee was proposed in [83]. With the information of user wireless channel quality and queue state information, the proposed algorithm classified all users into three categories and allocated the time-frequency resource blocks to three user categories in turn. Through differentiating the resource allocation, the proposed algorithm was proved to have the merits of reducing the data rate and improving the resource exploitation rate.

It can be seen that the above research work of resource allocation in 3G/4G networks focused on the system throughput, allocation fairness and average transmission latency, while did not consider the guarantee of QoS performance, including packet transmission delay. For resource-hungry application and service with strict QoS requirements, such as on-line gaming and interactive social events, it is not sufficient just to provide the guarantee on average transmission latency, but more necessary to enforce guarantees on

the upper bound of packet delays. In this area, a unified framework was proposed in [84] to provide the real-time service through utilising the stochastic approximation tools and convex optimisation, however, when this strategy is transplanted from LTE system to LTE-A system, there are some problems needed to be carefully dealt with, such as high-complexity and backward compatibility. In addition, a two-level downlink scheduling algorithm was proposed in [81] for real-time multimedia services in LTE networks. The proposed algorithm provided good performance of user fairness and has overcome the limitation of many prior works, however, it did not consider the users who has the pending data approaching to the deadline, and may experience a sudden decrease of the channel quality. For avoiding the violation of the target delay, the Head-of-Line (HoL) packets that need to be transmitted in present frame are not fully guaranteed in the design of [81], which may lead to serious packet loss especially for the edge-cell users, since the data quota calculated by the upper level frame in [81] is larger than that of HoL flows; if the arrival traffic becomes heavier due to service fluctuation, more radio resource will be allocated in [81] to the quota of the users who have good channel condition; in this case the edge-cell users would be forced in the situation of resource starvation. In order to address this issue, the performance of the edge-cell should be enhanced by taking into account of the HoL packet expiration; compared with the flows that sill have chance in the future TTIs, the flow approaching the deadline should be given a higher priority in the resource allocation to avoid the packet lost.

In addition, CA is one of the key technologies in LTE-A towards meeting the required wider bandwidth by aggregating multiple existing LTE carriers together [85]. In CA, LTE and LTE-A users are assigned into different CCs to maximise the diversity gain from the resource allocation perspective. However, the operation of user assignment would introduce the serious load unbalance among different CCs that one CC$'$s load is much heavier

than that of the other CCs due to the different channel quality experienced by mobile users. Load unbalance coupled with the issue of the QoS guarantee pose a challenging problem for resource allocation in LTE-A system. This problem becomes even more challenging in the presence of mobile users with different requirements in terms of bandwidth, tolerance to delay, and reliability.

2.4.2 Resource Allocation and Analytical Modelling in SDN

Resource allocation and analytical model are critical for SDN networks. This section surveys the latest work in the area of resource allocation and analytical modelling in the literature.

2.4.2.1 Resource Allocation of SDN Networks

SDN allows the underlying network to be programmed by the control plane, which makes it easier for the network provider to dynamically control and manage network resource and create value-added services. In this context, several research efforts [86] [87] [88] [89] [90] [91] [92] have been made in the area of the resource allocation to optimise the overall operation for SDN networks and leverage the capability of SDN networks to virtualise, deploy and manage emerging applications and services. For instance, in order to jointly optimise application performance and network utilisation, Wang et al. in [86] proposed an application-aware network resource allocation through SDN controller and optical switching. In order to overcome the limited rule space of SDN devices, Dong et al. in [87] designed a two-level rule space strategy in data plane and a novel cache prefetching mechanism to increase the utilisation of network resources. The novelty of this work is the integration of the modification of the flow entries with the prediction of the user mobility to significantly increase the hit probability of the flow table. Authors in [88] leveraged the capability of SDN architecture to realise the virtualisation of radio access network and

optimise the resource allocation for Internet of Things application. In order to provide reconfigurable networks for social big data analytics, a big data processing system powered by SDN was designed in [89] through integrating the transmission of SDN networks and the processing of Hadoop architecture. This work exploited the potential of SDN to build a high-performance network infrastructure among different processing units to accelerate the overall data processing; Li et al. [90] proposed an OFScheduler based on OpenFlow and used as a network optimiser for optimising MapReduce operations in a heterogeneous cluster. Qin et al. [91] designed a framework that employs SDN elements in Hadoop to reduce the time taken by data to reach the distributed processing nodes. Within each processing nodes, an online deduplication energy approach is developed in [92] to minimise the energy cost in data centre.

Although existing SDN work has made significant progress in network management and operation by leveraging SDN centralised controller, little attention is paid to the performance improvement in the data plane. Based on the separation of the control and data planes, network logics are implemented in a logically centralised controller; most of the existing work assumed that network switches should become as simple as possible, and adopted First In First Out (FIFO) scheme in data plane to process the arrival packets. Although, FIFO has been widely considered an effective approach to allocate network resources [18], it incurs serious issues of low global fairness and performance degradation in SDN paradigm, due to the inherent feature of SDN - feedback control loop between data plane and control plane. Therefore, there is an urgent need to develop an efficient packet scheduling in SDN networks to improve the global fairness and overall performance.

2.4.2.2 Analytical Modelling of SDN Networks

Due to the explosive growth on the volume of Internet traffic and the ever-increasing QoS requirements of emerging network applications, there have been timely and pressing demands to study the performance of SDN networks. Currently, the performance of SDN networks are mainly investigated by simulation experiments and analytical modelling. For the simulation experiments, Naous et al. [93] firstly implemented the OpenFlow Ethernet switch on the NetFPGA platform to provide high throughput and low complexity of forwarding switches. Antichi et al. [94] extended Naous work by designing a flexible OpenFlow based forwarding architecture through regular expression with the aim of supporting more network applications in data plane. The switches in the proposed architecture are capable of storing up to 200K flow information while satisfying the requirement of line rate processing. Bianco et al. [95] extended the OpenFlow switch implementation to the Linux platform based on OpenFlow specification, also meeting realistic line rates. These implementations of OpenFlow switches, however, were only realised on single platform, lacking the support for cross-platform implementation. To fill this gap, in [96], a modular and parameterised implementation of a hardware-based OpenFlow switch was proposed to implement SDN on three different platforms, i.e., NetFPGA, ML605 and DE4. Through performance comparison, this study showed that the switch design can be implemented on different platforms with minor performance variations.

As compared to simulation, analytical modelling has the potential to offer a significant reduction of the computation resource and time required for achieving the system performance [97] [98] [99] [100], especially when large-scale Internet with high-volume big data is considered in [12]. Azodolmolky et al. in [5] analysed the performance of the SDN architecture through exploiting the network calculus theory and achieved the boundary condition of the transmission latency and queue length. Based on the mea-

surements of the switching time in hardware OpenFlow switch, Jarschel et al. in [25] proposed an analytical model for SDN networks to estimate the packet sojourn time and packet loss probability. Mahmood et al. in [26] extended the work in [25] to investigate the performance of the SDN architecture with multi-node condition. In this study, both the data plane and control plane were simply modelled as M/M/1 queues. Furthermore, for analytical tractability and simplicity, all these existing models for SDN networks were primarily developed under the nonbursty Poisson arrivals. For big data transmission, the traffic patterns typically exhibit bursty and correlated nature. For instance, Beck et al. [28] revealed that the procedures of the big data analytics lead to the high burstness during the data transmission and more dynamic resource allocation are required to meet the QoS/QoE requirements. The authors in [27] discovered that the traffic behaviour of the big data exhibits the larger bursty at the range of 10-1000 microsecond. Liu et al. in [30] analysed the four popular big data applications (Hadoop, Spark, Shark and Impala) running on the experimental clusters. The real traffic was collected from the communications among these applications. The experimental results showed that the big data traffic results in the higher use of the network in a short time and exhibits the high degree of fluctuations and burstiness. Although the transmission of the big data presents the bursty pattern and significantly affects the provisioning of the network services, none of the existing analytical models for the SDN networks is capable of capturing such realistic characteristics. There is an urgent need to develop an analytical model that could accurately predicts the performance of SDN networks under the traffic patterns exhibited bursty and correlated features.

2.4.3 NFV and Analytical Modelling of Service Chains

Due to its profound impact in the future network, NFV has gained global awareness [101] [102] [103] and leads to a lot of research results reported in the literatures, for instance, to tackle the problem of the optimal Virtual Network Function (VNF) placement, Xia et al. [32] formulated this problem as a binary integer programming for minimising the overall optical/electronic conversions and designed a heuristic algorithm to achieve high computation efficiency. Moens et al. [33] addressed the similar problem through formulating the placement problem as an integer linear program with the aim of allocating a service chain onto the physical network minimising the number of servers used. In order to improve the performance of the NFV virtualised network to achieve the comparable performance with that of the network function deployed on the dedicated network device, Ge et al. [101] firstly conducted the comprehensive research and determine that industry standard servers may not provide satisfied performance for some network functions, such as DPI and NAT, and highlighted that hardware acceleration technology is a good alternative for improving the performance for VNFs. Yamazaki et al. [104] deployed virtual DPI on Application Specific Instruction-set Processor (ASIP) and achieved much better performances. Compared with ASIP solution, Intel [105] proposed a set of Data Plane Development Kit (DPDK) to accelerate the packet processing speed in the VNFs, which has been adopted by many vendors during designing their NFV solutions. In the standardisation process of NFV architecture, ETSI [106] launched the specification of "Network Function Virtualisation Performance & Portability Best Practises" to identify the performance requirements for Virtual Machines (VMs) and hardwares to assure predictable high performance. Experimentation tests were conducted in both bare metal and virtualisation environments for NFV use cases, such as DPI, C-RAN, BRAS, etc. The specification concluded that the predictable high performance could be achieved through following the

best practices listed in the specification. In addition, China Mobile conducted extensive field trails to test the performance of NFV and SDN architectures in C-RAN; the results from China Mobile report in [107] showed that common hardware can support multi-RAT technologies and achieve the comparable performance with traditional systems. The existing research work has achieved a lot of progresses in the performance improvement of NFV network, however based on the simulation trails, existing study can not accurately and quantitatively investigate the performance for the NFV architecture, especially with large scale and complex network configurations.

Modelling and analysis of the network functions and service has been a very challenging and attracts tremendous research efforts [108] [109] because analytical models can capture the inherent features of a complex system and yield significant insights into the system design and performance in a cost-effective way. For performance modelling and analytics, most of the existing studies appealed to the queueing theory [70], which is a fundamental mathematical approach to capture the behaviour of the network system. The classical queueing theory focuses on the average quantities in the equilibrium and derives the average system performances such as average latency, throughput and packet loss probability, however, for the QoS guarantee, it can be hardly used to investigate the performance of the service-guaranteed system due to the dynamic and on-demand features of the service provisioning. In this area, stochastic network calculus [73] [72] [74] has attracted research interests. Instead of giving the average performance metrics, it derives the worst-case of system performance. For instance, in order to achieve the available bandwidth, Lubben et al. [108] explored the properties of stochastic min-plus linear system theory, which expresses bandwidth availability in terms of bounding functions with defined violation probability, and accurately estimated the available bandwidth with random server in wireless communication system. This work, however, is only focusing on

modelling the service capability of the access network, lacking the support for modelling the end-to-end service provisioning. As a result, a new model was developed in [109] for characterising the service capability of the converged networks, from access network, core network, to datacenter networks. The analysis technique was developed with the aim of achieving the delay performance of the converged infrastructure and generally agnostic to the specific network implementation. However, this work did not consider the on-demand feature of the service provision; especially, when the service capabilities of VNFs are different due to their different network functions and also may change over the whole life-cycle in the manner of on-demand. Furthermore, the network functions in NFV chain may be added, removed or modified in order to continuously offer satisfied performance and forms new NFV chain. To the best of our knowledge, analytical modelling and analysis of NFV network with the features of dynamic service and scalable resource has not been reported in the existing literature.

2.5 Summary and Contribution

This chapter firstly introduced the fundamental knowledge of the network architectures of LTE-A, SDN and NFV; then the traffic patterns and the analytical tools that will be used in the derivation of the analytical models, were presented. Finally, a detailed state-of-the-art was given with focuses on the resource allocation and analytical modelling of LTE-A, SDN and NFV. In order to bridge the gaps identified in the state-of-the-art of Section 2.4, four aspects of innovation work are conducted in this study and will be introduced in the rest of this thesis: 1). to address the unbalanced load problem coupled with the issue of the QoS guarantee in LTE-A, a novel Cross-CC user migrating scheme is proposed, which consists of three cooperative and complemented schedulers to define, fulfil and optimise the transmission quotas in each TTI, with the aim of meeting QoS re-

quirements and optimising the overall resource utilisation; 2). according to the OpenFlow specification 1.3.3 [110], the queue structure in the forwarding devices is recommended to be designed with multiple queues, therefore, a PQ based packet scheduling is proposed in this research to improve the forwarding capability of SDN data plane; 3). in order to achieve a fundamental understanding of the performance of SDN networks, two analytical models are developed in this research to comprehensively investigate the performance of the SDN networks under the inputs of Poisson process and MMPP; and 4). in order to quantitatively study the dynamic and on-demand features of NFV network, stochastic network calculus is used in this research to achieve the capability of service guarantee in NFV network; instead of giving the average QoS metrics, the proposed analytical model based on stochastic network calculus provides the upper latency bound, which is very useful for practical network service provisioning and network planning.

Chapter 3

QoS-Aware Resource Allocation for LTE-A system with Carrier Aggregation

3.1 Introduction

Carrier Aggregation (CA) is regarded as a promising technique for LTE-A wireless communications to satisfy the ever-increasing bandwidth requirements [39][111]. However, this technical innovation puts forward new challenges on radio resource allocation in LTE-A systems such as serious unbalanced loads among different Component Carriers (CCs). To alleviate this problem, a Cross-CC user migration packet scheduling algorithm is proposed to provide real-time service in the LTE-A downlink transmission with CA, jointly considering system throughput, QoS constraints, and user fairness. The proposed scheme has three cooperative components: the higher level scheduler, the lower level scheduler and Cross-CC user migration scheme. (1) In the higher level scheduler, an innovative resource allocation algorithm defines frame-by-frame the amount of data that each real-time source should transmit to satisfy its delay constraint. (2) Once the higher level has accom-

plished its task, the lower level scheduler, every TTI, assigns Resource Blocks (RBs) using the proportional fair algorithms to fulfil the transmission quotas defined by higher level scheduler, by virtue of considering user average data rate in Proportional Fair (PF) algorithm, lower level scheduler achieves a higher fairness among users. (3) When the lower level scheduler finishes its allocation process, the base station will start the Cross-CC user migration process, it is motivated by decreasing the unbalance degree among the different CCs and will increase the system efficiency through globally utilising the resource of CCs that have accomplished their quotas in advance.

The remainder of this chapter is organised as follows. Section 3.2 outlines the radio resource allocation in LTE-A with focus on the architectural and physical aspects. Section 3.3 presents the proposed QoS-aware resource allocation scheme. The simulation results are shown and analysed in Section 3.4. Finally, Section 3.5 concludes the chapter.

3.2 Carrier Aggregation in LTE-A System

According to 3GPP Release10 [112], CA is capable of aggregating several LTE CCs (e.g. up to 5) to achieve a wider bandwidth; therefore, the maximum bandwidth for LTE-A User Equipments (UEs) can be up to 5 CCs of 20 MHz. In this study, LTE-A user and LTE-A UE are exchangeable. As CA leverages the existing LTE CCs to achieve the wider bandwidth, LTE-A system provides seamless backward compatibility to LTE users as shown in Fig. 3.1. The bandwidth of LTE CC supported by Rel-8 [113] specification is 1.4, 3, 5, 10, 15, and 20 MHz. Therefore, flexibility bandwidth can be achieved through appropriate CC configurations. The minimum resource that BS could assign is RB as shown in Fig. 3.2. For high-quality information transmission, the quality of the wireless channel on all CCs should be firstly estimated by Rel′8 and LTE-A users and feedback to the base station (e.g. eNB); according to the received channel quality information,

eNB performs various resource allocation strategies to provide network services. While the mobile devices always have limited power and computation, the number of CCs a user can support should be allocated as less as possible. While in order to maxmise the multi-user scheduling diversity, following the work in [81], LTE-A users are assumed to be allocated on all CCs, while the Rel8′ users can only be assigned to one CC. The optimisation of the number of the CCs is an important research and has been arranged as future work in Chapter 7.

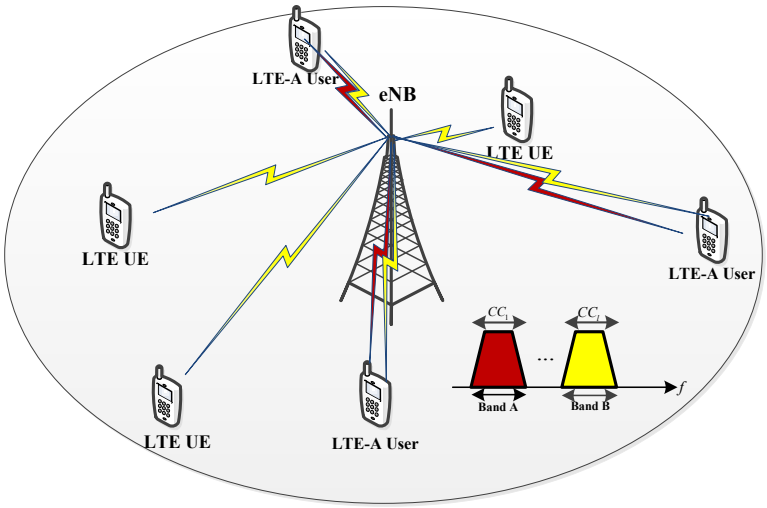

Figure 3.1: Network Scenario of LTE-A System with CA

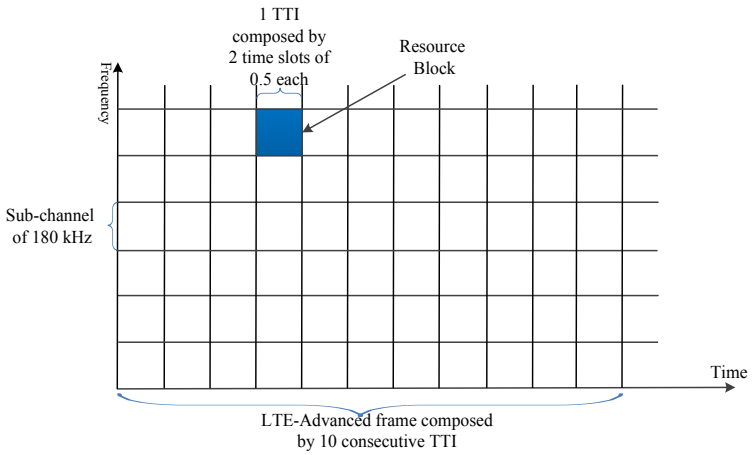

Figure 3.2: Time-Frequency Resource Block in LTE-A System

According to Release10 [112], there are three CA scenarios that eNB supports in the specification, including intra-band contiguous CA, intra-band non-contiguous CA and

inter-band non-contiguous CA, as shown in Fig. 3.3;

- Intra-band contiguous CA: a contiguous bandwidth wider than 20 MHz is used by CA as shown in Fig. 3.3a. In LTE, it is almost impossible to find such a wide bandwidth based on existing frequency allocation strategy. While in LTE-A, new spectrum band such as 3.5 GHz is harvested in the LTE-A scenario.

- Intra-band non-contiguous CA: multiple non-contiguous bandwidths in the same spectrum band are aggregated by CA as shown in Fig. 3.3b. Different countries have different spectrum allocation strategies, there are some individual and narrow bandwidths that are not occupied by other communication system, which could be utilised by CA in LTE-A system to form CCs and increase the spectrum utilisation.

- Inter-band Non-Contiguous CA: multiple contiguous or non-contiguous bandwidths in different spectrums bands are aggregated by CA as shown in Fig. 3.3c, for instance, bandwidths on 2GHz and 800MHz can be aggregated to form a wider bandwidth [114]; Through exploiting the bandwidths on different spectrum bands, LTE-A system achieves better performance in system performance and robustness to user mobility. Low spectrum has good performance on signal penetration and cell coverage, while high spectrum provides higher data transmission rates.

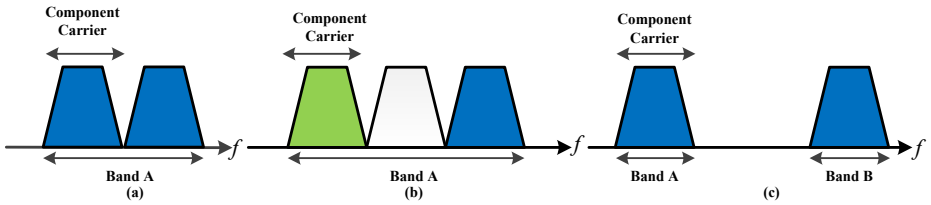

Figure 3.3: CA Scenarios in LTE-A System

CA provides the LTE-A system the benefit of the wider available bandwidth, however, it also introduces the additional challenge in radio resource allocation, for instance,

in the second and three scenarios, the non-contiguous bandwidths in the same or different spectrum bands may have different radio propagation characteristics; additional complexity in the design of radio frequency components in user devices may be introduced and advanced resource allocation algorithms are needed.

The support for both contiguous and non-contiguous CA of CCs with different bandwidths offers significant flexibility for efficient spectrum utilisation, and gradual re-farming of frequencies previously being used by other systems such as e.g. Global System for Mobile Communications (GSM) or Code Division Multiple Access (CDMA). While, the non-contiguous CA scenarios have additional implications in the radio network planning and the design of the Radio Resource Management (RRM) algorithms as shown in Fig. 3.4, for instance, different CCs would exhibit different path loss and Doppler shifts.

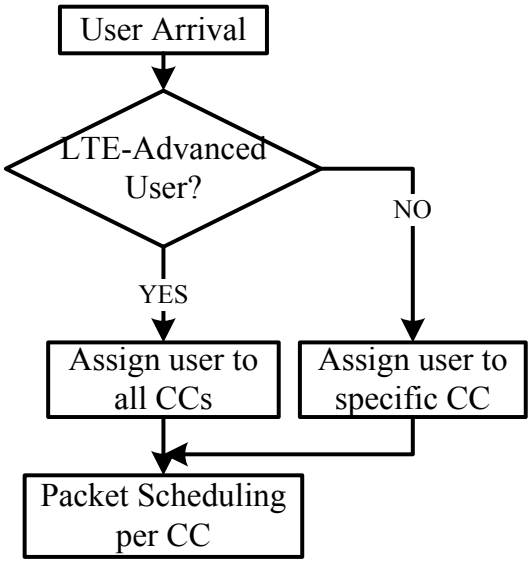

Figure 3.4: Component Carrier Allocation for LTE-A and LTE Users with CA

3.3 Cross-CC User Migration Scheme

In this section, a novel QoS-aware scheme of resource allocation is developed for provisioning real-time services in the downlink transmission of LTE-A. In order to achieve a good trade-off among the system throughput, user fairness and QoS constraints, the pro-

posed scheme is composed of three cooperative components as shown in Fig. 3.5. These three components interact with each other to efficiently and dynamically allocate radio resources to terminal users. According to the diverse delay requirements and the queue lengths, the higher level scheduler calculates two types of transmission quotas frame-by-frame: the transmission quota for Head-of-Line (HOL) packets and the transmission quota from Long Term Perspective (LTP). The task of the lower level scheduler is to assign RBs to fulfil two defined transmission quotas. In order to achieve a lower packet loss probability, the lower scheduler first offers service for HoL packets, since these packets are more likely facing violation of the delay constraints. The Cross-CC user migration scheduler follows the lower level scheduler to assign more resources to the users that cannot complete their transmission quotas. In this study, the proposed Cross-CC User Migration (CUM) algorithm mainly improves the performance of the downlink communication and will be implemented in the BS. In the following parts, these three cooperative components will be separately investigated in detail.

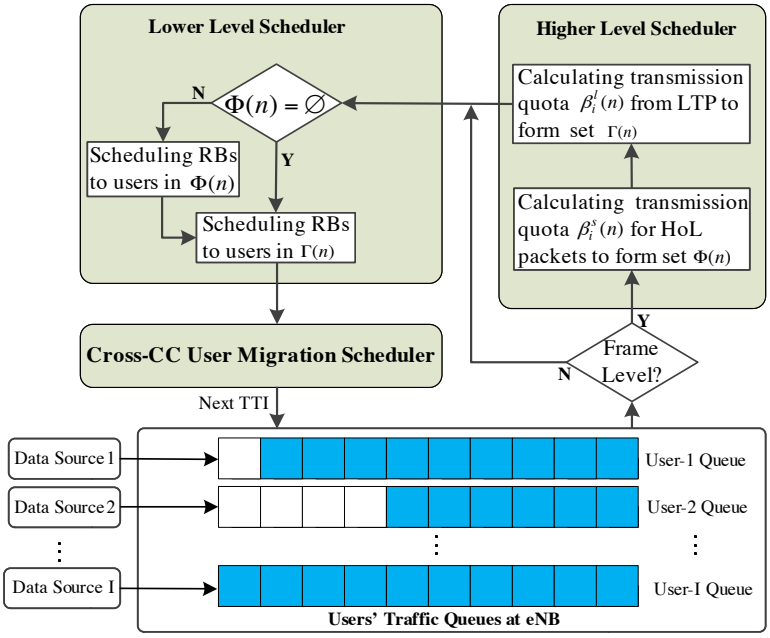

Figure 3.5: Structure of the CUM Scheme in LTE-A System

3.3.1 The Higher Level Scheduler

In order to achieve guarantees on the absolute packet delays, the higher level scheduler defines two types of transmission quotas as described above. These two quotas are complementary to each other. The quotas for HoL are designed to obtain the lower packet loss probability for guaranteeing the delay requirements when the quotas from LTP are not completed by the lower level scheduler. On the other hand, successfully fulfilling the quotas from LTP enables the systems to define the fewer quotas for HoL packets.

(1). Transmission Quotas for HOL Packets

For the real-time service provisioning, a packet failed to be delivered within its corresponding delay requirement τ_i, will be considered lost [116]. As shown in Fig. 3.6, the third packet with $\tau_i = 10\ ms$ arrives within the nth frame. It should be transmitted in the $(n+1)th$ frame. However, due to the transmission impediments of wireless communications such as path loss and interference, the third packet is blocked and is still in the queue at the end of the $(n+1)th$ frame. As a result, it is dropped by the eNB. In order to avoid dropping the HoL packets, in this part the higher level scheduler defines the transmission quotas for HoL packets to give them the higher priority in resource allocation.

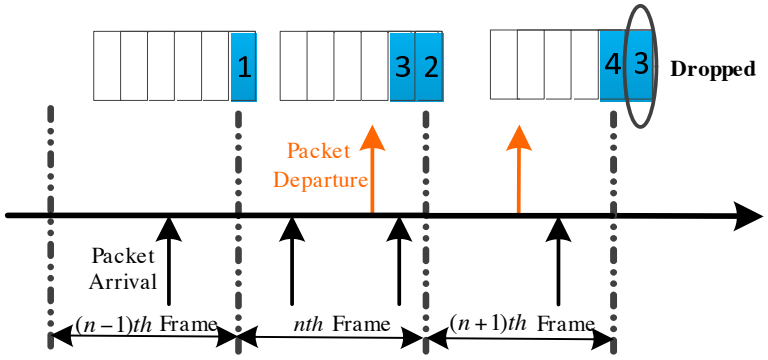

Figure 3.6: Real-time Packets Operation in eNBs

Let $x_i(n)$ denote the queue length of the ith user at the nth frame. $\alpha_i(n)$ and $\beta_i(n)$, respectively, denote the numbers of packets that arrive in and depart from the queue during the nth frame. Then the queue length of the ith user at the beginning of the $(n+1)th$ frame

can be calculated as follows:

$$x_i(n+1) = x_i(n) + [\alpha_i(n) - \beta_i(n)] \tag{3.1}$$

For real-time services, the packets for the ith user arrive at the eNB during the nth frame, then the deadlines of these packets are fixed as $t(n) + \tau_i$. Let M_i denote the number of frames that the packets for the ith user should be delivered. M_i can be computed as:

$$M_i = ceil(\tau_i / TTI) \tag{3.2}$$

From the perspective of FIFO, in order to satisfy the delay requirement, the number of packets departing from the queue from the $(n+1)th$ to the $(n+M_i-1)th$ frame should be larger than those stored in the queue during the nth frame. Thus,

$$\sum_{z=n}^{n+M_i-1} \beta_i(z) \geq \alpha_i(n) \tag{3.3}$$

Transposing $M_i - 2$ items from the left side of the above inequality, to the right side, it can be equivalently rewritten as

$$\beta_i(n+M_i-1) \geq max[\alpha_i(n) - \sum_{z=n}^{n+M_i-2} \beta_i(z), 0] \tag{3.4}$$

By imposing $n+M_i-1 = n$, the transmission quota for HoL packets can be obtained and the above inequality becomes

$$\beta_i^s(n) \geq max[x_i(n-M_i+1) - \sum_{z=n-M_i+1}^{n-1} \beta_i(z), 0] \tag{3.5}$$

where $\beta_i^s(n)$ is the number of HoL packets for the ith user that should be transmitted

during the nth frame so as to avoid packets loss. The higher level scheduler forms a transmission set $\Gamma(n)$, only the users that the corresponding transmission quota $\beta_i^s(n) \neq 0$ can be put in this set to receive the service from the lower level scheduler.

(2). The Transmission Quotas from LTP

In order to offer guarantees on the absolute bounds of packet delays, the higher level scheduler calculates, from the long term perspective, the transmission quotas for each user to meet delay constraints. Herein the long term perspective means the packets arriving in the queue during the nth frame are distributed into $n+M_i-1$ frames for transmission. In what follows, we will calculate the transmission quotas from LTP in each frame.

As defined in Eq. (3.6), $x_i(n)$ is the queue length for the ith user at the beginning of the nth frame. Let $h_i(n)$ denote a pulse response that indicates the relationship between the queue length and the transmission quota. Then the transmission quota from LTP, $\beta_i^l(n)$, can be described as following. The symbol $*$ represents convolution.

$$\beta_i^l(n) = h_i(n) * x_i(n) \tag{3.6}$$

where the pulse response is given by:

$$h_i(n) = \sum_{z=0}^{M_i-1} c_i(z)\delta(n-z) \tag{3.7}$$

where M_i is calculated by Eq. (3.2), and $c_i(z)$ is the pulse response coefficients. To satisfy the actual waiting time smaller than the delay requirements, $c_i(z)$ in the above equation is designed as a strictly decreasing function and calculated as

$$\begin{aligned} c_i(z) &= 0, && z = 0 \\ c_i(z) &= \tfrac{M_i-z}{M_i-1}, && z = 1,...,(M_i-1) \end{aligned} \tag{3.8}$$

The derivation of the transmission quota from LTP is based on a discrete-time linear control theory [81].

$$\beta_i^l(n) = x_i(n) + \sum_{z=2}^{M_i-1} [x_i(n-z+1)$$

$$-x_i(n-z+2) - \beta_i^l(n-z+1)]c_i(z) \tag{3.9}$$

After obtaining the transmission quotas from LTP, the higher level scheduler establishes a transmission set $\Gamma(n)$. Only the user that the transmission quota $\beta_i^l(n) \neq 0$ can be put in this set and will receive the resources from the lower level scheduler when the users in set $\Phi(n)$ have finished their transmission quotas.

3.3.2 The Lower Level Scheduler

The performance of the higher level scheduler is determined by the allocation results from the lower level scheduler, thus the lower level scheduler plays a critical role in the proposed CUM scheme. For achieving a higher level of fairness among different users, the lower level scheduler adopts the PF algorithm in resource allocation[14]. The basic principle is to assign the RBs to users with best metric $m_{i,j,k}^{PF}$. To obtain this metric, the lower level scheduler should have the information of the average transmission rate $\overline{R}_i(k)$ and the instantaneous data rate $r_i^j(k)$ for the ith user during the kth TTI. The average transmission rate is updated in every RB by

$$\overline{R}_i(k) = \varepsilon \overline{R}_i(k-1) + (1-\varepsilon)R_i(k) \tag{3.10}$$

where $R_i(k)$ is the data rate transmitted by the ith user. The parameter ε is used to tune the trade-off between the spectrum efficiency and fairness. The larger value of ε means the better fairness. The smaller value of ε results the worse fairness.

Then the allocation metric $m_{i,j,k}^{PF}$, the ratio of the instantaneous data rate $r_i^j(k)$ for the ith user on the jth RB over the average data rate $\overline{R}_i(k)$, is calculated as follows:

$$m_{i,j,k}^{PF} = \frac{r_i^j(k)}{\overline{R}_i(k)} \tag{3.11}$$

It is worth noting that the proposed scheme is capable of guaranteeing the same bounded delay by regarding a temporary channel quality drop or a sudden dramatic traffic increase. It takes into consideration the left pending packets, scheduling them in the next frame, allocating a greater amount of data to be transmitted and giving higher priorities during Cross-CC user migration process, which will be discussed in the following part.

3.3.3 The Cross-CC User Migration Scheduler

Due to characteristics of wireless communications, the users achieving good channel qualities may accomplish their transmission quotas in advance compared with their counterparts with poor channels, which results in serious unbalanced loads among CCs. In order to relieve this problem, a Cross-CC user migration scheduler is designed in this part for decreasing the unbalance degree of loads and assigning extra resources to the users that are unable to accomplish their transmission quotas timely.

In the proposed scheduler, the users are no longer served by the fixed CC. The dominant CC can be changed if there is any CC that has finished the allocated quotas. And in order to keep the backward compatibility for LTE systems, the number of CC that LTE users can communicate with is mandatory to be one. Then the specific procedure of user allocation for the Cross-CC user migration scheduler presents as follows. When the lower level scheduler has finished the resource allocation at the kth TTI, the eNB will check the transmission set $\Gamma(n)$ to see whether there is any empty set. If $\Gamma(n) = \emptyset$ in the mth CC, it is equivalent to the case that the quota in this CC has been finished. Then the eNB will

select a user to receive the migration process from its dominant CC to the mth CC. In order to enable the lower level scheduler to accomplish its allocation task timely, herein the user that has the largest ratio of the remainder of transmission quota over the average transmission rate will be selected.

Let $L_i(k)$ denote the data quota left for the ith user to transmit. $\bar{r}_i(k)$ and $r_{i,j}(k)$ present the average transmission rate and the instantaneous transmission rate during the kth TTI on the jth RB, respectively. $\bar{r}_i(k)$ is given by

$$\bar{r}_i(k) = \frac{1}{N_{RB}} \sum_{j=1}^{N_{RB}} r_{i,j}(k) \tag{3.12}$$

where N_{RB} is the number of RBs available for the ith user to occupy. Then, the user selection criterion is designed as:

$$i^* = \underset{i}{\operatorname{argmax}} \left(\frac{L_i(k)}{\bar{r}_i(k)} \right) \tag{3.13}$$

The mth CC will serve the selected user i^* in the rest of the TTIs during the nth frame. By allowing users to change their dominant CC during resource allocation, the proposed scheme improves the resource utilization from two aspects: 1) decreasing the resource waste in the CC that has not accomplished its data quota, and 2) increasing the resource utilisation in the CC that has fulfilled its allocated data quota.

3.4 Performance Evaluation

In this section, the performance of the CUM scheme is evaluated through a downlink multi-cell LTE-A system-level simulator. We will first present the simulation scenarios, including the cell topology, wireless channel, CC configuration and traffic generation model. Based on the developed simulator, we will investigate the performance of the pro-

Table 3.1: LTE-A System Simulation Settings

Parameter	Setting/Description
Test scenario	3GPP Macro-cell case #1 (19 sites)
CA pattern	4 CCs at 2.0 GHz frequency, with 10 MHz per CC
Number of PRBs per CC	50 (12 subcarriers per PRB)
Sub-frame duration	1 ms (11 OFDM data symbols plus 3 control-symbols)
Modulation and coding schemes	QPSK (1/5, 1/4, 1/3, 2/5, 1/2, 3/5, 2/3, 3/4),16-QAM (2/5, 9/20, 1/2, 11/20, 3/5, 2/3, 3/4, 4/5, 5/6) ,64-QAM (3/5, 5/8, 2/3, 17/24, 4/5, 5/6, 7/8, 9/10)
CQI reporting	1 CQI per 3 PRBs; 1.6 dB quantization step; log normal error with 1dB standard deviation
Layer 2 PS	Proportional-Fair
Transmission Block Error Rate target	10%
Admission control constraint	Maximum 80 users per cell (Mixed user scenario with 20% LTE-Advanced users)
Traffic type	Poisson arrival with fixed queue length of 2 Mbits

posed algorithm compared with the well-known Two Level Downlink Scheduling (TLDS) scheme.

3.4.1 Simulation Scenarios

The simulation environment is set based on 3GPP specification defined in [113]. A scenario of 19 hexagonal cells is conducted with the reference cell surrounded by two ties cells. The detailed system parameters and settings are listed in Table 3.1 [42] [116] [14]. The wireless channel is modelled in terms of distance-dependent path loss, shadowing fading and multipath Rayleigh fading with each independent fading path generated by Jakes Model [15]. The traffic flow for the user is modelled as the Poisson process.

The details of the simulation scenario is described as follows:

- Multi-cell topology: the network topology in the designed LTE-A simulator consists of 19 hexagonal cell as shown in Fig. 3.7. The centre cell provides the network service for the UE in the middle; other 18 cells continuously generate the interference and noise to the UE for simulating the practical network condition.

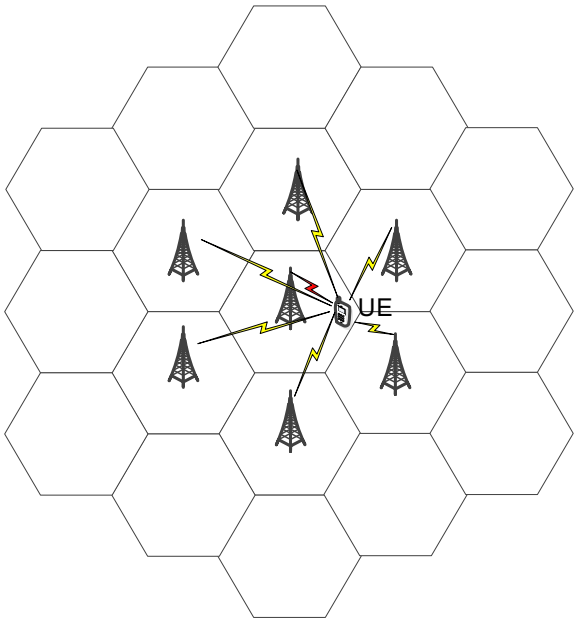

Figure 3.7: Multi-cell Topology for LTE-A System Simulator

- CC configuration: 4 CCs are adopted at the spectrum band of 2.0 GHz; each CC is assigned with the bandwidth of 10 MHz and has 50 Physical Resource Blocks (PRBs); each PRB has 12 subcarriers; thus each CC has up to 600 subcarriers at one time slot (1 ms).

Given the network topology and CC configuration, the structure of the LTE-A simulator is represented in Fig. 3.8, consisting of traffic generator module, user mobility management module, channel generator module, eNBs and UEs.

- Traffic generator module: the maximum number of user per cell is set to be 80, 20% of which is LTE-A users. The traffic generator module is used to simulate downlink traffic from Internet to UEs; the traffic for the ith UE will be generated according to

Poisson process with the generation rate λ_i, in the unite of the packets per second. The total traffic eNB received can be described as a Poisson process with arrival rate λ_t, calculated by $\lambda_t = \sum_{i=1}^{80} \lambda_i$.

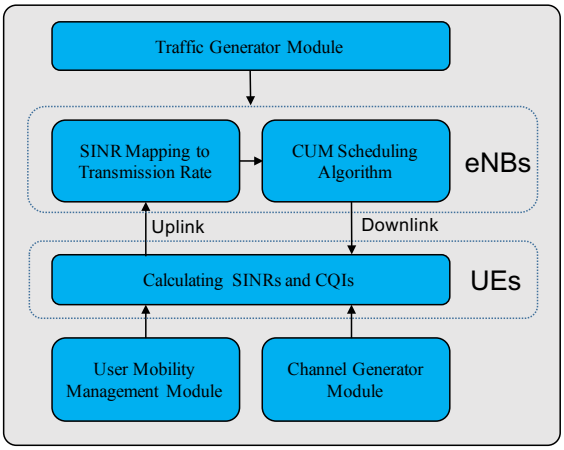

Figure 3.8: Component Structure of LTE-A Simulator.

- User mobility management module: user mobility management module is used to generate and manage UE locations; at the start of each simulation, the UEs will be randomly positioned in the centre cell with coordinate [x,y], given a random speed value, v, and a random mobility angle, θ. During the simulation, the users will move a certain distance in the centre cell at each TTI. User mobility management module will use the following equations to update the UE locations:

$$x_i^{new} = x_i^{old} + v_i * TTI * cos(\theta_i) \tag{3.14}$$

$$y_i^{new} = y_i^{old} + v_i * TTI * sin(\theta_i) \tag{3.15}$$

In order to avoid the user cross the cell edge, user mobility management module will check the distance between UEs to the eNB at each TTI and change the mobility direction if the distance is larger than the cell radius. UE locations data generated by the mobility module will be stored in an excel document in advance. During the

Table 3.2: Channel Parameters in Hata Model

f (GHz)	h_B(m)	h_M(m)	d(Km)
2	150	1	5

simulation, eNBs will read the position data from this file to acquire the locations of UEs, calculate the channel quality and process resource allocation strategy.

- Wireless Channel Model: several factors are considered in the simulator to simulate wireless channel, including shadow fading [117], multi-path Rayleigh fading [118] and distance-related path loss [119].

- Pathloss model: Hata model [120] is widely used in wireless communications to estimate the channel behaviour such as diffraction, reflection and scattering. As the working spectrum is set to be 2 GHz, COST 231-Hata model [121] is used in the simulator to estimate the path loss.

$$\begin{aligned} P_{Hata} = 46.3 + 33.9 * log(f/1MHz) - b(h_B/1m) - a(h_M/1m) + \\ (44.9 - 6.55log(h_B/1m))log(d/1Km) + C_M \end{aligned} \tag{3.16}$$

The parameters in Eq. (3.16) are listed in Table 3.2, where f is the carrier frequency, h_B and h_M are heights of BS and UE respectively, and d is the distance between BS and UE.

For the small-medium network size, the value of C_M in COST 231 Hata model is set to be 0; and the values of $a(h_M)$, $b(h_M)$ are calculated by

$$a(h_M) = (1.1log(f/1MHz) - 0.7) * h_M/1m - 1.56log(f/1MHz) + 0.8 \tag{3.17}$$

$$b(h_M) = 13.82log(h_B/1m) \tag{3.18}$$

- Shadow fading: shadow fading, due to the presence of the large obstruction, obscures the wireless signal between the eNBs and UEs. It is modelled by a log-normal distribution with 0 mean and 8 dB of standard deviation in the simulator [122]. Shadow fading for the ith UE on the jth RB at the time t is denoted as $S_{i,j}(t)$.

- Multi-path Rayleigh Fading: Jake Model [123][124] is adopted in the simulator to model the multi-path Rayleigh fading, denoted as $M_{i,j}(t)$. Jake Model has good characteristic to capture the effect of the user mobility such as Doppler effects.

With the path-loss model, shadow fading and multi-path Rayleigh fading, the overall channel gain, $G_{i,j}(t)$, can be calculated as [120]

$$G_{i,j}(t) = 10^{(P_{i,j}(t)/10)} * 10^{(M_{i,j}(t)/10)} * 10^{(S_{i,j}(t)/10)} \tag{3.19}$$

Based on the achieved channel gain, UEs leverage the approach in [120] to calculate the Signal Interference plus Noise Rate (SINR) and forward the SINR together with Channel Quality Index (CQI) to eNB [125]; Once eNB receives the SINR and CQI information, it maps the SINR to transmission rata that UEs can be achieved and conducts the proposed CUM algorithm.

3.4.2 Performance Analysis

In this section, the performance results of the proposed CUM scheme are compared with those of the Two-Level Downlink Scheduling (TLDS) scheme [81] which has been shown to outperform the other existing scheduling strategies [2]. In order to fully evaluate the performance of the proposed scheme, the performance comparison will be conducted in three aspects: Packet Loss Probability, Average Queue Length and Throughput per User.

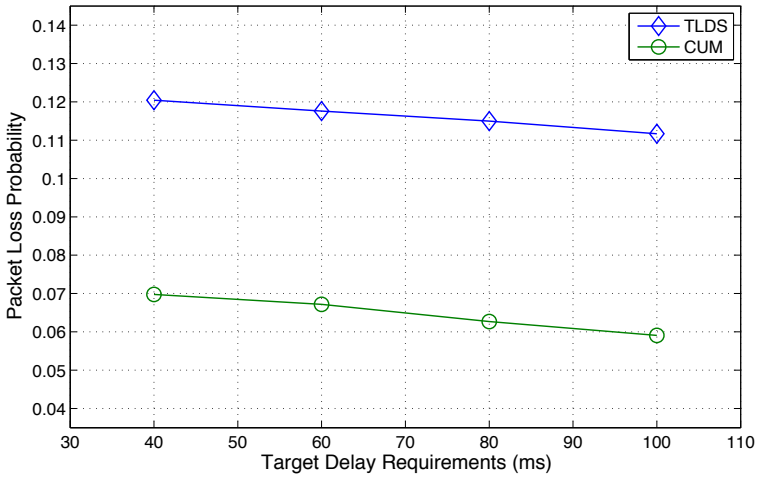

Figure 3.9: Comparison of Packet Loss Probability.

3.4.2.1 Packet Loss Probability

Regarding real-time applications, the packet loss probability is a standard metric widely used to evaluate the QoS offered by the system at network layer [81] [116] [2]. The packet loss probability for the proposed CUM scheme is shown in Fig. 3.9. The performance results of TLDS are also depicted. It can be seen from the figure that CUM achieves a significant improvement over the TLDS; the gain is always greater than 40%. The reason for achieving the improved performance can be explained as follows: for real-time service, sudden temporary channel disturbance causes more packets facing the expiration of deadline, and radio resource is limited in scheduler. As a result more packets are dropped during data transmission. To alleviate this problem, the proposed scheme defines transmission quotas for HoL packets, offering them extra priority for receiving radio resources, and thus the lower packet loss probability is achieved.

3.4.2.2 Average Queue Length

The relative gain in the average queue length by adapting the proposed CUM scheme over the TLDS is depicted in Fig. 3.10, subject to the different requirements for target delays. It is shown that the proposed method provides the much lower average queue length com-

pared with the TLDS. This is because, in the radio resource allocation, the transmitter favors the users that are geographically closer to the eNB, and starves the further users, which results into the high queue length for poor channel users. To relieve this problem, the Cross-CC user migration scheduler migrates the users at the less advantageous positions to receive more radio resource from other CCs and yields good performance in terms of the lower average queue length.

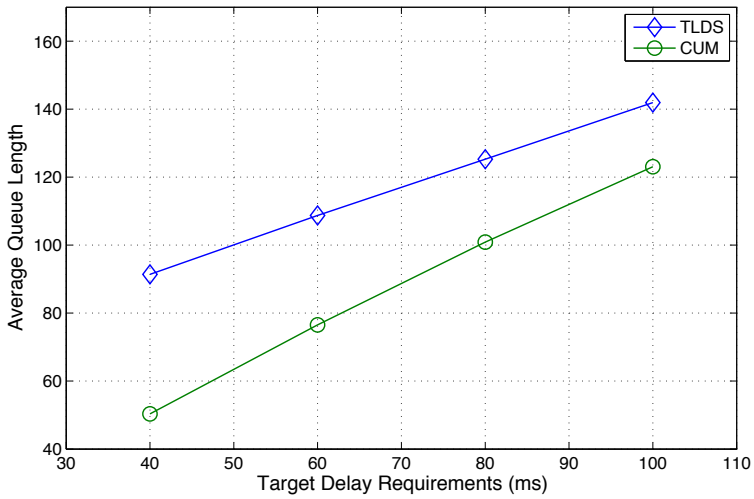

Figure 3.10: Comparison of Average Queue Length.

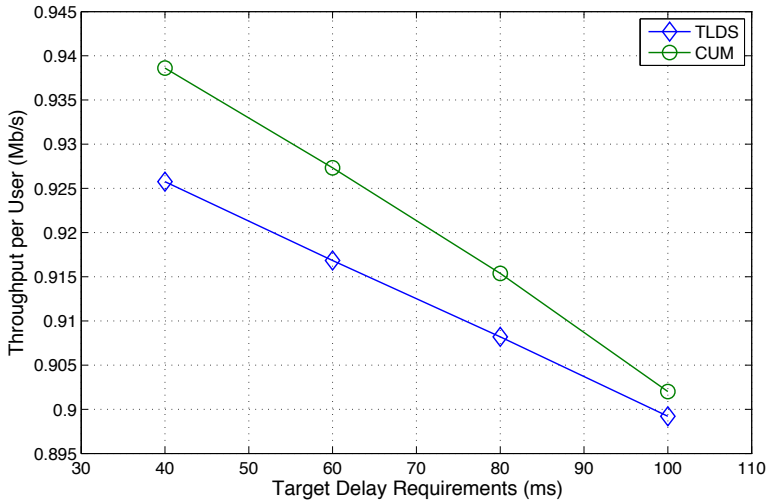

Figure 3.11: Comparison of Throughput per User.

3.4.2.3 Throughput per User

Fig. 3.11 shows the throughput per user for both scheduling schemes with different delay requirements. It can be seen that, when the delay requirement is 40ms, the proposed CUM scheme outperforms TLDS. However, the gain gradually decreases as the delay requirement increases. This change can be explained as follows. Adapting transmission quota for HoL in resource allocation yields the better fairness for poor channel quality users at the expense of system efficiency. To relieve this drawback, a Cross-CC user migration scheduler is developed in CUM scheme to achieve high throughput per user. However, the benefit is reduced with the increase of the target delay requirements, because the larger value of M_i is defined in Eq. (3.2) for the lower delay demand and it will lead to the lower transmission quota as calculated in Eq. (3.9). As a consequence, less migration process will be implemented, which results in the lower throughput per user.

3.5 Summary

This chapter has investigated QoS-aware resource allocation for LTE-A system with CA, taking into account the system efficiency, user fairness and QoS requirements. We have proposed a novel resource allocation algorithm that consists of three components to efficiently and dynamically allocate radio resources to users, enabling LTE-A system to achieve an improvement in real-time service provisioning and keep backward compatible to LTE systems. The simulation results have demonstrated that the proposed scheduling scheme outperformed the well-known Two-Level downlink scheduling scheme in terms of the packet loss probability, average queue length and throughput per user.

Chapter 4

Performance Modelling of Preemption-based Packet Scheduling for Data Plane in Software Defined Networks

4.1 Introduction

Software Defined Networking (SDN) is proposed with the aim of simplifying network management and improving service flexibility and has attracted considerable research interests [93][94][95][91][90][126]. However, with the migration of the network logic from data plane to SDN centralised controller, existing studies always assume that network switches should become as simple as possible and adopts First In First Out (FIFO) scheme in data plane to process the arrival packets. Although, FIFO has been widely considered an effective approach [18], it incurs serious issues of low global fairness and performance degradation in SDN paradigm, due to the inherent feature-feedback control loop between data plane and control plane of SDN networks.

To address this problem, this chapter presents a Preemption-based Packet-Scheduling (P^2S) scheme to improve the global fairness and reduce the packet loss rate in SDN data plane. Different from equally processing the feedback packets from SDN controller and those from other forwarding devices, P^2S offers the high priority to the packets arriving from the SDN controller for resource scheduling in the data plane. In order to quantitatively investigate the performance of P^2S, an analytical model is developed to capture the loop control, limited buffer resource, and preemption features of the P^2S scheme. The developed model is further leveraged to analyse and pinpoint the performance bottleneck of the SDN architecture. Both theoretical analysis and simulation experiments are conducted to demonstrate that this preemption-based scheduling scheme can achieve the better system performance compared to the traditional data plane packet scheduling in terms of global fairness index and packet loss probability.

The rest of this chapter is organised as follows. Section 4.2 presents the details of the P^2S scheme. An analytical model is developed in Section 4.3 to investigate the quantitative performance of P^2S scheme. Section 4.4 presents extensive simulation experiments to evaluate the performance of the P^2S scheme and validate the accuracy of the proposed analytical model. In Section 4.5, the performance analysis of SDN architecture is carried out and feasible solutions are provided based on the developed model. Finally, Section 4.6 concludes this chapter.

4.2 Preemption-based Packet Scheduling (P^2S) in SDN networks

This section will firstly describe the working mechanism of SDN and then present the motivation and design details of the P^2S scheme. The parameters used in this chapter are listed in Table 4.1.

Table 4.1: Key Notations Used in the Derivation of the Model in Chapter 4

T_i	The time when the ith packet arrives at the queue
λ_{in}	The arrival rate of the low priority queue
λ_{up}	The arrival rate of uplink queue
λ_{ctr}	The arrival rate of SDN controller
λ_{down}	The arrival rate of downlink queue
λ_h	The arrival rate of the high priority queue
μ_s	The service rate of SDN switch
μ_c	The service rate of SDN controller
W_{tot}	The end-to-end average waiting time
W_h	The average waiting time in the high priority queue
W_l	The average waiting time in the low priority queue
P_{hit}	The hitting probability of the flow table
W_{up}	The average waiting time in the uplink queue
W_{ctr}	The average waiting time in the queue of SDN controller
W_{down}	The average waiting time in the downlink queue
$W_{tot}^{P^2S}$	The end-to-end average waiting time for PQ scheduling
λ_{ctr}^{eff}	The effective arrival rate for SDN controller
P_k	The probability that there are k packets in the queueing system
w_r	The residual time of the packets in service
w_d	The delay experienced by the packets in the low and high priority queue
w_a	The Additional waiting time caused by the high priority queue for the packets in the low priority queue

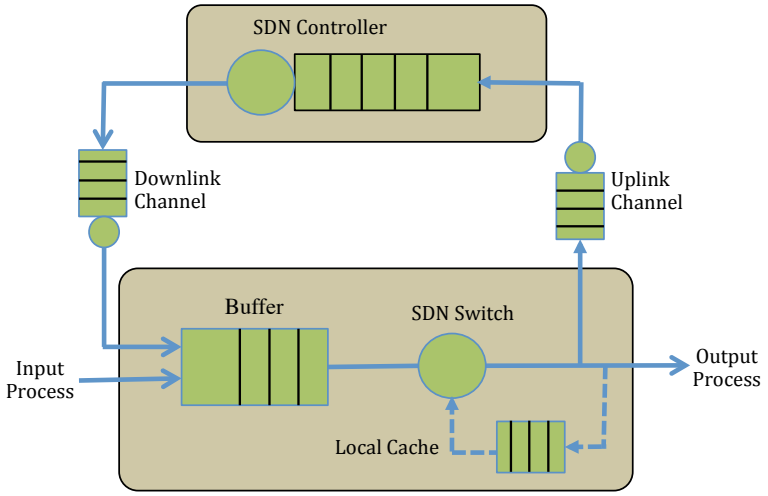

Figure 4.1: SDN Architecture with FIFO Scheme

4.2.1 Packet Scheduling in SDN networks

This study focuses on the data plane in SDN architecture, as shown in Figure 4.1. This architecture operates as follows [45]: When a packet arrives at SDN switch, it will wait in the queue for service if the switch server is busy. Once the server becomes idle, the first packet in the buffer is popped out and transferred to switch server. Each server keeps a flow table to store, retrieve and modify routing information. A flow table consists of multiple flow entry, each of which has three fields: match, action and statistic. If the server holds the corresponding flow entry in the flow table, this packet will be served according to the action field of the matching flow entry. If the packet fails to match any entry in the flow table, the switch server sends the whole or partial package (i.e., the packet header) to the SDN controller through the uplink channel, in order to consult how to process the unmatched packet. When the partial transmission strategy is adopted, the unmatched packet is stored in the local cache and waits for the reply message from the SDN controller. Once SDN controller receives the request message from SDN switches, based on a series of routing and forwarding calculations, it will generate a response message and send it out through the downlink channel. When the switch receives the response message, it stores the routing information in the flow table and processes the packet according to the action field. Herein, during the whole process, a packet that fails to match entries in the flow table has to traverse the switch server twice.

4.2.2 Preemption-based Packet Scheduling

In the SDN network architecture, due to the existence of feedback control loop, there are two types of packets arriving at the data plane: the packets from other forwarding devices and the packets coming from SDN controller. To simplify the forwarding device, most of the existing studies adopt simple FIFO scheme [18] to forward packets in data plane.

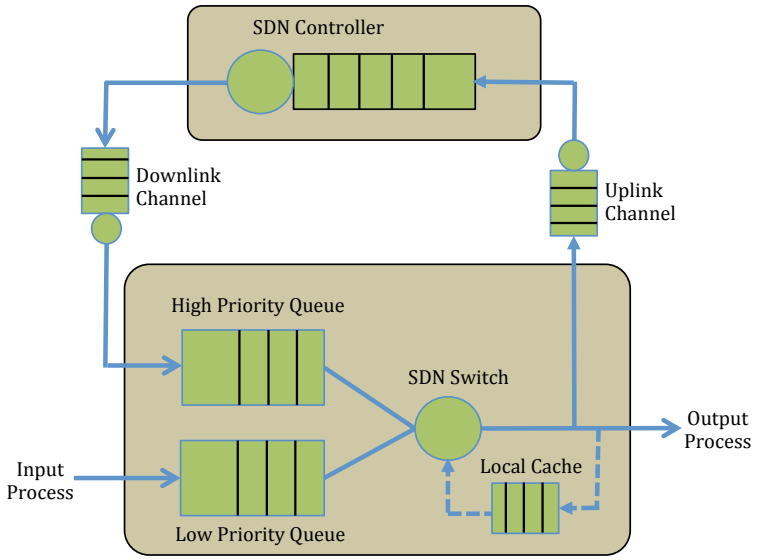

Figure 4.2: SDN Architecture with P^{2}S Scheme

This can be described as follows:

$$I = max\{t - T_i\} \tag{4.1}$$

where t is the current time and T_i is the time when the ith packet enters into the waiting queue. FIFO scheduling scheme as shown in Fig. 4.1 serves the packet with the longest waiting time, I, in the queue system. However, the packets coming from the SDN controller often encounter serious unfairness. As described in the above SDN working mechanism, the packet miss-matching the flow entry in the flow table is sent to or partially sent to the SDN controller. When the replied package arrives at SDN switch, this packet has to be buffered in the queue of data plane and competes with the newly arriving packets for the forwarding service. Therefore, FIFO can hardly provide the global fairness for packet scheduling in SDN, and thus leads to high packet loss probability. In order to avoid these performance degradations, the packets from SDN controller should be given an extra priority in data plane packet processing. Herein, P^{2}S scheme achieves this objective by differentiating the packets from the neighbouring forwarding devices and SDN

controller. To this end, two types of queues are designed in the data plane as shown in Fig. 4.2: high priority queue and low priority queue. Packets coming from the SDN controller enter into the high priority queue. The new packets arriving from the neighbouring forwarding devices enter into the low priority queue. The packets in the high priority queue preemptively have the priority for receiving the service and the packets belonging to the low priority queue can only be served when the high priority queue is empty. As a result, the packet feedback from SDN controller is served with the strict high priority and the residual service is provided to the low priority queue. In consideration of the SDN data plane, uplink channel, SDN control plane and downlink channel as a whole system, the preemption mechanism achieves the better global fairness for the packets. In order to obtain the quantitative performance metrics of this preemption-based packet scheduling, an analytical model will be derived in the next session.

4.3 Analytical modelling

The traffic model plays an important role in analysing the performance of packet scheduling techniques [19]. We therefore consider a dynamic model with Poisson arrivals. The arrival and departure of packets in the system are modelled as a birth-death process. This process is a special case of continuous-time Markov process, where the states represent the current number of packets in the system, and the transitions occur between neighbouring states. The "birth" is the transition towards increasing the number of the packets in the system by 1, and a "death" is the transition towards decreasing the number of the packets in the system by 1 [18].

In SDN paradigm, the service modes of data plane, uplink channel and downlink channel follow $M/M/1$ process [127], where M means Markov process; the service model in the control plane follows $M/M/1/K$ process where K represents the maximum number of

packets that can be accommodated in the SDN controller, which demonstrates the process of the admission control in SDN networks. The packet arrivals follow a Poisson distribution, and the service time follows a negative exponential distribution. The following notations are used to derive the analytical model: λ_l, λ_{up}, λ_{ctr}, λ_{down} and λ_h denote the arrival rates of the low priority queue, uplink channel, SDN controller, downlink channel and the high priority queue; Denote the arrival rate for the SDN switch as λ_l, as the packets arriving the SDN switches will enter the low priority queue, therefore $\lambda_l = \lambda_{in}$; μ_s and μ_c denote the service rates of SDN switch and controller respectively. L is the average number of packets in the queue; W_{tot} is the average end-to-end latency; W_h and W_l are the average waiting times of packets in the high and low priority queues, respectively.

In what follows, the end-to-end system performance of SDN architecture with P^{2}S scheme is investigated. When a packet is served by switch server, it may fail to match the flow table and need to be cached in the local storage. Therefore, the end-to-end latency, W_{tot}, consists of two parts and can be described as follows:

$$W_{tot} = W_{hit} * P_{hit} + W_{miss} * (1 - P_{hit}) \tag{4.2}$$

where W_{hit} and W_{miss} are the average latency experienced by an arrival packet when it matches or misses the flow entry. P_{hit} is the probability that a packet finds its corresponding flow entry in the flow table. Within the P^{2}S scheme, the traffic belonging to the low priority queue can be served only when the high priority queue is empty. Let W_l and W_h denote the average latency that a packet experiences in the low and high priority queues. Eq. (4.2) can be re-written as:

$$W_{tot}^{\mathrm{P^2S}} = W_l * P_{hit} + (W_l + W_{up} + W_{ctr} + W_{down} + W_h) * (1 - P_{hit}) \tag{4.3}$$

According to the working mechanism of SDN, the effective traffic entering the queuing system of the uplink channel is a fraction, $1-P_{hit}$, of the traffic generated by the other SDN switches [19]. Let λ_{in} represent the traffic entering the data plane from other SDN switches; as the splitting of a Poisson process is again a new Poisson process, λ_{up} (the traffic rate entering the uplink channel queue) can be obtained by splitting λ_{in} with the probability $1-P_{hit}$ and can be written as $\lambda_{up} = \lambda_{in} * (1-P_{hit}) * (1-P_l)$. As the buffer size of the uplink channel is infinite, the rate of traffic, λ_{ctr}, entering the queue of SDN controller is equal to λ_{up}. The buffer size of the SDN controller is K. The new arrival requests may be dropped when the queue is full. Let P_c denote the probability that a packet is lost in SDN controller, the effective traffic entering SDN controller queue is indicated by $\lambda_{ctr}^{eff} = \lambda_{ctr} * (1-P_c)$ [14]. Similar to the uplink case, the traffic rate for the downlink channel and the high priority queue are denoted as $\lambda_h = \lambda_{down} = \lambda_{ctr}^{eff}$.

To determine P_c for calculating the effective traffic entering the SDN controller, let us first calculate the probability that there are k packets in the queue, given by [128]:

$$P_k = \begin{cases} P_0 \prod_{i=0}^{k-1} \frac{\lambda_i}{\mu_{i+1}}, & if \quad 1 \leq k \leq K \\ 0, & if \quad K < k \end{cases} \tag{4.4}$$

where P_0 is the probability that there is no packet in the queue system, and $\sum_{i=0}^{K} P_i = 1$. Then P_0 is calculated by

$$P_0 = \left(1 + \sum_{k=1}^{K} \prod_{i=1}^{k} (\frac{\lambda_i}{\mu_{i+1}})\right)^{-1} \tag{4.5}$$

Inserting Eq. (4.5) into Eq. (4.4) and setting $k = K$, then the probability P_c that an

arriving packet finds the finite buffer full can be written as

$$P_c = P_K \tag{4.6}$$

Given the service rates of the uplink channel, the SDN controller and the downlink channel, μ_{up}, μ_{ctr} and μ_{down}, the average latency of the uplink channel, the SDN controller and the downlink channel, W_{up}, W_{ctr} and W_{down}, can be derived through the following equation [70]:

$$W = 1/(\mu - \lambda) \tag{4.7}$$

After obtaining W_{up}, W_{ctr} and W_{down}, the difficulty to derive the end-to-end latency, $W_{tot}^{\mathrm{P^2S}}$, is transferred to calculate W_h and W_l. Within the P^{2}S scheme, the packets belonging to the high priority queue have the absolute priority to be served by SDN switch. Therefore, the service rate for the high priority packet, μ_h, is equal to that of the SDN switch, μ_s. The arrival rate of the high priority queue is $\lambda_h = \lambda_{in} * (1 - P_{hit}) * (1 - P_c)$. W_h can be easily obtained through Eq. (4.7). In order to derive W_l, let us mark an arrival packet from other SDN switches and calculate the time it has to wait before starting service in the switch server. The delay can be represented as the sum of three components: the residual time of the packet found in service, w_r; the delay experienced by the packet in the low and high priority queues, w_d; and the additional waiting time caused by the high priority packets arriving when the marked packet is waiting in the low priority queue, w_a. W_l can be written as

$$W_l = w_r + w_d + w_a \tag{4.8}$$

Based on the utilisation law [70], w_r is given by

$$w_r = \frac{\lambda_{in} + \lambda_h}{\mu_s^2} \tag{4.9}$$

When the tagged packet arrives at the low priority queue, it may see that there are L_l packets in the low priority and L_h packets in the high priority. Each packet takes an average time $1/\mu_s$ to be served. Applying the Little Law, the average waiting time, w_d, is

$$w_d = \frac{W_l * \lambda_{in} + W_h * \lambda_h}{\mu_s} \tag{4.10}$$

In addition, the number of packets arriving at the high priority queue when the tag packet is waiting in the low queue for service, is $W_l * \lambda_h$. Then, w_a can be described as

$$w_a = \frac{W_l * \lambda_h}{\mu_s} \tag{4.11}$$

Inserting Eqs. (4.9)-(4.10) into Eq. (4.11) and after a series of calculation, the average latency experienced by a packet in the low queue, W_l, is given by

$$W_l = \frac{\lambda_{in} + \lambda_h + \lambda_h W_h \mu_s}{\mu_s(\mu_s - \lambda_{in} - \lambda_h)} \tag{4.12}$$

Inserting Eq. (4.12) into Eq. 4.3, we can obtain the average packet latency with the P^{2}S scheme.

4.4 Performance Comparison and Model Validation

The performance of the P^{2}S scheme is evaluated through developing and conducting a discrete-event SDN simulator in Objective Modular Network Testbed in C++ (OM-

NeT++) [129]. The buffer size at SDN controller, K, is set to be 10 to reflect the access control in SDN controller. The transmission rates of the uplink and downlink channel, λ_{up} and λ_{down} are set to 100 packets per second. The packets arriving at the data plane are characterised by a Poisson process. The service time follows a negative exponential distribution. In the following subsections, we firstly evaluate the performance of the P^2S scheme compared to the traditional FIFO scheme in terms of packet loss probability and service fairness. Then the accuracy of the developed analytical models is validated through varying the arrival packet rate, the hit probability of the flow table, and the switch and controller service rates.

4.4.1 Performance Comparison between P^2S and FIFO schemes

4.4.1.1 Global Fairness Index

In this part, the well-known Jain's fairness index [130] is used to evaluate the global fairness of the two packet scheduling schemes in the SDN data plane. From Fig. 4.3, we can see that P^2S can improve the fairness index over FIFO. When the heavy traffic arrives at the SDN controller and switch and if the hit probability is low, the forwarding service of P^2S have the better global fairness. The reason for the poor performance of FIFO as compared to P^2S can be explained as follows: In the FIFO scheduling scheme, the packets that have failed to match the flow table need enter the same queue for service. Overall, these packets experience much higher delay because of the feedback loop of the uplink channel, SDN controller and downlink channel. In FIFO, the switch treats the packets from the SDN controller equally with the packets from other switches, these packets from the SDN controller experience the longer overall delay. As a result, FIFO cannot guarantee the fairness among packets and also result in a serious issue of high packet loss probability in data plane. P^2S scheme offers priority for the packets from SDN controller

and thus achieves the better better performance in terms of both the global fairness index and packet loss probability.

In order to elaborate the aforementioned performance improvement clearly, the average latencies of packets matched and failed in the flow table are both showed in Fig. 4.4. It can be seen that the average latency of both the packets missing the flow entry in P^{2}S is lower than those in FIFO and the average latency of packets matching in the flow entry in P^{2}S is higher than those in FIFO. The results demonstrate that P^{2}S sacrifices the performance of the packets from other SDN switches and can improve the service of the packets that have experienced serious delay in control plane.

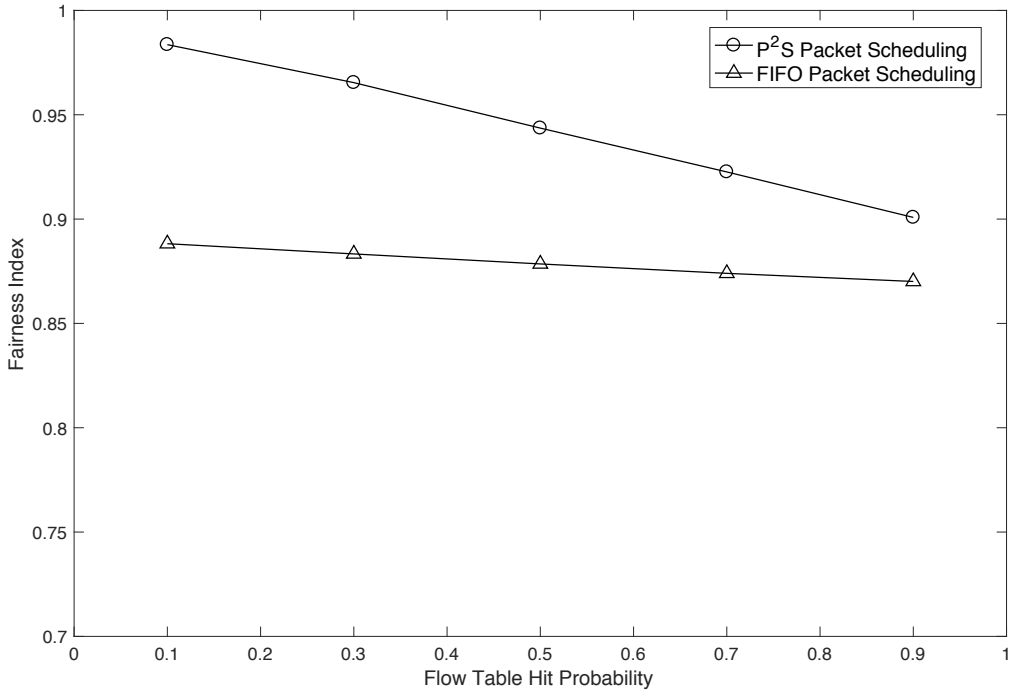

Figure 4.3: Fairness Index of P^{2}S and FIFO with Different Hit Probabilities in Flow Table

4.4.1.2 Packet Loss Probability

The relative gain in packet loss probability by using P^{2}S over FIFO is shown in Fig. 4.5, with different packet hit probabilities in the flow table. P_{hit} varies from 0 to 1. When P_{hit} is set to 1, each newly arrived packet can find the corresponding flow entry in the

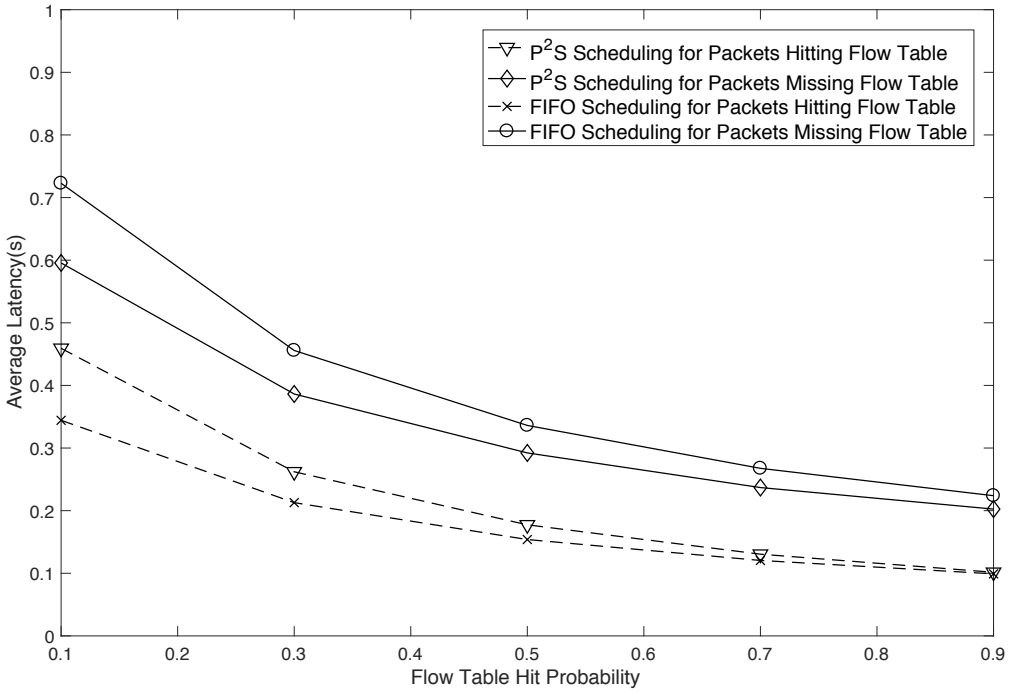

Figure 4.4: Average Latency of Packets Hitting and Failing in Matching the Flow Table of P^{2}S and FIFO

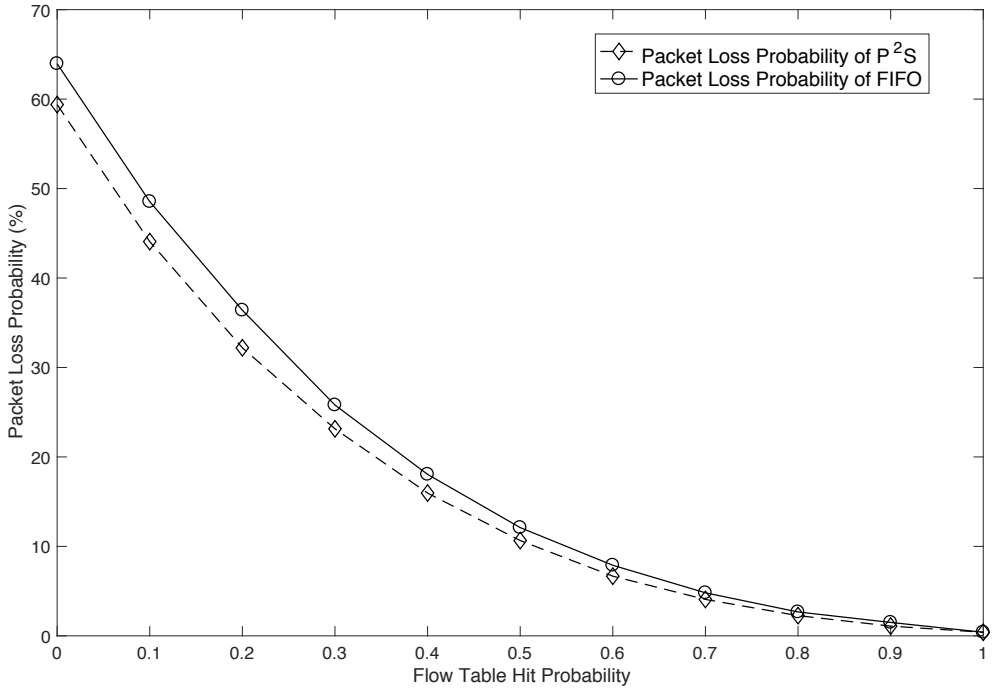

Figure 4.5: Packet Loss Probability of P^{2}S and FIFO with Different Hit Probability of Flow Table

flow table, without the need of the loop communication with control plane. When P_{hit} is set to be 0, the flow table is empty and SDN is in the initial state. The header of the

newly arrived packet will be abstracted and sent to controller for requesting the forwarding policy. When the forwarding policy is replied back to data plane, SDN switch inserts the forwarding policy into the flow table. So P^2S provides these packets the priority in switch server and achieves the lower packet loss probability. In addition, the average packet loss probability drops dramatically as the hit probability increases. This is because, increasing the hit probability results in less packets to be sent back to the SDN controller. More packets can be directly forwarded to the next hop and experience less packet latency, leading to the lower packet loss probability. When $P_{hit} = 1$, all packets can find the flow entries in the flow table and the packet loss probability reaches the lowest value.

4.4.2 Validation of the Analytical Model

From the above discussion, we have seen that the P^2S scheme offers the better performance than FIFO. In this part, the developed analytical model is validated by varying the traffic arrival rate, flow table hit probability and the service rates of the SDN switch.

4.4.2.1 Effects of Flow-entry Hit Probability

In order to achieve a comprehensive and accurate performance comparison, the service rate of the SDN switch and controller, μ_c and μ_s, are considered for three different cases to investigate the effects of the hit probability on average latency: Case (I) $\mu_c > \mu_s$ ($\mu_c = 40$, $\mu_s = 20$); case (II) $\mu_c = \mu_s = 30$; and case (III) $\mu_c < \mu_s$ ($\mu_c = 20$, $\mu_s = 40$); The figures reveal a good match between the analytical and simulation results, therefore giving confidence in the accuracy of the proposed model. Fig. 4.6 shows that the analytical results predicted by the model are very accurate at most cases. However, some discrepancies exist between the model and simulation results in Case (I). This is because the input of the uplink channel is a fraction of output process and is modelled as Poisson process. This approximation is taken in most cases except when most packets are forwarded to the SDN

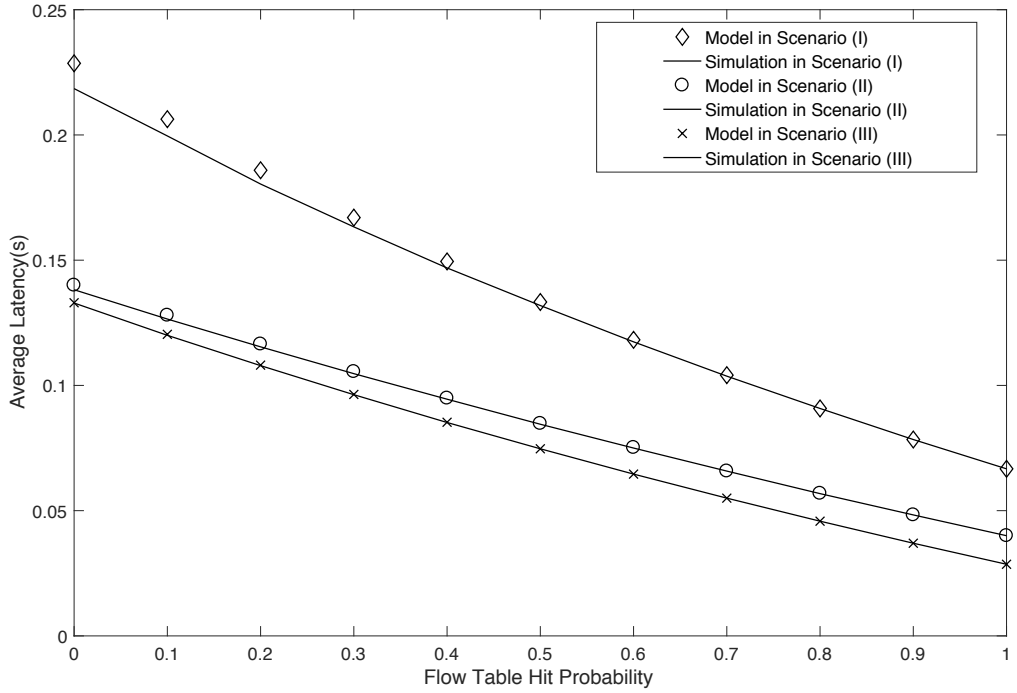

Figure 4.6: Average Latency Predicted by the Model and Simulation with Different Hit Probability of Flow Table

controller and the arrival rate of the input traffic is approaching to that of the switch. Nevertheless, the extensive comparison between the analytical results and those obtained from simulation experiments reveals that the model possesses an acceptable level of accuracy, and its tractability makes it a practical and cost-effective evaluation tool.

4.4.2.2 Effects of Traffic Arrival Rate and Service Rate of SDN Switch

Figs. 4.7 and 4.8 depict the analytical results predicted by the model against those provided by the simulation experiments in SDN networks. In these figures, the horizontal axis represents the traffic rate, λ_{in} and the service rate of SDN switch, μ_s, respectively. The vertical axis denotes the latency obtained from the developed model and simulator. The figures reveal that the results obtained from the analytical model closely match those from the simulation experiments.

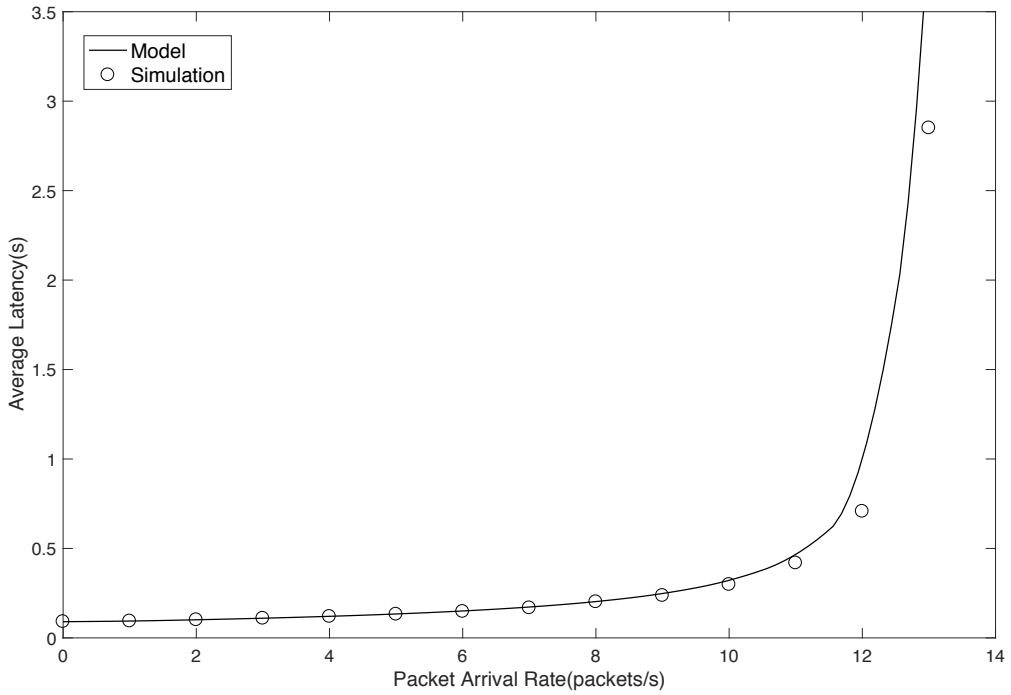

Figure 4.7: Average Latency Predicted by the Model and Simulation with Different Traffic Arrival Rate

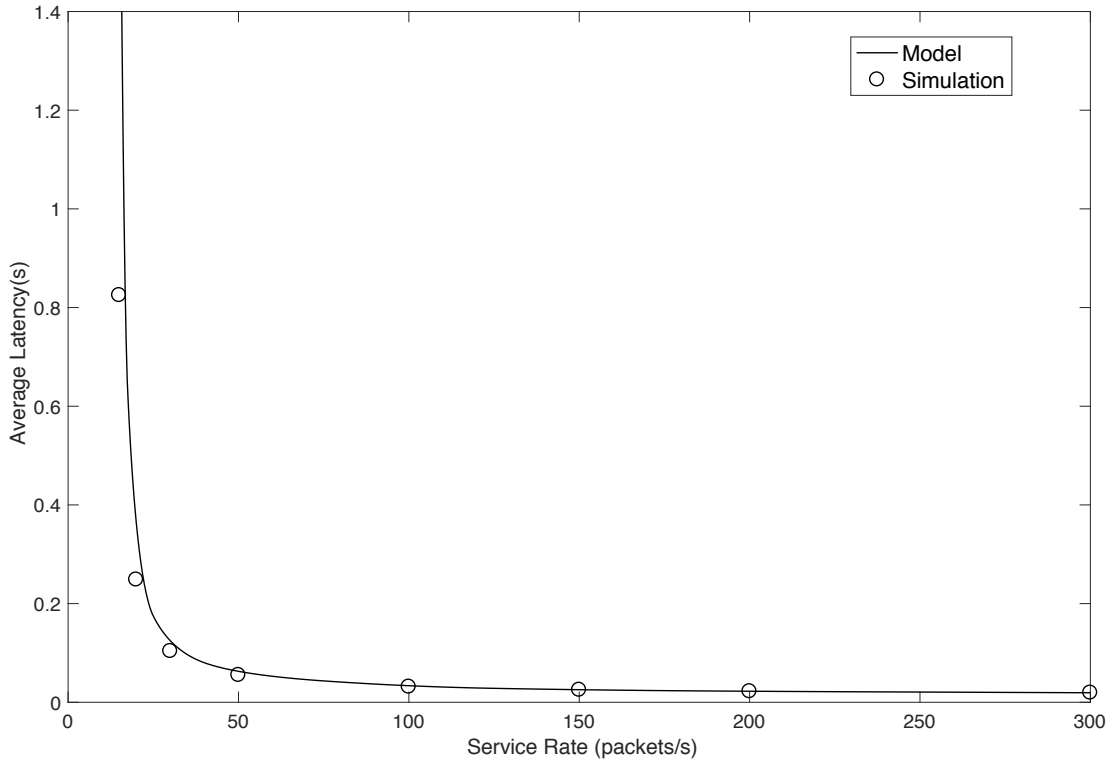

Figure 4.8: Average Latency Predicted by the Model and Simulation with Different Service Rate of SDN Switch

4.5 Applications of the Analytical Model

In this section, we will use the developed analytical mode to investigate the performance of the SDN networks. The traffic feedback to the SDN controller is affected by the flow table hit probability, P_{hit}. Increasing P_{hit} from 0 to 1 indicates that more forwarding policies are inserted into the flow table. Eq. (4.4) can be written as

$$W_{tot} = W_{miss} + (W_{hit} - W_{miss}) * P_{hit} \tag{4.13}$$

From Eq. (4.5), $W_{miss} > W_{hit}$, therefore, the average latency, W_{tot} is a decreasing function of the hit probability, P_{hit}. Therefore, the increment of the hit probability results in the lower average latency. As shown in Fig. 4, the average delay is the highest with $P_{hit} = 0$ and lowest with $P_{hit} = 1$. The above results reveal that SDN centralised control indeed introduces serious packet forwarding delay compared to the traditional network architecture.

In order to avoid the negative effects of SDN architecture on scalability [131], according to the description in Section 4.3, we should increase the flow table hit probability to reduce the number of packets feedback to the SDN controller. Therefore, in the practical deployment of SDN networks, in order to avoid the disruptive degradation in Quality-of-Service (QoS), the flow table of SDN switches can be filled by the flow entries copied from traditional network devices through building the communication of the SDN controller and traditional network management platform. Given the quantitative relationship between the resource provisioning and the performance results, the analytical model can be used as a useful analytical tool in the SDN network plan and deployment.

4.6 Summary

In this chapter, we have investigated the working mechanism of SDN architecture and presented a P^2S scheme to enhance the global fairness index and reduce the packet loss probability. P^2S offers the high priority to the packets that fail to match any entry in the flow table in order to reduce the packet delay, increase the global fairness index, and reduce the packet loss probability. In addition, a new analytical model for predicting the packet latency has been developed to achieve quantitative performance evaluation of the P^2S scheme. Extensive simulation experiments have been conducted to validate the accuracy of the analytical model. The performance results can reveal the quantitative relationship between the given system resources and the achievable QoS and thus can be used in the stages of SDN network plan and deployment.

Chapter 5

Performance Modelling and Analysis of Software Defined Networking under Bursty Multimedia Traffic

5.1 Introduction

Software Defined Networking (SDN) is an emerging architecture for the next-generation Internet, providing unprecedented network programmability to handle the explosive growth of Big Data driven by the popularisation of smart mobile devices and the pervasiveness of content-rich multimedia applications. In order to quantitatively investigate the performance characteristics of SDN networks, several research efforts from both simulation experiments and analytical modelling have been reported in the current literature. Among those studies, analytical modelling has demonstrated its superiority in terms of cost-effectiveness in the evaluation of large-scale networks. However, for analytical tractability and simplification, existing analytical models are derived based on the unrealistic assumptions that the network traffic follows the Poisson process which is suitable to model non-bursty text data and the data plane of SDN is modelled by one simplified

Single-Server-Single-Queue (SSSQ) system. Recent measurement studies have shown that, due to the features of heavy volume and high velocity, the multimedia big data generated by real-world multimedia applications reveals the bursty and correlated nature in the network transmission. With the aim of the capturing such features of realistic traffic patterns and obtaining a comprehensive and deeper understanding of the performance behaviour of SDN networks, this chapter presents a new analytical model to investigate the performance of SDN in the presence of the bursty and correlated arrivals modelled by Markov Modulated Poisson Process (MMPP). The Quality of Service (QoS) performance metrics in terms of the average latency and average network throughput of the SDN networks are derived based on the developed analytical model. To consider realistic multi-queue system of forwarding elements, Priority Queueing (PQ) system is adopted to model SDN data plane. To address the challenging problem of obtaining the key performance metrics, e.g., queue length distribution of PQ system with a given service capacity, a versatile methodology extending the Empty Buffer Approximation (EBA) method [132] is proposed to facilitate the decomposition of such a PQ system to two SSSQ systems. The validity of the proposed model is demonstrated through extensive simulation experiments. To illustrate its application, the developed model is then utilised to study the strategy of the network configuration and resource allocation in SDN networks.

The rest of this chapter is organised as follows: Section 5.2 illustrates the working principle of the PQ-based SDN architecture. Section 5.3 derives the comprehensive analytical model to investigate the average latency and network throughput of SDN networks subject to bursty and correlated traffic. The accuracy of the developed model is validated in Section 5.4 through extensive simulation experiments. Section 5.5 adopts the developed model to conduct the performance analysis of SDN architecture. Finally, Section 5.6 concludes this study.

5.2 Priority-Queue based SDN Architecture

This study focuses on the SDN architecture with the PQ system in the data plane, as illustrated in Fig. 5.1. The PQ system consists of two types of queues: the low priority queue and the high priority queue. The packets transmitted from the SDN controller enter the high priority queue and those arriving from the neighbouring forwarding devices enter the low priority queue. During the packet scheduling, the packets in the high priority queue have the priority for receiving the service and the packets belonging to the low priority queue can only receive service when there is no packet in the high priority queue. According to the system design in [133], the buffer sizes of the high priority queue, Uplink Channel (UC) queue and Downlink Channel (DC) queue, are considered to be infinite, and the buffer sizes of the SDN controller and the low priority queue are set to be finite, denoted by K_c and K_l, respectively. According to [134], the working mechanism of the PQ-based SDN system architecture is as follows: when arriving at the SDN switch, the packet waits in the low priority queue for service if the buffer is not fully occupied and the Switch Server (SS) is busy. Once the SS becomes idle and there is no packet in the high priority queue, the first packet in the low priority queue is popped out and transferred to the SS. If the flow table in the switch holds the corresponding entry, this packet will be served immediately according to the action field of the matching flow entry. Otherwise, if the packet does not match any entry in the flow table, the switch needs to send the whole or partial package (i.e., the packet header) to the SDN controller through the UC to consult how to process the unmatched packet. When the partial transmission strategy is adopted, the unmatched packet is stored in the local cache and waits for the response message from the SDN controller. Once receiving the request message from SDN switches, the controller generates a response message based on a series of routing and forwarding calculations and sends the result out through the DC. When arriving at the SDN switch,

the packets of the response message enter the high priority queue if the SS is busy. Once the SS becomes idle, the first packet in the high priority queue is forwarded to the SS. When receiving the response message, the SDN switch stores the routing information as the entries of the flow table and leverages the action field of the entry to process the packet. Herein, during the whole process, the packet that fails to match the entries of the flow table has to traverse the SS twice. The parameters of the derivation of the analytical model are listed in Table 5.1.

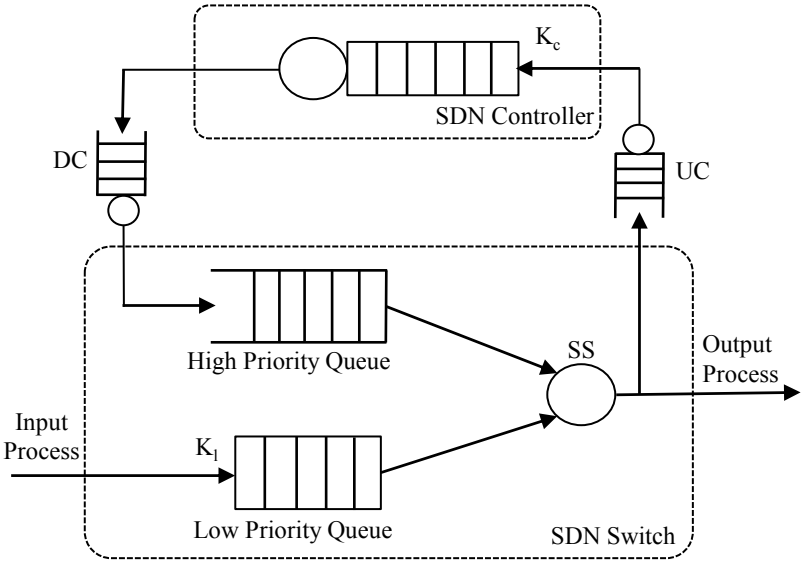

Figure 5.1: The PQ-based SDN System Architecture

Table 5.1: Key Notation Used in the Derivation of the Model in Chapter 5

K_c	The buffer size of the SDN controller
K_l	The buffer size of the low priority queue
$Latency$	The average latency in the SDN architecture
Lat_{hit}	The average latency for the packets hitting the flow table
Lat_{miss}	The average latency for the packets missing the flow table
ξ	The hitting probability of flow table
D_l, D_h	The average delay in the low and high priority queues
D_u, D_d	The average delay in the uplink and downlink channels
D_c	The average delay in the SDN controller

$T_{a,i}$	The interarrival time between the ith and $(i+1)th$ packets arriving at the PQ system
$T_{d,i}$	The interdeparture time between the ith and $(i+1)th$ packets arriving at the PQ system
$T_{s,i}$	The time of the ith packet spending at the PQ system
μ_l	The service rate of the low priority server
μ_h	The service rate of the high priority server
μ_s	The service rate of the SDN switch
L_l	The average number of packets in the $SSSQ_l$
L_h	The average number of packets in the $SSSQ_h$
L_t	The average number of packets in the PQ system
Q_i, Λ_i	The infinitesimal generator matrix and the arrival rate matrix of the $MMPP_i$ input traffic
l_i	The average queue length of $SSSQ_l$
$l_i^{(1)}$	The first moment of l_i
ζ	The stop condition of the recursion loop
Pb_l	The probability that an arriving packet finds $MMPP_{in}/M/1/K_l$ full
$MMPP_l^{in\to e}$	The effective traffic entering the low priority queue
$Q_l^{in\to e}$, $\Lambda_l^{in\to e}$	The infinitesimal generation and rate matrix of $MMPP_l^{in\to e}$
$\mathbf{P}$	The steady-state probability vector of $MMPP$
$min\{\mathbf{Z}(\rho,\rho)\}$	The minimum number in the diagonal line of the matrix $\mathbf{Z}$
$\dot{P}_n$	The probability that an arriving packet observes there are n packets in the $SSSQ_l$ system
$E\left[T_{d,i}\right]$ and $E\left[T_{d,i}^3\right]$	The first moment and the third moment of the interdeparture time
$c^2(T_{d,i})$	The squared coefficient variation of the interdeparture time
$Cov(T_{d,i}, T_{d,(i+1)})$	The covariance of two successive interdeparture times
$L(s)$	The Laplace-Stieltjes transform of the service time distribution
x_k	The stationary probability that the number of the packets in the system is k
$\tilde{A}_{,k}(x)$	The probability that when a departure happens there is at least one packet in the system
$P(k,x)$	The probability that there are k packets arriving at the system during the length of x time
$P(z,x)$	The z transformation of $P(k,x)$
$\tilde{L}(x)$	The cumulative distribution function of exponential distribution

f_m	The miss probability of the flow table
$MMPP_u^{out}$	The output process of the UC queue
Q_u^{in} and Λ_u^{in}	The infinitesimal generator and the rate matrix of $MMPP_u^{in}$
m_j	The mean arrival rate, $E\left[T_{a,j}\right]$
v_j	The second moment, $E\left[T_{a,j}^2\right]$
p_j	The third moment, $E\left[T_{a,j}^3\right]$
$r_j(t)$	The covariance function, $Cov(T_{a,j}, T_{a,(j+1)})$
$\tau_{,j}$	The time constant of the $MMPP_j$ process
$MMPP'_t$	The approximate of the $MMPP_t$
h_i and $h_i^{(2)}$	The mean and the second moment of the service time

5.3 Derivation of the Analytical Model

The average latency in the SDN architecture can be obtained by the weighted sum of the packet latencies, Lat_{hit} if the packet hits the entry of the flow table, and Lat_{miss} if the packet misses the flow entry. The packet arriving at the SDN switch can successfully find the flow entry in the flow table with the probability, ξ. Then, the average latency, $Latency$, can be written as follows:

$$Latency = \xi Lat_{hit} + (1-\xi) Lat_{miss} \tag{5.1}$$

Based on the system description in Section 5.2, Lat_{hit} and Lat_{miss} are given by

$$Lat_{hit} = D_l \tag{5.2}$$

$$Lat_{miss} = D_l + D_u + D_c + D_d + D_h \tag{5.3}$$

where D_l, D_u, D_c, D_d, and D_h are the average delay in the low priority queue, the UC

queue, the controller queue, the DC queue and the high priority queue, respectively.

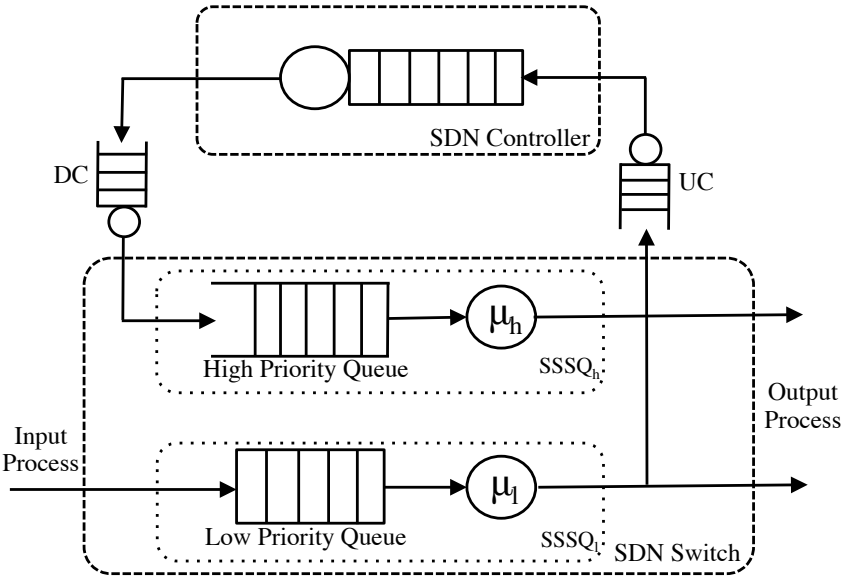

Figure 5.2: Decomposition of a PQ System to Two SSSQ Systems in SDN Forwarding Devices

Directly deriving these values is intractable under the input of MMPPs because it is difficult to calculate the additional delay for the packets in the low priority queue due to the ones in the high priority queue. In order to address this issue, inspired by the well-known Kleinrock's independence approximation [29], a novel queueing decomposition approach is developed in this study to transform a PQ system into two SSSQ systems. Therefore, instead of directly modelling the complex PQ system subject to bursty traffic, the task of the performance evaluation of SDN architecture is achieved by analysing the two but relatively simple systems, $SSSQ_l$ and $SSSQ_h$ as shown in Fig. 5.2. There have been a few publications that appeared in the literature to investigate the queueing decomposition. For instance, Jin. et al. in [135] proposed a method that can achieve the service rates of the two queues for the decomposed SSSQ system with the input of fractional Brownian motion (FBM) traffic. Liu et al. in [24] further extended the decomposition method from the traffic of FBM to MMPP. These studies adopted EBA method [136] and, for analytical tractability, assumed that the high priority queue has the negligible impact

on the overall queue length of the PQ system and concluded that the overall queue length of the PQ system is almost exclusively formed by the queue length of the low priority queue. As a result, the queue length distribution of the PQ system can be approximated as that of the low priority queue. Although high accuracy is achieved by these studies when the low priority queue is poured by heavy traffic and high priority queue by light traffic, they can hardly capture the comprehensive performance evaluation of the PQ system under various traffic load conditions, especially for the case of the overloaded traffic in the high priority queue. In order to bridge this gap, an enhanced EBA approach is proposed and described in the following section.

5.3.1 Decomposition of the Priority Queue System

In order to successfully decompose a PQ system into two SSSQ systems, let us firstly analyse the relationship among the interdeparture time, the interarrival time and the sojourn time. Let $T_{a,i}$ (the subscript a represents the arrival process) denote the interarrival time between the ith and $(i+1)th$ packets arriving at the PQ system. Let $T_{d,i}$ (the subscript d represents the departure process) denote the interdeparture time between ith and $(i+1)th$ packets leaving the PQ system. Let $T_{s,i}$ and $T_{s,(i+1)}$ (the subscript s denotes the sojourn process) be the time of the ith and $(i+1)th$ packets spending at the PQ system, which includes queueing time and serving time. After simple derivation, the relationship among $T_{a,i}$, $T_{d,i}$ and $T_{s,i}$ can be denoted as $T_{d,i} = T_{s,(i+1)} - T_{s,i} + T_{a,i}$. From this equation, it can be seen that $T_{d,i}$ is determined by two parts: $T_{s,(i+1)} - T_{s,i}$ and $T_{a,i}$. Herein, $T_{a,i}$ is only determined by the input process characterised by $MMPP_l^{in}$ (the subscript l represents the low priority queue and the superscript in denotes the input traffic). As the input traffic does not change, then if the relationship among $T_{a,i}$, $T_{d,i}$ and $T_{s,i}$ is still valid after the decomposition of the PQ system, the sojourn time should be kept unchanged during the

the queueing decomposition.

According to the Little's law [137], this condition can be equivalently transferred to keep the average number of packets in the PQ system unchanged. The key issue to satisfy this condition during the PQ decomposition is to achieve the service capabilities of the $SSSQ_l$ and $SSSQ_h$, namely, μ_l and μ_h respectively. Recall that EBA can only achieve high accuracy when the low priority queue is poured with heavy traffic and high priority queue with light traffic, it can hardly capture the comprehensive performance evaluation of the PQ system under various traffic load conditions. In this study, we extend the EBA method to derive μ_l and μ_h. Since the SS provides the absolute priority for the packets in the high priority queue, the newly arriving packets in the low priority queue can hardly have impact on the serving process of the high priority queue. Therefore, the equivalent service rate of the $SSSQ_h$, μ_h, can be achieved as $\mu_h = \mu_s$. Then, the main difficulty in the decomposition of the PQ system transfers to the calculation of the equivalent service rate of the $SSSQ_l$. Inspired by EBA method, the average number of packets in the $SSSQ_l$, L_l, can be calculated by subtracting the average number of packets in the $SSSQ_h$, L_h, from the average number of packets in the PQ system, L_t. This relationship can be expressed as follows:

$$L_l = L_t - L_h \tag{5.4}$$

The average number of packets in an $SSSQ_i$ (the subscript i represents different types of queueing systems) system with $MMPP_i$ traffic input can be calculated as follows [66] [138]:

$$L_i = {l_i}^{(1)} + [\frac{1}{\lambda_i^m}\pi_i\Lambda_i - l_i](e\pi_i + Q_i)^{-1}\Lambda_i e \tag{5.5}$$

where $e = (1,1)^{-1}$, $\pi_i = (\pi_{1i}, \pi_{2i}) = (\varphi_{1i}, \varphi_{2i})/(\varphi_{1i} + \varphi_{2i})$; Q_i and Λ_i are the infinitesimal

generator matrix and the arrival rate matrix of the $MMPP_i$ input traffic. l_i is the average queue length of the $SSSQ_i$ system; $l_i^{(1)}$ is the first moment of l_i; l_i and $l_i^{(1)}$ can be calculated based the method in [66]. For the low priority queue, after achieving the average number of packets in the $SSSQ_l$ in Eq. (5.4), the service rate of $SSSQ_l$, μ_l can be calculated based on Eq. (5.5) through iterative algorithm, which applies a search over feasible region [0, μ_s]. The search algorithm recursively calculates the average number of packets $L_l{}'$ until satisfies $|L_l{}' - L_l| < \zeta$, where ζ is a small value, e.g., 10^{-8} specifying the stop condition for the recursion loop.

In what follows, we will derive the arrival traffic processes for the $SSSQ_l$, the $SSSQ_h$, and the PQ system, respectively.

5.3.2 Input Traffic Process of the Low Priority Queue

Since the buffer size of the $MMPP_l^{in}/M/1/K_l$ (the arrival traffic in low priority queue follows the *MMPP* process) queueing system is limited as K_l for modelling the low priority queue, the packets arriving at the SDN networks will be dropped when the $SSSQ_l$ is full. Let Pb_l indicate the probability that an arriving packet finds $MMPP_l^{in}/M/1/K_l$ full. The traffic effectively entering the queueing system is a fraction $(1 - Pb_l)$ of the total traffic arrived. As the splitting of an *MMPP* generates a new *MMPP*, let $MMPP_l^{in\to e}$ represent the effective traffic entering the queueing system. $MMPP_l^{in\to e}$ can be calculated by splitting $MMPP_l^{in}$ with the probability $(1 - Pb_l)$. Based on the principle of MMPP splitting process [67], the infinitesimal generation $Q_l^{in\to e}$ and rate matrix $\Lambda_l^{in\to e}$ of $MMPP_l^{in\to e}$ can be given by

$$Q_l^{in\to e} = Q_l^{in} = \begin{bmatrix} -\varphi_{1l} & \varphi_{1l} \\ \varphi_{2l} & -\varphi_{2l} \end{bmatrix} \tag{5.6}$$

$$\Lambda_l^{in\to e} = (1-Pb_l)\Lambda_l^{in} = \begin{bmatrix} (1-Pb_l)\times\lambda_{1l} & 0 \\ 0 & (1-Pb_l)\times\lambda_{2l} \end{bmatrix} \tag{5.7}$$

To compute the blocking probability, Pb_l, let us first analyse the bivariate Markov chain of the $SSSQ_l$ system. The state (s,n) in this Markov chain denotes that the Markov chain of $MMPP_l^{in}$ is in state s, ($s = \{0,1\}$), and there are n packets in the $SSSQ_l$, ($0 \leq n \leq K_l$). The transmission rate from the state $(0,n)$ to $(1,n)$ is φ_{1l}, and the rate from state $(1,n)$ to $(0,n)$ is φ_{2l}. φ_{1l} and φ_{2l} are given by Q_l^{in}. The transmission rate from state $(0,n)$ to $(0,n+1)$ is the packet arrival rate, λ_{1l}, and from state $(1,n)$ to $(1,n+1)$ is λ_{2l}. λ_{1l} and λ_{2l} can be achieved from Λ_l^{in}. The rate out of the state $(s,n+1)$ to state (s,n) is the service rate of $SSSQ_l$, μ_l. In order to calculate the blocking probability, the transmission matrix, G, should be built based on the state-transition-rate diagram. Given the number of the state of the bivariate Markov chain, $2K_l$, the dimension of the transmission matrix should be $2K_l * 2K_l$. Based on the balance equations of the bivariate Markov chain, the transmission matrix can be expressed by the transmission rates linking different states. After achieving the transmission matrix, let us calculate the steady-state probability vector $\mathbf{P}$, where $\mathbf{P} = (P(0,0),P(0,1),...,P(0,K_l),P(1,0),P(1,1),...,P(1,K_l))$. Let $\mathbf{e}$ represent a $2K_l$ unit vector. The steady-state probability vector, $\mathbf{P}$, satisfies the following equations:

$$\mathbf{PZ} = \mathbf{0} \qquad \mathbf{Pe} = \mathbf{1} \tag{5.8}$$

Solving the above equations yields the probability $\mathbf{P}$ as

$$\mathbf{P} = \mathbf{u}(\mathbf{I} - \Re + \mathbf{e})^{-\mathbf{1}} \tag{5.9}$$

where $\Re = \mathbf{I} + \mathbf{Z}/min\{\mathbf{Z}(\rho,\rho)\}$ and $min\{\mathbf{Z}(\rho,\rho)\}$ represents the minimum number in

the diagonal line of the matrix $\mathbf{Z}$. $\mathbf{u}$ denotes any row vector of the $\Re$. After achieving $\mathbf{P}$, the probability that there are n packets in the $SSSQ_l$ system, P_n, can be calculated as $P_n = \sum_{s=0}^{1} P_{s,n}$. With P_n, let us calculate, $\dot{P}_n$, which is the probability that an arriving packet observes there are n packets in the $SSSQ_l$ system. $\dot{P}_n$ is given as follows [139]:

$$\dot{P}_n = \left(\sum_{n=0}^{K_l} \mathbf{P}_n \times \Lambda_l^{in} \times \mathbf{e} \right)^{-1} \mathbf{P}_n \times \Lambda_l^{in} \times \mathbf{e} \tag{5.10}$$

The blocking probability is equal to the probability that a packet arrives at the system and observes that the queue is full, therefore, $Pb_l = \dot{P}_{K_l}$.

5.3.3 Output Traffic Process of the Low Priority Queue

The output process of the PQ system subject to an MMPP arrival process will be partially fed to SDN controller, playing critical role in deriving the input process of the high priority queue. Based on the study in [140], the output process of the priority queue no longer possesses the property of MMPP. In order to address this issue to achieve a tractable analytical model, a matching method is leveraged in this section to use an MMPP process characterised by four parameters (λ_1, λ_2, φ_1, and φ_2), to approximately model the output process of the low priority queue. We employ the selection method in [140] to choose the four statistics of the interdeparture process to match the four MMPP parameters: the first moment and the third moment of the interdeparture time, $E\left[T_{d,i}\right]$ and $E\left[T_{d,i}^3\right]$, the squared coefficient variation of the interdeparture time $c^2(T_{d,i})$, and the covariance of two successive interdeparture times $Cov(T_{d,i}, T_{d,(i+1)})$.

The moments of the inter-departure time, $T_{d,i}$, can be written as

$$E\left[T_{d,i}^n\right] = (-1)^n \left[\sum_{i=0}^{n-1} \frac{n!}{i!} L^i(0) x_0 U^{-(n-1)}(0) e \right] + (-1)^n L^{(n)}(0), \tag{5.11}$$

where $U(0) = Q - \Lambda$ and $L(s)$ is the Laplace-Stieltjes transform of the service time distribution, given by $L(s) = \mu/(s+\mu)$. Let x_k denote the stationary probability that the number of the packets in the system is k once a departure occurs, and x_0 and x_1 can be achieved based on the method in [66].Then, the first three moments of the inter-departure time can be easily achieved from Eq. (5.11) as follows:

$$E\left[T_{d,i}\right] = l - x_0 U^{-1}(0)e \tag{5.12}$$

$$E\left[T_{d,i}^2\right] = L^{(2)}(0) - 2lx_0 U^{-1}(0)e + 2x_0 U^{-2}(0)e \tag{5.13}$$

$$E\left[T_{d,i}^3\right] = -L^3(0) - 3L^{(2)}(0)x_0 U^{-1}(0)e + 6lx_0 U^{-2}(0)e - 6x_0 U^{-3}(0)e \tag{5.14}$$

The squared coefficient of variation of the interdeparture time $c^2(T_{d,i})$, can be obtained from Eqs. (5.12)-(5.13), given by $c^2(T_{d,i}) = \left(E\left[T_{d,i}^2\right] - (E\left[T_{d,i}\right])^2\right)/(E\left[T_{d,i}\right])^2$. The covariance of two successive interdeparture times is given by

$$\begin{aligned} Cov(T_{d,i}, T_{d,(i+1)}) = {} & lx_0 U^{(-1)}(0)e - \left(x_0 U^{(-1)}(0)e\right)^2 + x_1 A_0'(0)U^{(-1)}(0)e \\ & + x_0 U^{(-1)}(0)K(0)A_0(0)U^{(-1)}(0)e + x_0 K(0)A_0'(0)U^{(-1)}(0)e \end{aligned} \tag{5.15}$$

where $l = 1/\mu$ and $K(0) = (A-\Lambda)^{-1}\Lambda$. Let $\tilde{A}_k(x)$ denote the probability that when a departure happens there is at least one packet in the system and the next departure occurs no later than x with k arrivals during the service time. Then, the transform matrix of $\tilde{A}_k(x)$ can be calculated as follows:

$$A_k(s) = \int_0^\infty e^{-sx} d\tilde{A}_k(x) = \int_0^\infty e^{-sx} P(z,x) d\tilde{L}(x) = \int_0^\infty e^{-sx} e^{[(Q-\Lambda)+z\Lambda]x} d\tilde{L}(x) \tag{5.16}$$

where $P(z,x)$ is the z transformation of $P(k,x)$ and is calculated by $P(z,x) = e^{[(Q-\Lambda)+z\Lambda]x}$. $P(k,x)$ is the probability that there are k packets arriving at the system during the length of x time. Given $U(0) = Q - \Lambda$, the cumulative distribution function of exponential distribution, $\tilde{L}(x)$, is achieved by $\tilde{L}(x) = 1 - e^{\mu x}$. $A_0(0)$ and $A_0^{'}(0)$ can be readily derived from Eq. (5.16), i.e., $A_0(0) = \mu[\mu I - U(0)]^{-1}$ and $A_0^{'}(0) = -A_0(0)[\mu I - U(0)]^{-1}$. Then the four parameters of the output process of the low priority queue can be derived from Eqs. (5.11)-(5.16) based on the method in [140].

5.3.4 Input Traffic Process of the High Priority Queue

Recall that the packet arriving at SDN switch has the probability, $(1-\xi)$, missing the flow entry in the flow table and a proportional amount of the output traffic will be sent to the SDN controller through the UC. The traffic arriving at the UC, denoted by $MMPP_u^{in}$, is a fraction of output traffic from the $SSSQ_l$. This fraction, f_m, is equal to the miss probability as $f_m = 1 - \xi$. Based on Eqs. (5.6)-(5.7), the infinitesimal generator, Q_u^{in}, and the rate matrix, Λ_u^{in} of $MMPP_u^{in}$ can be achieved. Let $MMPP_u^{out}$ be the output process of the UC queue, which is characterised by the infinitesimal generator, Q_u^{out}, and rate matrix Λ_u^{out}. Given the transmission rate of the UC, μ_u, the output process of the UC can be achieved based on the matching approach described in Section 5.3.3. Since there is no packet dropped in the transmission of the UC [133], the traffic arriving at the SDN controller, $MMPP_c^{in}$ is equal to the output process, $MMPP_u^{out}$ of the UC. Since the buffer size of the SDN controller, K_c, is finite, when the packet arrives at the SDN controller, there is a probability, Pb_c, that the arriving packet is dropped when the queue becomes full. Pb_c can be obtained using Eqs. (5.8)-(5.10). The effective traffic entering the queueing system of SDN controller is a fraction $(1 - Pb_c)$ of traffic arriving at the controller. As the splitting of an $MMPP$ is again a new $MMPP$, let $MMPP_c^{in \to e}$ denote the effective traffic

entering the queueing system. $MMPP_c^{in\rightarrow e}$ can be obtained by splitting $MMPP_c^{in}$ with the probability $(1-Pb_c)$. Following the matching approach described in Section 5.3.3, the output process from the $MMPP_c^{in\rightarrow e}/M/1/K_c$ queue, parameterised by Q_c^{out} and Λ_c^{out} can be readily obtained. Similar to the analysis of the UC, the input and output processes of the DC, $MMPP_d^{in}$ and $MMPP_d^{out}$ can be obtained. Again, due to infinite DC queue, the traffic arriving at the high priority queue in SDN architecture, denoted by $MMPP_h^{in}$, is the output process from the DC, $MMPP_d^{out}$.

5.3.5 Total Traffic Process of the Priority Queue System

Since the superposition of multiple *MMPPs* is again an *MMPP* [66], let $MMPP_t$ denote the superposition of the $MMPP_l$ and $MMPP_h$. The number of states in the $MMPP_t$ is the production of those of the $MMPP_l$ and $MMPP_h$, which brings the complex computations in the iterative process to calculate μ_l. In order to achieve an efficient analytical model, inspired by [141], a two-state $MMPP'_t$ is constructed in this study to approximate the $MMPP_t$. For the clarification, let m_j, v_j, p_j and $r_j(t)$ be the mean arrival rate, $E\left[T_{a,j}\right]$, the second moment, $E\left[T_{a,j}^2\right]$, the third moment, $E\left[T_{a,j}^3\right]$ and the covariance function, $Cov(T_{a,j},T_{a,(j+1)})$ of the $MMPP_j$ (where $j=\{l,h\}$). Let τ_j denote the time constant of the $MMPP_j$ process, caculated by $\tau_j=\frac{1}{v_j}\int_0^\infty r_j(t)dt$. Then, the four parameters of $MMPP'_t$, m'_t, v'_t, p'_t and τ'_t, are given by:

$$m'_t=\sum_{j\in\{l,h\}} m_j \quad v'_t=\sum_{j\in\{l,h\}} v_j \quad p'_t=\sum_{j\in\{l,h\}} p_j \quad \tau'_t=\sum_{j\in\{l,h\}} \frac{v_j}{v'_t}\tau_j \tag{5.17}$$

After obtaining these four parameters, the infinitesimal generator, Q'_t, and rate matrix Λ'_t can be easily obtained based on the matching procedure in [142], which will be used to approximate the infinitesimal generator, Q_t, and rate matrix Λ_t of $MMPP_t$. The accuracy of this approximation will be evaluated in Section 5.4. With the $MMPP_l$, $MMPP_h$ and

$MMPP_t$, the service rate of $SSSQ_l$ can be calculated from the iteration process in Section 5.3.1.

According to [66], the average sojourn time in a $MMPP_i/M/1$ queueing system is given by

$$D_i = \frac{1}{\rho_i}\left\{\frac{1}{2(1-\rho_i)}\left[2\rho_i + \lambda_i^m h_i^{(2)} - 2h_i((1-\rho_i)g_i + h_i\pi_i\Lambda_i)(Q_i + e\pi_i)^{-1}\lambda_i\right] - \frac{1}{2}\lambda_i^m h_i^{(2)}\right\} \tag{5.18}$$

where ρ_i is the utilisation rate of the server, given by $\rho_i = \lambda_i^m/\mu_i$. h_i and $h_i^{(2)}$ are the mean and the second moment of the service time, given by $h_i = 1/\mu_i$ and $h_i{}^{(2)} = 2/\mu_i{}^2$, respectively. g_i is the steady state vector of the matrix G_i and can be achieved based on the methods in [66].

The average sojourn time in the low priority queue, the UC queue, the queue in the SDN controller, the DC queue and the high priority queue, can be computed by Eq. (5.18). Finally, the average latency can be obtained from Eq. (5.1).

During the whole lifecycle of the packet in the PQ system, packets will be dropped in the queues of SDN switch and controller once the buffers become full. Therefore, the average throughput, $Throughput$, can be obtained as

$$Throughput = \lambda_l^m(1-Pb_l)(\xi + (1-\xi)(1-Pb_c)) \tag{5.19}$$

5.3.6 Implementation of the Model

In order to implement the developed analytical model, an algorithm is described in this section for calculating the average latency and the average throughput of PQ-based SDN networks.

Algorithm 1: The procedure for calculating the average latency of PQ-based SDN networks

Input: The service rates of SDN controller, switch, UC, and DC, μ_c, μ_s, μ_u and μ_d; the buffer sizes of low priority queue and controller queue, K_l and K_c; the flow table hit probability, ξ; the infinitesimal generator and rate matrix of $MMPP_l^{in}$, Q_l^{in} and Λ_l^{in}; the recursive gap, $\mu_{gap} = \mu_s$; the service rate of $SSSQ_l$, $\mu_l = 0$; the recursive stop condition, $\zeta = 10^{-8}$; and the initial recursive difference, $diff = 10$;

Output: The average latency and the average throughput of the PQ-based SDN networks, *Latency* and *Throughput*.

while $|dif| > \zeta$ **do**

  if $dif > 0$ **then**

    $\mu_l = \mu_l + \mu_{gap}$;

  else

    $\mu_l = \mu_l - \mu_{gap}$;

  end

  1. Calculate the blocking probability for the low priority queue, Pb_l, using Eq. (5.10);

  2. Compute the infinitesimal generator and rate matrix for effective input process of the low priority queue, $Q_l^{in\to e}$ and $\Lambda_l^{in\to e}$, using Eqs. (5.6)-(5.7);

  3. Calculate the four matching parameters, the infinitesimal generator, and the rate matrix for the output process of the low priority queue, $E\left[T_{d,i}\right]$, $E\left[T_{d,i}^2\right]$, $E\left[T_{d,i}^3\right]$, $Cov(T_{d,i}, T_{d,(i+1)})$, Q_l^{out} and Λ_l^{out}, using Eqs. (5.11)-(5.16);

  4. Calculate the infinitesimal generator and the rate matrix for the input process of the UC, Q_u^{in} and Λ_u^{in}, using Eqs. (5.6)-(5.7);

  5. Calculate the infinitesimal generator and the rate matrix for the output process of the UC, Q_u^{out} and Λ_u^{out}, using Eqs. (5.11)-(5.16);

  6. Calculate the blocking probability of the controller queue, Pb_c, using Eq. (5.10);

  7. Compute the infinitesimal generator and rate matrix for the effective input process of the controller queue, $Q_c^{in\to e}$ and $\Lambda_c^{in\to e}$, using Eqs. (5.6)-(5.7);

  8. Calculate the infinitesimal generator and the rate matrix for the output process of the controller queue, Q_c^{out} and Λ_c^{out}, using Eqs. (5.11)-(5.16);

  9. Calculate the infinitesimal generator and the rate matrix for the input process of the DC, Q_d^{in} and Λ_d^{in}, using Eqs. (5.6)-(5.7);

  10. Calculate the infinitesimal generator and the rate matrix for the output process of the DC, Q_d^{out} and Λ_d^{out}, using Eqs. (5.11)-(5.16);

  11. Calculate the infinitesimal generator and the rate matrix for the total traffic process of the PQ system, Q_t and Λ_t, using Eq. (5.17);

  12. Calculate the average queue lengths of the low priority queue, the high priority queue, and the PQ system, L_l, L_h and L_t, respectively, using Eq. (5.5);

  13. Calculate the value of the queue length difference, $diff$, using Eq. (5.4);

  14. Update the recursive gap, $\mu_{gap} = \mu_{gap}/2$;

end

15. Calculate the average sojourn times in the low priority queue, the UC, the SDN controller, the DC, and the high priority queue, D_l, D_u, D_c, D_d, and D_h, respectively, using Eq. (5.18);
16. Calculate the average latency in the PQ-based SDN architecture, *Latency*, using Eqs. (5.1)-(5.3);
17. Calculate the average throughput in the PQ-based SDN architecture, *Throughput*, using Eq. (5.19).

5.4 Validation of the Model

To validate the accuracy of the developed analytical model, we have developed a discrete-event simulator in the Objective Modular Network Testbed in C++ (OMNeT++) simulation environment [129]. 95% confidence intervals is adopted in this study to collect the simulation results when the simulation experiment reaches the steady state. The traffic arriving at the SDN switch follows the $MMPP_l^{in}$ process, characterised by the infinitesimal generator Q_l^{in} and the rate matrix Λ_l^{in}. Extensive simulation experiments have been conducted by varying the network parameters, including buffer sizes, switch service rate, controller service rate, UC and DC capacities, different flow table hit probability, various MMPP traffic inputs. However, for the sake of specific illustration and without loss of generality, the result comparisons between the analytical model and simulation experiments are presented in terms of the average latency and average throughput with different combinations of system parameters, which are set as follows:

* Service rate of SDN switch: μ_s = 80, 40, 20 packets/second;

* Service rate of SDN controller: μ_c = 60, 30 packets/second;

* Transmission rates of UC and DC: $\mu_u = \mu_d$ = 5, 10 packets/second;

* Flow table hit probability: ξ = 0.5;

* Buffer sizes of the low priority queue and the controller queue, K_l = 128 packets and K_c = 256 packets;

Table 5.2: System Configuration Parameters for SDN Networks in Performance Evaluation

	I		*II*		*IV*		*IX*	
Scenarios	A	B	A	B	A	B	A	B
φ_{1l}	0.13	0.13	0.06	0.06	0.008	0.008	0.09	0.09
φ_{2l}	0.15	0.15	0.03	0.03	0.004	0.004	0.06	0.06
μ_u	5, 10	10	5, 10	10	5, 10	10	5, 10	10
μ_d	5, 10	10	5, 10	10	5, 10	10	5, 10	10
μ_s	80	40, 20	80	40, 20	80	40, 20	80	40, 20
μ_c	60	30	60	30	60	30	60	30
ξ	0.5	0.5	0.5	0.5	0.5	0.5	0.5	0.5
K_l	128	128	128	128	128	128	128	128
K_c	256	256	256	256	256	256	256	256

* The infinitesimal generator, Q_l^{in}, of $MMPP_l^{in}$, representing different degrees of traffic burstiness and correlation.

$$Q_l^{in} = \begin{bmatrix} -0.3 & 0.3 \\ 0.015 & -0.015 \end{bmatrix} \quad Q_l^{in} = \begin{bmatrix} -0.09 & 0.09 \\ 0.06 & -0.06 \end{bmatrix}$$

$$Q_l^{in} = \begin{bmatrix} -0.06 & 0.06 \\ 0.03 & -0.03 \end{bmatrix} \quad Q_l^{in} = \begin{bmatrix} -0.008 & 0.008 \\ 0.004 & -0.004 \end{bmatrix}$$

Figs. 5.3-5.6 present the average latency and throughput predicted by the analytical model and simulation experiments for different network configurations. The system configuration parameters for performance evaluation are listed in Table 5.2. The horizontal axis represents the traffic rate, λ_{1l}^{in}, when the Markov chain of *MMPP* process stays in state 1. For clarity of the description, the traffic rate, λ_{2l}^{in} is set to be zero. These figures show that the developed model provides a good degree of matching with the simulation

experimental results under different network configurations. In addition, the subfigures reveal that the average latency and average throughput significantly increase when the arrival traffic rate goes up (subfigures (a) and (b)). In this case, the uplink and downlink channels become the bottleneck for the system performance improvement even though SDN switch and controller have adequate service capacity. When sufficient transmission capabilities are allocated to the uplink and downlink channels, with the practical configuration of the finite buffer in the forwarding devices, the average latency and average throughput would reach a stable point once the incoming traffic exceeds the service capacity that the SDN switch can provide (subfigures (c) and (d)). In this case, packets will be dropped as the buffer is full and the service capacity of the switch becomes the performance bottleneck for SDN networks. Therefore, in order to avoid the service degradation and Service Level Agreement (SLA) violation, the developed model can be used as a practical and cost-effective tool to gain insights into the performance of SDN networks in the presence of bursty and correlated multimedia traffic.

5.5 Performance Analysis

The accuracy of the proposed analytical model has been investigated in the above section. In this section, the developed model is adopted to conduct the performance evaluation of the SDN architecture. The system configuration parameters for performance analysis are listed in Table 5.3.

5.5.1 Effects of the Flow Table Hit Probability

In order to investigate the impact of flow table hit probability on the performance of SDN networks, Fig. 5.7(a) presents the average latency predicted by the developed analytical model against varying traffic arrival rate with different flow table hit probabilities ($\xi = 0$, 0.5 and 1); the service rates of the SS, DC, SDN controller and UC, μ_s, μ_d, μ_c and μ_u are

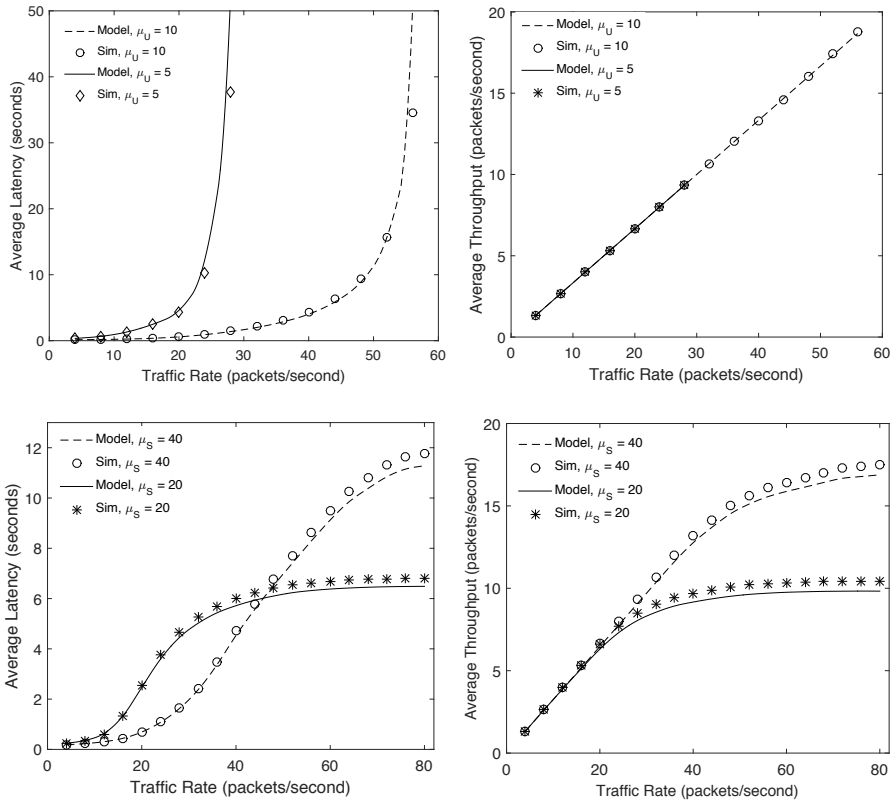

Figure 5.3: Average Latency and Throughput Predicted by the Model and Simulation in Case I

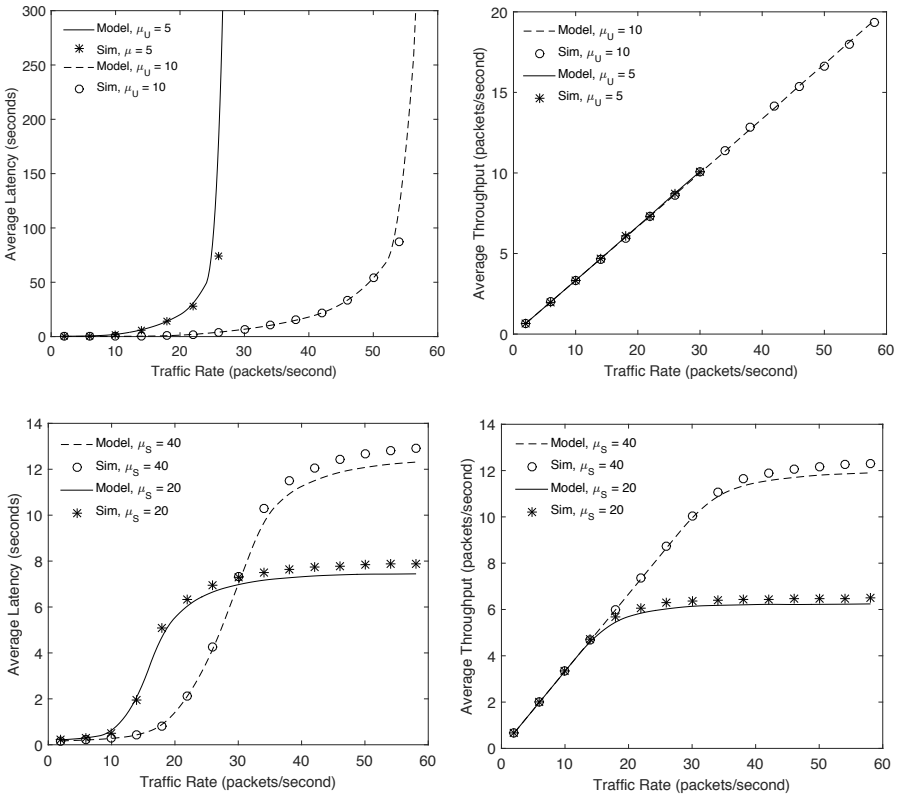

Figure 5.4: Average Latency and Throughput Predicted by the Model and Simulation in Case II

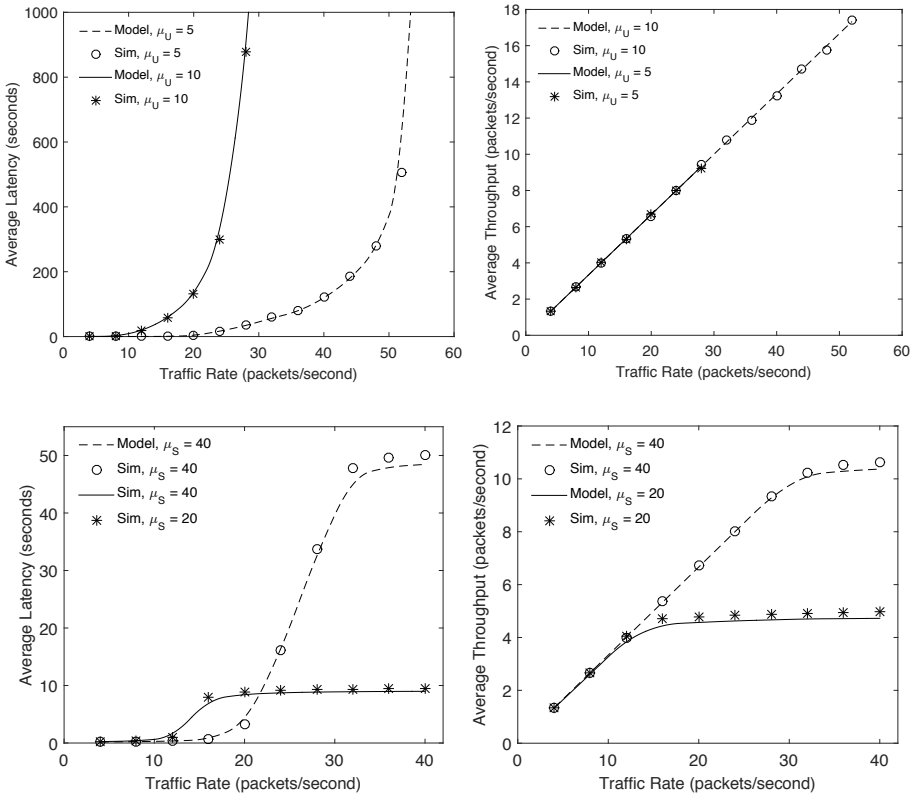

Figure 5.5: Average Latency and Throughput Predicted by the Model and Simulation in Case IV

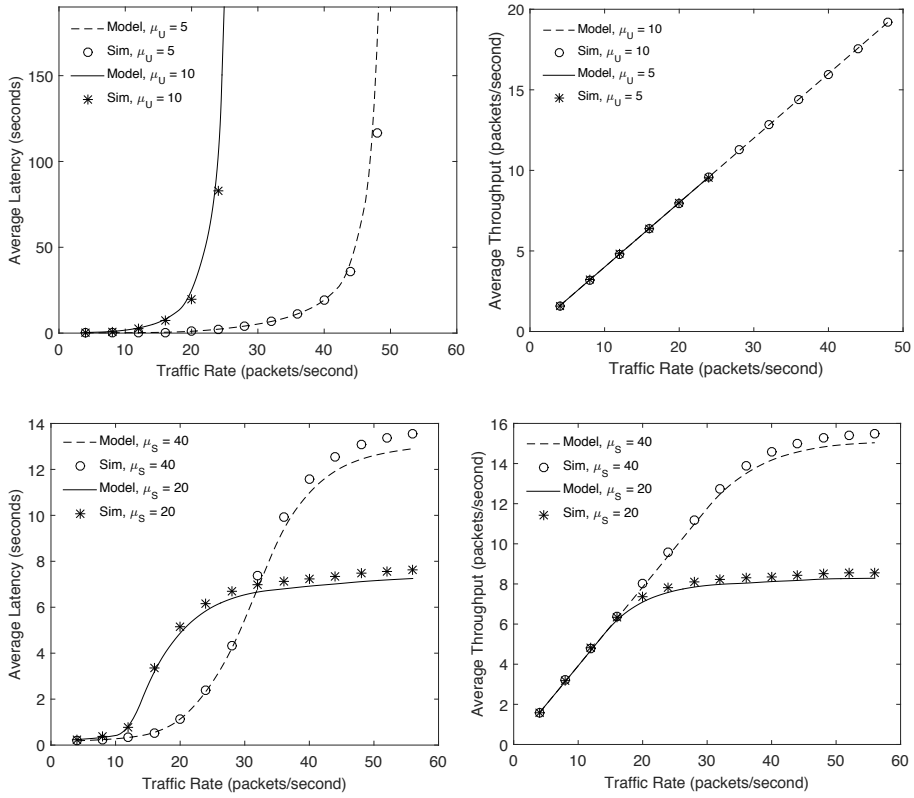

Figure 5.6: Average Latency and Throughput Predicted by the Model and Simulation in Case IX

set to be 20 packets/second, 10 packets/second, 30 packets/second and 10 packets/second, respectively; and the buffer sizes of the low priority queue and SDN controller queue, K_s and K_c, are set to be 128 and 256 packets. When $\xi = 1$, each new arriving packet can find the forwarding rule in the flow table, without the loop communication with the SDN controller. This case can be used to approximate the forwarding mechanism of the traditional network architecture, where network control resides in the forwarding devices. When $\xi = 0$, no flow entry is stored in the flow table and the SDN networks is in its initiation stage. For each arriving packet failing to match the entry in the flow table, the header of the new arrival packet will be forwarded to the controller for requesting the necessary forwarding rule. $\xi = 0.5$ represents the case that 50% of the arriving packets can match the rules in the flow table. In addition, Fig. 5.7(b) presents the average latency obtained from the model against varying flow hit probability from 0 to 1 with the fix step of 0.1. From these two figures, we can see that the average latency of SDN networks becomes better with the increase in the flow table hit probability and reaches the highest level when the hit probability is equal to 1. This relationship shows that the analytical model is very useful for the practical network deployment and management. For instance, in order to avoid the disruptive QoS degradation of network service in the early stage of network deployment, network routing information would be cached in the flow table in advance. During this installation process, the analytical model can be used as a cost-effective tool to quantitatively calculate the threshold of the flow table to satisfy a required network latency.

5.5.2 Effects of the Resource Allocation

The efficient resource allocation plays an important role in SDN networks to provide services with the required QoS guarantee. In what follows, the impact of the resource

Table 5.3: System Configuration Parameters for SDN Networks in Performance Analysis

φ_{1l}	φ_{2l}	μ_u	μ_d	μ_s	μ_c	ξ	K_l	K_c	λ_{1l}^{in}	λ_{2l}^{in}
0.09	0.06	10	10	20	30	0, 0.5, 1	128	256	/	0
0.09	0.06	10	10	20	30	/	128	256	25	0
0.09	0.06	20	20	30, 60	30, 60	0.5	128	256	/	0
0.09	0.06	20	20	30	/	0.5	128	256	25	0

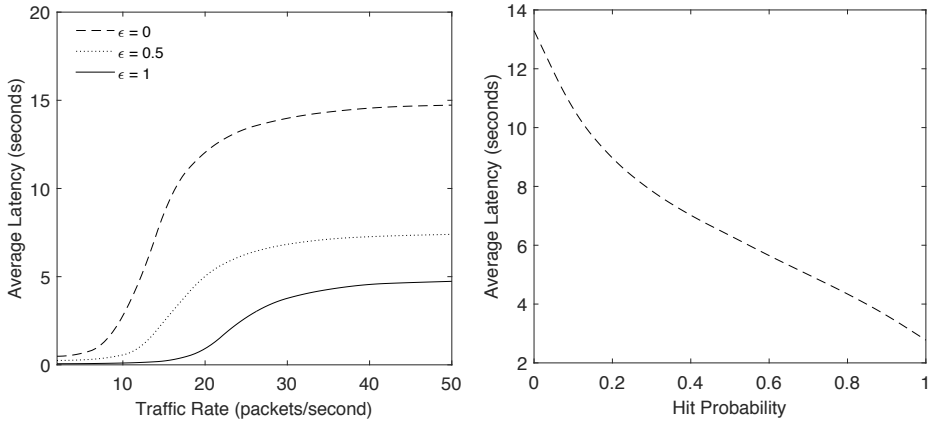

(a) (b)

Figure 5.7: Impact of the Flow Table Hit Probability on the Average Latency

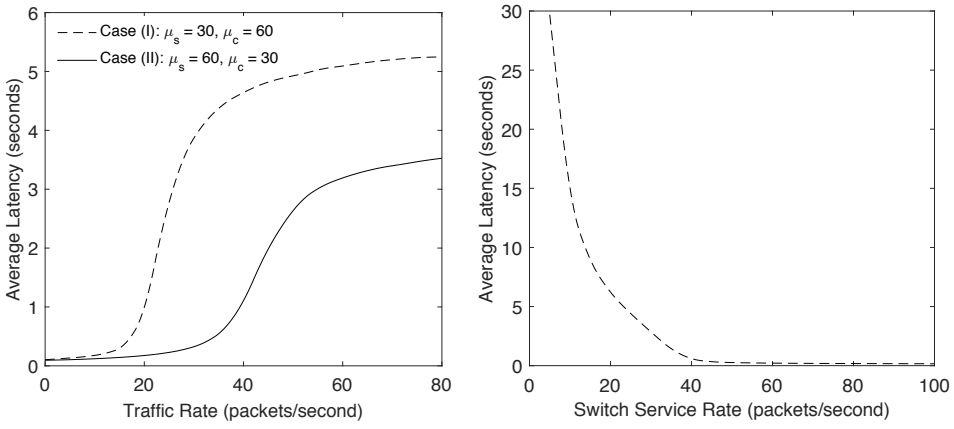

(a) (b)

Figure 5.8: Impact of the Service Capacity of SDN Switch on the Average Latency

allocation on the performance of SDN networks in terms of the average latency will be investigated. For the sake of illustration, a PQ-based SDN system with two scenarios of resource allocations is firstly considered: Case (I) $\mu_c > \mu_s$ (e.g., $\mu_c = 60$, $\mu_s = 30$) and Case (II) $\mu_c < \mu_s$ (e.g., $\mu_c = 30$, $\mu_s = 60$). The infinitesimal generator of the MMPP arrivals is set as $\varphi_{1l} = 0.09$ and $\varphi_{2l} = 0.06$; the transmission rates of both the UC and DC, μ_u, μ_d, are set to be 20 packets/second; and the buffer sizes of the SDN switch queue and controller queue, K_l, K_c, are set to be 128 packets and 256 packets, respectively. The flow table hit probability, ξ, is set to be 0.5. Fig. 5.8(a) depicts the results of the average latency under the two cases and shows that Case (II) provides the lower average latency compared to that by Case (I). From the analytical model, the effective traffic entering the queue of the SDN controller, $MMPP_c^{in\to e}$, is derived through two splitting procedures of the $MMPP_l^{in}$ (one splitting is in the queue of SDN switch and the other is in that of SDN controller) using Eqs. (5.6)-(5.10). The input of the *SS* is the superposition of the traffic from the $SSSQ_h$ and $SSSQ_l$, where the input of $SSSQ_h$ is statistically the output traffic from the SDN controller as there is no packet lose during the transmission from the controller to the $SSSQ_h$. It is therefore readily to see that the traffic load of the SDN switch is heavier than that of the SDN controller in the PQ-based SDN system architecture, leading to the phenomenon shown in the figure that the higher capacity allocated to the SDN switch could bring the lower average latency of the whole system. Furthermore, in order to achieve a deeper understanding of the impact of the data plane on the overall system performance, the quantitative relationship between the service rate of the SDN switch and the average latency is achieved through the developed model, as presented in Fig. 5.8(b). It can be seen that the average latency significantly reduces with the increase in the service rate of the SDN switch from 5 packets/s to 40 packets/s.

5.6 Summary

This chapter has proposed an analytical model for SDN architecture in the presence of MMPP arrivals capturing the traffic characteristics of multimedia applications. A PQ system has been adopted to model SDN data plane to capture the multi-queue nature of forwarding devices. A versatile method extending the EBA has been proposed to facilitate the decomposition of such a PQ system to two SSSQ systems in order to facilitate the derivation and improve the tractability of the analytical model. The key performance metrics including average latency and average network throughput have been derived by the model. The accuracy of the proposed model has been validated through extensive OMNeT++ simulation experiments. The validation results have revealed that the average latency and the average throughput predicted by the developed analytical model reasonably match those obtained from the simulation experiments. The analytical model has been adopted as a cost-effective tool to study the impact of flow table hit probability and the service resource allocation in the SDN controller and the switch on the system performance.

Chapter 6

Stochastic Performance Analysis of Network Function Virtualisation of Future Internet

6.1 Introduction

With the explosive increase in demand for wireless broadband services to deliver content-rich and resource hungry applications, traditional network architecture struggles to provide the satisfied network performance in terms of flexibility, scalability and reliability, due to its inherent features such as hardware-based service provision, multiple protocols co-existence and manual configuration and management. New and flexible networks are needed to cope more efficiently with the quick pace imposed by the evolution of the digital world. Future Internet is expected to support a multitude of new services and applications with very diverse requirements, mainly including higher traffic volume, lower latency, huge number of devices, etc. Network Function Virtualisation (NFV) has been proposed as a promising architecture for Future Internet, greatly enhancing the flexibility and Capital Expense (OPEX) and Operational Expense (OPEX) [143] [144] [103]. In order to fully

harvest the merits of NFV for network operators, there is an urgent need and opportunity to use the probabilistic features of stochastic network calculus to investigate the dynamic features of NFV. To bridge this gap, this work proposes a first novel comprehensive analytical model based on stochastic network calculus to investigates end-to-end performance of NFV networks. In detail, it addresses the two related challenges: 1) to characterise and model the traffic process and service process of NFV networks to capture the dynamic and on-demand features; and 2) to derive the performance bounds for the end-to-end service with the input of the required Service Level Agreements (SLAs). Through jointly exploiting the Exponentially Bounded Burstness (EBB) and Moment Generation Function (MGF) [71], the Stochastic Arrival Curves (SAC) and Stochastic Service Curves (SSC) can be achieved with different types of arrival traffic and service model. In addition, the leftover service technology and statistical multiplexing are also exploited to derive the end-to-end system performance.

The organisation of this chapter is summarised as follows: Section 6.2 presents the working mechanism of NFV service chain. Section 3 forms an abstracted mathematical model for NFV chain. Section 6.4 describes the methodology for deriving the end-to-end performance of NFV chain. The stochastic arrival and service curves are investigated based on MGFs; end-to-end latency bound is derived based on convolution feature of stochastic network calculus. The numerical results of the analytical model are discussed in Section 6.5. Finally, Section 6.6 concludes this study.

6.2 NFV Service Chain

The network architecture [58] launched by European Telecommunications Standards Institute (ETSI) gives a guide on how to design, implement and manage the NFV including the underlying physical resources, VNF management and service orchestration and oper-

ation. The key concept in ETSI NFV architecture is NFV service chain, which defines a list of individual network functions and the sequence policy and Service Level Agreement (SLA) requirements among these functions.

In order to demonstrate how the NFV chain is deployed in the practical network, we exemplify a cloud based service for mobile user to visit web server as shown in Fig. 6.1. The transmission network covers the LTE-A based access network, service provider network, and datacenter network. Within the network domains, through leveraging NFV technology, the dedicated network devices have been replaced by the common server; network functions are implemented and managed through NFV MANO. In Fig. 6.1, the end user sends a request to base station through access network. Based on service type, this message may be processed by various Virtual Network Functions (VNFs) within the base station, including Mobility Management Entity (MME), Authentication, Authorisation, and Accounting (AAA), Policy and Charging Rules Function (PCRF), Deep Packet Inspection (DPI), Service Gateway (S-Gateway) and Packet Data Network Gateway (P-Gateway); when the packet leaves access network and enters the ingress router (Provider Edger Router (PE router)) of service provider network. One or more network functions, such as Firewall, Load Balance and WAN Optimiser, would be offered by the service provider network to the arrival packets for guaranteeing the SLA, reliability and security requirements. To simplify the packet transmission in the core network, most of the exiting service provider network uses the Multi-protocol Label Switch (MPLS) to replace TCP/IP forwarding. Herein, Provider Edge (PE) routers A and B reside in the edge of the service provider network, responsible for label processing. In order to realise the packet transmission following the sequence of service chain, PE Router A will insert the MPLS labels of the Firewall, Load Balance and WAN Optimiser in the label stack of the packet. The label of firewall service will be at the top of the stack, followed by the labels for load

balancer service and WAN optimiser. The MPLS devices inside the provider network will check the top label to route the traffic and add/remove/swap the top label according to the service required. Therefore, packet will flow through paths according to the label sequence in the label stack and will achieve service chaining in sequence. When the packet leaves the PE Router B and arrives at the datacenter network, VNFs such as Firewall and Quality of Service (QoS) monitor would be offered before it visits the web server.

For NFV technology, NFV chain is characterised by its dynamic and on-demand features. Through implementing the network function in the manner of software, NFV functions can be easily added, removed or modified in the service chain at any time during the overall life-cycle of the service provision. For instance, a DPI service or an AAA verification can be installed in the datacenter network when the packet arrives at the datacenter network to improve the security. Another important merit of NFV is that the underlying virtual resource, such as storage space, computing speed and network transmission quality, can be upgraded to continuously and quickly satisfy the up-level service requirement. Although NFV chain brings a lot of benefits for service provider and network operator to manage and deploy network services, the dynamic and on-demand features pose unprecedented challenge for the quantitive performance analysis. In the next section, the working mechanism of service chain will be abstracted into mathematical model for further performance evaluation.

6.3 System Model

In order to quantitatively investigate the performance of the NFV networks, the service chain in Fig. 6.1 needs to be firstly abstracted and modelled. Based on the stochastic network calculus presented in Chapter 2, NFV service chain scenario in Fig. 6.1 is modelled as a queueing network in Fig. 6.2. In the abstracted NFV model, the arrival traffic

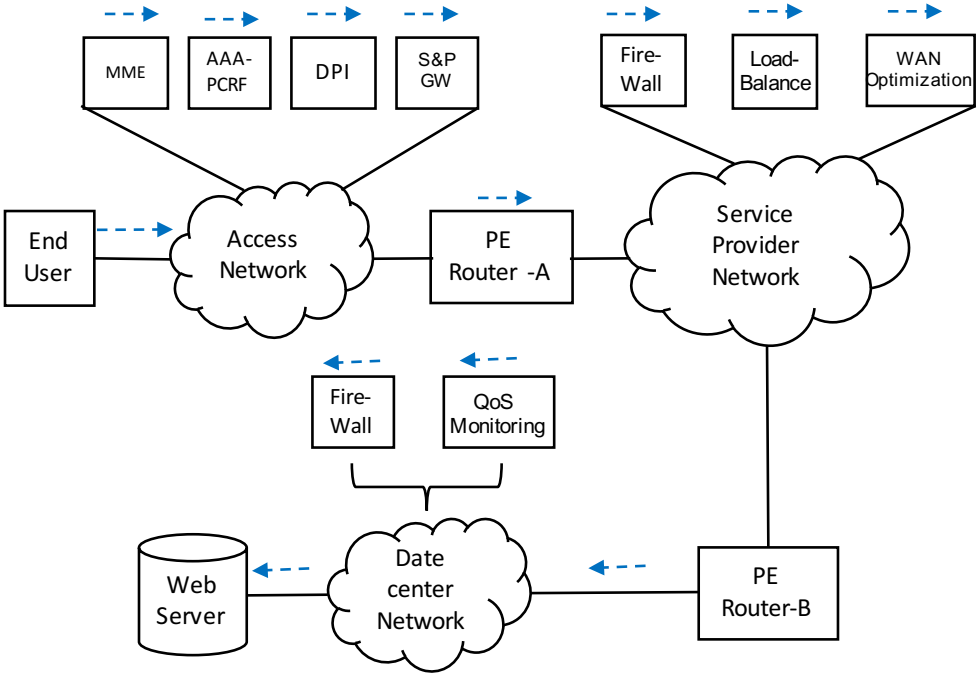

Figure 6.1: End-to-End NFV Chain Deployment

for each server consists of two kinds of traffic: through traffic generated by the end user in Fig. 6.1, and cross traffics that complete the resource with the through traffic. As the physical server is shared by multiple NFV chain, cross traffics are used to capture the effects of resource completion. The NFV chain that we are interested is named as through traffic in this research[74]. Let $A_{th_i}(t)$ and $A_{cr_i}(t)$ denote the through and cross traffic for the ith server. Within the abstracted NFV model, the through traffic, $A_{th_i}(t)$, is generated by MMPP and the cross traffic, $A_{cr_i}(t)$, is generated as Poisson Process. The number of the cross-traffic in the ith server is set to be m_i. The first server in the abstracted model is set to be memory-less on-off server to represent the wireless communication channel; for the other servers, service process, $S_i(t)$ follows the exponential distribution with different system parameters to model various VNFs in the access, service provider and datacenter networks. The total number of the VNFs in the service chain is set to be $n-1$. The departure process is denoted as $D(t)$. As SLA requirements for service provisioning should be met by the network operators, this work assumes the transmission bandwidth between two

VNFs in NFV chain can be guaranteed by the underlying NFV Infrastructure (NFVI). It is worth noting that the service model in Fig. 6.2 considers the following three important aspects:

Table 6.1: Key Notation Used in the Derivation of the Model in Chapter 6

$A_{th_i}(t)$	The through traffic for the ith server
$A_{cr_i}(t)$	The cross traffic for the ith server
m_i	The number of the cross-traffic in the ith server
$S_i(t)$	The service process for the ith server
$D(t)$	The departure process of the NFV system
$\lambda_{,i}^{j}$	The arrival rate for the jth cross traffic in the ith server
$A_{cr_i^j}(t)$	The jth cross traffic in the ith server
A_{cr_i}	The total arrival process of cross traffic in the ith server
$W(t)$	The latency bound of end-to-end latency
ε	The violation probability
$M_A(\theta, t-\tau)$	The MGF of an arrival process, $A(t)$
ρ	The effective bandwidth
θ	The free parameter
τ	The time interval
b_S	The burstness of the service process
b_A	The burstness of the arrival process
τ^*	The time interval that the inequality achieves the minimum
$1/v$	The packet size
$N_{cr_i}^{j}$	The numbers of the packets arriving at the ith server from the jth cross source
$M_{N_{cr_i}^{j}}(\theta, t-\tau)$	The MGF of $N_{cr_i}^{j}$
φ_1	The transmission rate from the state 1 to state 2 of $MMPP$
φ_2	The transmission rate from the state 2 to state 1 of $MMPP$
λ	The arrival rate when $MMPP$ is in state 1
σ	The free parameter under the constraint of θ
$A_{Agg_i}(t)$	The aggregation arrival process of cross traffic in the ith server
p_{on}	The probability that the state of the wireless channel is 'on'

μ_i	The service rate of the ith server
$M_{th_i}(-\theta, t-\tau)$	The MGF of the leftover service for the through traffic

- Cross Traffic

  As discussed in the previous paragraph, multiple VNFs may share the same underlying physical or virtual servers in order to achieve the higher resource utilisation. However, this co-existence deployment strategy poses a challenging issue for service quality guarantee, for instance, how to consider the negative impact of the cross traffic that belongs to other NFV chains on the through NFV chain should be carefully considered.

  Within the abstracted model, as shown in Fig. 6.2, the cross traffic is modelled as $A_{cr_i}(t)$, and the number of the cross traffic for the ith server is m_i. The traffic rate for the cross traffic in the server is set to be λ_i^j. Use $A_{cr_i^j}(t)$ to denote the jth cross traffic in the ith server; then the total accumulative cross traffic for the ith server, A_{cr_i} is equal to $A_{Agg_i}(t) = \sum_{j=1}^{m_i} A_{cr_i}^j$. In section 6.5, we will investigate the impact of m_i and λ_i^j on the end-to-end performance bound. Furthermore, in order to simplify the model derivation, leftover service technique [72] will be used in this study to calculate the service available for the through VNF in the present of the cross VNFs.

- Dynamic Feature

  The second issue for modelling NFV networks is how to capture the dynamic feature of the NFV chain, including the processing ability of each VNF and add or removal of specific NFV during the service provisioning. In Fig. 6.2, the service

capability of the each VNF in service chain is denoted as $S_i(t)$, which is modelled as a random server during performance derivation. The capacity of the each server can be modified in the manner of the on-demand. Thanks to the associativity property of the min-plus convolution, the multiple nodes NFV chain can be abstracted as a single equivalent system. Let $S(t)$ denote the service process of the overall NFV chain, by leveraging the associativity property, $S(t)$ can be expressed as the convolution of the individual service process, shown as $S(t) = S_1 \otimes S_2 \otimes \cdots \otimes S_n$. Let the number of the VNFs in a service chain be as n, which is a free parameter during the whole performance derivation. The final end-to-end system performance will be a function of n. In case that a VNF is removed or added into the service chain, the analytical model can immediately capture this effect and quickly achieve the new performance bounds for the modified service chain by uploading the value of n accordingly. The details of the performance derivation will be studied in Section 6.4.

- SLA Oriented NFV Model

  For network operators, the network service is booked and offered in the manner of SLA constraints. Strict requirement will be applied to the probability of service violation or availability. In this area, analytical model to be designed is expected to derive the system performance in term of SLA guarantee not just the basic average QoS metrics. For this reason, the stochastic network calculus is exploited in this research to study the performance of NFV networks. Stochastic network calculus is based on the probability theory and defines the mathematical relationship between the SLA requirement and probability that this demand can be met with a given network resource. For instance, let w denote the latency bound for end-to-end

service chain and ε be the violation probability that w can not be guaranteed, the aim of analytical model is to achieve the relation between w and ε, to calculate w if ε is given, and vice versa. According to [73], the relation between w and ε can be expressed as,

$$P(W(t) > w) \leq \varepsilon \tag{6.1}$$

Through exploring the useful results of stochastic network calculus, the analytical model to be developed in this research will be capable of capturing the SLA properties and thus has the potential value for network operators to conduct the network plan and management.

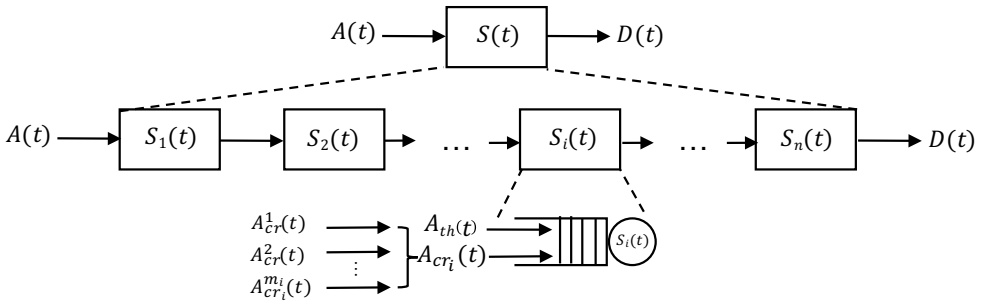

Figure 6.2: Abstracted Model of NFV Chain

6.4 Derivation of the Performance Model

In this section, we will first derive the SACs and SSCs for two types of the arrival traffic (Poisson Process and MMPP) and two kinds of server model (On-off Wireless Channel Model and Exponential Service Model). With SACs and SSCs, the leftover service technology [74] is leveraged in this research to calculate the service resources available for through traffic in the presence of the cross traffics. After achieving the effective SSCs, a single equivalent system is envisioned to replace multiple server NFV chain based the associativity property of the min-plus convolution. Finally, end-to-end performance bound

is calculated with the SAC of the through NFV traffic and SSC of the convolution network.

6.4.1 Moment Generating Function (MGF) and Exponentially Bounded Burstiness (EBB)

In order to achieve the SACs for arrival traffic and SSCs for abstracted servers in Fig. 6.2, two envelopes named MGF and EBB are utilised in this work to achieve the statistical bounds. For the simplification, we present the derivation of the statistical performance bounds for the arrival process. The service statistical performance bounds can be obtained similarly in [74].

In the statistic [145], the MGF of an arrival process, $A(t)$, is defined as $M_A(\theta, t-\tau) = E[e^{\theta A(\tau,t)}]$, where θ is a free parameter with the constraint of τ. Given the affine envelop of $A(t)$, the MGF of the arrival process is bounded by

$$E[e^{\theta A(\tau,t)}] \leq e^{\theta((\rho(t-\tau)+\sigma)} \tag{6.2}$$

where ρ and σ are the function of the free parameter θ.

EBB is a stochastic envelop for arrival process, $A(t)$. Given the violation probability, $\varepsilon(b)$, that $A(t,\tau)$ is larger than an affine envelop $\rho(t-\tau)+b$, EBB is defined as,

$$P(A(t,\tau) > \rho(t-\tau)+b) \leq \varepsilon(b) \tag{6.3}$$

where $\varepsilon(b)$ is defined as a exponential function of b, given by $\varepsilon(b) = \alpha e^{-\theta b}$.

In the statistics [145], the generic Chernoff bound for a random variable, X, is defined as,

$$P(X > x) = P(e^{\theta X} > e^{\theta x}) \leq \frac{E[e^{\theta X}]}{e^{\theta x}} \tag{6.4}$$

By applying the Chernoff bound in Eqs. (6.2)-(6.3), the EBB can be rewritten as,

$$P(A(t,\tau) > \rho(t-\tau)+b) \leq \varepsilon(b) \leq \frac{E[e^{\theta A(t,\tau)}]}{e^{\theta[\rho(t-\tau)+b]}} \leq \frac{e^{\theta[\rho(t-\tau)+\sigma]}}{e^{\theta[\rho(t-\tau)+b]}} = e^{\theta\sigma}e^{-\theta b} \tag{6.5}$$

Compared with EBB in Eq. (6.3), the violation probability, $\varepsilon(b)$ is equal to $e^{\theta\sigma}e^{-\theta b}$.

6.4.2 Stochastic Arrival Curves

The abstracted NFV model comprises of two types of the traffics, the data traffic served by the cross NFV chains and the voice traffic served by the through NFV chain. Poisson process is used for modelling the data traffic and MMPP for voice traffic [146]. In this part, the SACs of the Poisson process and MMPP are derived respectively; the packet size is set to be $1/v$. The adoption of $1/v$ is to simplify the mathematical derivation. As discussed in the Section 6.2, there are m_i NFV cross chains existing for the ith server. In this section, a stochastic multiplexing approach will be presented to calculate the total accumulative traffic for the individual server.

6.4.2.1 Poisson Traffic

We denote that the numbers of the packets and bits arriving at the ith server from the jth cross source during the time interval $[0,t]$ are denoted as $A^j_{cr_i}$ and $N^j_{cr_i}$ respectively. Given the packet size $1/v$, then $A^j_{cr_i} = N^j_{cr_i}/v$. Assume the MGF of $N^j_{cr_i}$, is set to be $M_{N^j_{cr_i}}(\theta,t-\tau)$, the MGF of $A^j_{cr_i}$, can be calculated as follows,

$$M_{A^j_{cr_i}}(\theta,t-\tau) = E[e^{\theta A^j_{cr_i}}] = E[e^{\theta N^j_{cr_i}/v}] = M_{N^j_{cr_i}}(\theta/v,t-\tau) \tag{6.6}$$

In [145], the distribution of a Poisson process is $P[N(t)=k] = e^{-\lambda t}(\lambda t)^k/k!$, where λ

is the average arriving rate. Correspondingly, then the MGF of $N_{cr_i}^j$ can be calculated as,

$$M_{N_{cr_i}^j}(\theta, t-\tau) = E[e^{\theta N_{cr_i}^j}] = \sum_{k=0}^{+\infty} [(\lambda_i^j t)^k / k!] e^{-\lambda_i^j t} e^{\theta k} = e^{-\lambda_i^j t(e^\theta - 1)} \tag{6.7}$$

where λ_i^j is the arrival rate for the *jth* NFV cross traffic source at the *ith* server. Then $A_{cr_i}^j(t)$ has the MGF, $M_{A_{cr_i}^j}(\theta, t-\tau)$, to be $e^{-\lambda_i^j t(e^\theta - 1)}$; and the affine envelop model, $E[e^{\theta A_{cr_i}^j(t-\tau)}] \leq e^{\theta[\rho_i^j(t-\tau)+\sigma_i^j]}$, with the parameters $\rho_i^j = \frac{\lambda_i^j(e^{\theta/v}-1)}{\theta}$ and $\sigma_i^j = 0$.

6.4.2.2 MMPP Traffic

The through traffic, $A_{th}(t)$, is modelled by MMPP process with two states. The transmission rate from the state 1 to state 2 is φ_1; the transmission rate from the state 2 to state 1 is φ_2; when Markov chain is in state 1, the arrival rate for through traffic is λ; when Markov chain is in state 2, there is no arrival for through traffic.

The MGF of $A_{th}(t)$ is defined as $M_{A_{th}}(\theta, t-\tau) = E[e^{\theta A_{th}}]$ According to [72], the $M_{A_{th}}(\theta, t-\tau)$ can be calculated as,

$$E[e^{\theta A_{th}}] = \begin{bmatrix} \frac{\varphi_2}{\varphi_1+\varphi_2} & \frac{\varphi_1}{\varphi_1+\varphi_2} \end{bmatrix} exp\left(\begin{bmatrix} -\varphi_1 + \theta\lambda & \varphi_1 \\ \varphi_2 & -\varphi_2 \end{bmatrix} t \right) \begin{bmatrix} 1 \\ 1 \end{bmatrix} \tag{6.8}$$

From [147], Eq. (6.8) can be simplified as,

$$E[e^{\theta A_{th}}] \leq e^{\theta\lambda - \varphi_1 - \varphi_2 + \sqrt{(\theta\lambda + \varphi_2 - \varphi_1)^2 + 4\varphi_1\varphi_2}} \tag{6.9}$$

The affine envelop of the arrival process, $A_{th}(t)$, is defined as,

$$E[e^{\theta A_{th}(\tau,t)}] \leq e^{\theta(\rho_{a_{th}}(t-\tau)+\sigma_{a_{th}})} \tag{6.10}$$

After comparing Eq. (6.10) with Eq. (6.9), $\rho_{a_{th}}$ and $\sigma_{a_{th}}$ can be achieved as $\rho_{a_{th}} = \frac{1}{2\theta}(\theta\lambda - \varphi_1 - \varphi_2 + \sqrt{(\theta\lambda + \varphi_2 - \varphi_1)^2 + 4\varphi_1\varphi_2})$ and $\sigma_{a_{th}} = 0$.

6.4.3 Stochastic Multiplexing

For the ith server, there are m_i cross traffics served by cross NFV chains. A stochastic multiplexing approach [74] is applied in this part to combine m_i cross traffics into one equivalent aggregation traffic, which avoids the complex model derivation, especially providing an efficient solution for calculating the leftover service in Section 6.4.4.3. As denoted in Section 6.2, let $A^j_{cr_i}(t)$ represent the jth cross traffic for the ith server. For a lossless system, $A_{Agg_i}(t)$ is equal to the sum of $A^j_{cr_i}(t)$, shown as $A_{Agg_i}(t) = \sum_{j=1}^{m_i} A^j_{cr_i}(t)$. Based on this equation, it can be easily seen the relationship between the MGFs of the individual cross traffic process and the aggregated traffic process.

The MGF of the aggregated traffic, $M_{A_{Agg_i}}(\theta, t-\tau)$, is given by

$$M_{A_{Agg_i}}(\theta, t-\tau) = E[e^{\theta A gg_i(t-\tau)}] = E[e^{\theta \sum_{j=1}^{m_i} A^j_{cr_i}(t-\tau)}] = \prod_{j=1}^{m_i} e^{\theta A^j_{cr_i}(t-\tau)} \tag{6.11}$$

Given the affine envelop model of $A^j_{cr_i}(t)$, $E[e^{\theta A^j_{cr_i}(t-\tau)}] \leq e^{\theta[\rho_i^j(t-\tau)+\sigma_i^j]}$, $M_{A_{Agg_i}}(\theta, t-\tau)$ can be rewritten in the following equation,

$$M_{A_{Agg_i}}(\theta, t-\tau) \leq e^{\theta[\rho_{Agg_i}(t-\tau)+\sigma_{Agg_i}]} \tag{6.12}$$

where $\rho_{Agg_i} = \prod_{j=1}^{m_i} \rho_i^j$ and $\sigma_{Agg_i} = \prod_{j=1}^{m_i} \sigma_i^j$;

From the perspective of the ith server, the m_i cross traffics can be regarded as an aggregation traffic, $A^j_{cr_i}(t)$, with parameters ρ_{Agg_i} and σ_{Agg_i}, which are calculated from individual cross traffic, $A^j_{cr_i}(t)$.

6.4.4 Stochastic Service Curves

SSCs give the bound of the least service available in the system for the arrival traffic. Two kinds of the service models are envisioned in the abstracted NFV model, memoryless off-on service process and exponential service process. Memoryless off-on process is used to model the dynamic wireless channel [147] and exponential process is for normal NFV server [148]. This section investigates how to achieve the SSCs for both the off-on service process and exponential process. As the cross traffic served by cross NFV chains exists at each VNF node and competing the network, computing and storage resources with the through NFV chain, an efficient approach to calculate the leftover service will be exploited to obtain the effective resource left for the through NFV service chain.

6.4.4.1 On-off Wireless Channel Model

Off-on wireless channel has two states (on and off) during service provisioning. When the channel is in the "on" state, it provides a constant transmission at rate r; Once the channel is in the "off" state, the wireless channel does not provide any service. Let P_{on} denote the probability that the state of the wireless channel is "on"; and $1-P_{on}$ denote the probability that wireless channel is in "off" state. Let $X(t)$ be the service available at time interval t, it is a two states Bernoulli variable, $P(X(t)=r)=P_{on}$ and $P(X(t)=0)=1-P_{on}$. MGF of $X(t)$, $M_X(-\theta,t)$, can be expressed as,

$$M_X(-\theta,t)=E[e^{-\theta X(t)}]=P_{on}*e^{-\theta r}+1-P_{on} \tag{6.13}$$

Let $S_1(\tau,t)$ denote the cumulative service in time interval $[\tau+1,t]$, which is equal to the sum of the $X(t)$ over time interval $[\tau+1,t]$, expressed as $S_1(\tau,t)=\sum_{\upsilon=\tau+1}^{t}X(\upsilon)$.

Then the MGF of $S_1(\tau,t)$, $M_S(-\theta,t)$, can be achieved as,

$$M_S(-\theta,t) = E[e^{-\theta S(t)}] = E[e^{-\theta \Sigma_{\upsilon=1}^{t} X_\upsilon}] \tag{6.14}$$

As $A(t)$ follows iid Bernoulli distribution, Eq. (6.14) transfers to

$$M_S(-\theta,t) = \{E[e^{-\theta X(t)}]\}^t = \{M_X(-\theta,t)\}^t = (P_{on} * e^{-\theta r+1-P_{on}})^t = e^{-\theta t \frac{ln(P_{on}*e^{-\theta r}+1-P_{on})}{-\theta}} \tag{6.15}$$

Therefore, $S_1(\tau,t)$ has the MGF of $E[e^{-\theta S_1(t-\tau)}] \leq e^{-\theta[\rho_{S1}(t-\tau)-\sigma_{S1}]}$ with the parameter $\rho_{S1} = \frac{ln(P_{on}*e^{-\theta r}+1-P_{on})}{-\theta}$ and $\sigma_{S1} = 0$.

6.4.4.2 Exponential Service Model

According to [72], the MGF of service process, $S_i(\tau,t)$, is defined as $M_{S_i}(-\theta,t-\tau) = E[e^{-\theta S_i(\tau,t)}]$ with parameter $-\theta$ for $\theta > 0$. Applying the affine service envelop, $S_i(\tau,t) \geq \rho(t-\tau) - b_s$, to $M_{S_i}(-\theta,t-\tau)$ achieves the following equation,

$$E[e^{-\theta S_i(\tau,t)}] \leq e^{-\theta(\rho_{s_i}(t-\tau)-\sigma_{s_i})} \tag{6.16}$$

The relation between the packets and bits is $S_i = N_{s_i}/v$; then the MGF of service process, $M_{s_i}(-\theta,t-\tau)$, is calculated as,

$$M_{s_i}(-\theta,t-\tau) = M_{N_{s_i}}(-\theta/v,t-\tau) \tag{6.17}$$

Similar to the derivation process of the SACs, the MGF of service process can be achieved by,

$$M_{N_{s_i}}(-\theta/v,t-\tau) = e^{-\mu_i t(e^{-\theta}-1)} \tag{6.18}$$

where μ_i is the service rate for the ith server. Then $S_i(t)$ has the MGF, $M_{S_i}(-\theta, t-\tau)$, to be $e^{-\mu_i t(e^{-\theta}-1)}$; the affine envelop model, $E[e^{-\theta A_{S_i}(t-\tau)}] \leq e^{-\theta[\rho_{s_i}(t-\tau)+\sigma_{s_i}]}$, with the parameters $\rho_{s_i} = \frac{\mu_i(e^{-\theta/v}-1)}{-\theta}$ and $\sigma_{s_i} = 0$.

6.4.4.3 Leftover Service

For each server, we are interested in the the service available for the through traffic, not for the cross traffic. Therefore, the main work for this part is to calculate the amount of the service offered to the through traffic in the existence of the cross traffic, named leftover service, which is an important notion in stochastic network calculus. Let $A_{t_i}(t)$ be the total cumulative arrival at the ith server, which consists of through traffic, $A_{th_i}(t)$, and total cross traffic, $A_{Agg_i}(t)$. Let $D_{t_i}(t)$ be the total cumulative departure from the ith server, which consists of the departures from through traffic, $D_{th_i}(t)$, and the total departures from cross traffic, $D_{Agg_i}(t)$. Let $S_i(\tau,t)$ denote the service available at the ith server during the time interval $[\tau+1,t]$. The following inequality holds for $S_i(\tau,t)$, $A_{t_i}(\tau,t)$, and $D_{t_i}(\tau,t)$,

$$D_{t_i}(t) \geq \min_{\tau\in[0,t]} (S_i(\tau,t) + A_{t_i}(t)) \tag{6.19}$$

Assume the last busy time is τ^*, when $\tau = \tau^*$, the right side of the inequality achieves the minimum. Inserting $A_{th_i}(t)$, $A_{Agg_i}(t)$, $D_{th_i}(t)$, and $D_{Agg_i}(t)$ in Eq. (6.19), it can be written as

$$D_{th_i}(t) \geq A_{th_i}(\tau^*) + \{S_i(\tau^*,t) - [D_{Agg_i}(t) - A_{Agg_i}(\tau^*)]\}_+ \tag{6.20}$$

where the subscript "$+$" means nonnegative value. For the cross traffic, the departure bits can not be larger than the arrival bits, denoted as $D_{Agg_i}(t) \leq A_{Agg_i}(t)$. Eq. (6.20) can be further written as

$$D_{th_i}(t) \geq A_{th_i}(\tau^*) + \{S_i(\tau^*,t) - [A_{Agg_i}(t) - A_{Agg_i}(\tau^*)]\}_+ \tag{6.21}$$

In Eq. (6.21), $A_{Agg_i}(t) - A_{Agg_i}(\tau^*) = A_{Agg_i}(\tau^*, t)$; Since τ^* denotes the last busy time that can be determined in advance, we use minimum operation to generalise τ^* as τ. Eq. (6.21) becomes

$$D_{th_i}(t) \geq \min_{\tau \in [0,t]} \{[S_i(\tau,t) - A_{Agg_i}(\tau,t)]_+ + A_{th_i}(\tau)\} \tag{6.22}$$

For through traffic, the following inequality holds for $A_{th_i}(t)$, $S_{th_i}(t)$, and $D_{th_i}(t)$,

$$D_{th_i}(t) \geq \min_{\tau \in [0,t]} \{S_{th_i}(t) + A_{th_i}(\tau)\} \tag{6.23}$$

where $S_{th_i}(t)$ is the leftover service for the through traffic in the existence of the cross traffic. From Eq. (6.22) and Eq. (6.23), the leftover service, $S_{th_i}(t)$, is calculated as $S_{th_i}(t) = \{[S_i(\tau,t) - A_{Agg_i}(\tau,t)]_+$.

As $S_{th_i}(t)$ and $A_{Agg_i}(\tau,t)$ are stochastically independent, the MGF of the leftover service, $M_{th_i}(-\theta, t-\tau)$, can be calculated as

$$\begin{aligned} M_{th_i}(-\theta, t-\tau) = E[e^{-\theta S_{th_i}(t-\tau)}] &= E[e^{-\theta[S_i(\tau,t) - A_{Agg_i}(\tau,t)]_+}] \\ &= E[e^{-\theta S_i(\tau,t)}] E[e^{\theta A_{Agg_i}(\tau,t)}] \\ &\leq e^{-\theta[\rho_{S_i}(t-\tau) - \sigma_{S_i}]} e^{\theta[\rho_{Agg_i}(t-\tau) + \sigma_{Agg_i}]} \\ &= e^{-\theta[(\rho_{S_i} - \rho_{Agg_i})(t-\tau) - (\sigma_{S_i} + \sigma_{Agg_i})]} \end{aligned} \tag{6.24}$$

From Eq. (6.24), the MGF of $S_{th_i}(t)$ can be achieved from $E[e^{-\theta S_{th_i}(t-\tau)}] \leq e^{-\theta[\rho_{th_i}(t-\tau) - \sigma_{th_i}]}$, with the parameters $\rho_{th_i} = \rho_{S_i} - \rho_{Agg_i}$ and $\sigma_{th_i} = \sigma_{S_i} + \sigma_{Agg_i}$.

6.4.5 End-to-end Latency Bounds

From Sections 6.4.2 and 6.4.4, we achieved the envelop models for the arrival process and service process. For the through traffic, the envelop is shown as:

$$A_{th}(\tau,t) \leq (\rho_{A_{th}} + \delta)(t-\tau) + b_{A_{th}} \tag{6.25}$$

where δ is used to demonstrate a sample path and the probability for $A_{th}(\tau,t)$ to satisfy the above inequality is equal to $\varepsilon(b_{A_{th}}) = e^{\theta\sigma_{A_{th}}} e^{-\theta b_{A_{th}}}/(1-e^{-\theta\delta})$. For the service process of the entire NFV chain, the envelop is shown as:

$$S(\tau,t) \geq (\rho_S - \sigma)(t-\tau) - b_S \tag{6.26}$$

where the probability for $A_{th}(\tau,t)$ to meet the above inequality is equal to $\varepsilon(b_S) = e^{n\theta\sigma_S}/(1-e^{-\theta\sigma})^n$.

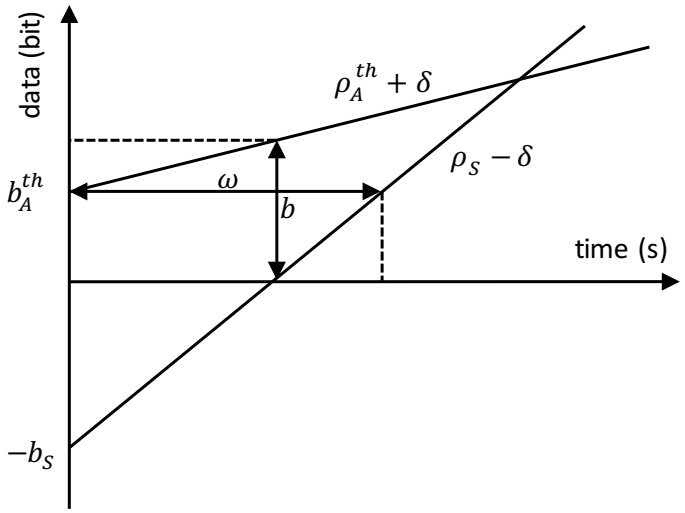

Figure 6.3: End-to-End Latency Bound from SSC and SAC

For the NFV system stability, it is required that the service envelop should be always larger than the arrival envelop, $\rho_{A_{th}} + \delta < \rho_S - \delta$, and $\delta < (\rho_S - \rho_{A_{th}})/2$. In order to simplify the description, we draw two envelops on one 2-dimension figure. From Fig.

6.3, the stability condition is shown as that the slope of the service envelop is larger than that of the arrival envelop.

For stochastic network calculus, the end-to-end upper bound lantecy, w, is defined as

$$W(t) \leq \min\{w \geq 0 : \max\{A_{th}(\tau,t) < D(\tau,t+w)\}\} \tag{6.27}$$

where W(t) is the system latency at time t.

With the MGFs of the traffic process and overall service process, the upper bound latency in Eq. (6.27) can be achieved in the following in [147]

$$w = \inf_{\theta>0}\left[inf\left[\tau : \tfrac{1}{\theta} ln\left(\textstyle\sum_{s=\tau}^{\infty} M_{A_{th}}(\theta, s-\tau) M_S(-\theta, s) - ln\varepsilon\right) \leq 0\right]\right] \tag{6.28}$$

Under the First In First Out (FIFO) scheduling strategy, the work in [149] gave the approach to solve the above inequality.

The end-to-end delay bound, w, can be achieved when τ satisfies the following condition:

$$\frac{1}{\theta} ln\left(\textstyle\sum_{s=\tau}^{\infty} M_{A_{th}}(\theta, s-\tau) M_S(-\theta, t-\tau) - ln\varepsilon\right) \leq 0 \tag{6.29}$$

In [149], the geometric series approach is exploited to solve the above inequality. Under the stability condition, $\rho_{A_{th}}(\theta) \leq \rho_S(-\theta)$, τ has the lower bound described as

$$\tau \geq \frac{\sigma(\theta)}{\rho_S(-\theta)} + \frac{n * ln\gamma - ln\varepsilon}{\theta \rho_S(-\theta)} \tag{6.30}$$

where γ is calculated by $\gamma = 1 + \frac{1}{1-e^{-\theta(\rho_S(-\theta)-\rho_{A_{th}}(\theta))}}$; then the end-to-end lower bound is achieved as $w = inf_{\theta>0}[inf[\tau]]$; and the backlog bound is $b = inf_{\theta>0}[\sigma(\theta) + (ln\gamma - ln\varepsilon)/\theta]$.

6.5 Numerical Results and Analysis

In this section, we first evaluate the accuracy of the developed analytical model; then the analytical model is used to study the impacts of the number of the NFV nodes, the arrival rates of cross traffic and violation probability on the end-to-end performance of NFV networks, with the aim of achieving the fundamental understanding of the NFV networks in the real network deployment.

6.5.1 Performance Evaluation

Following the apprach to validate the analytical model in [150], the accuracy of the proposed performance model is conducted through the comparisons with the exact queueing and comprehensive simulations with different network settings [73][147] [151].

6.5.1.1 Comparison of Analytical Model Results with Exact Queueing Results

In the literature [152], the exact bound of a queueing network is derived based on the assumption that the arrival packets are served by FIFO scheduling algorithm and M/M/1 queueing theory is used to model the queue behaviour. In order to evaluate the developed model compared with the exact bound results, this section simplifies the abstracted model in Section 6.3 as follows: the through traffic and cross traffic for the ith server, $A_{th_i}(t)$ and $A_{cr_i}(t)$, follow Poisson process with arrival rates: $\lambda_{th}$and λ_{cr_i}. The servers provide the independent and exponentially distributed service for arriving packets with service rate: μ_i. Then the utilisation rate of the server is $\rho_{s_i} = \frac{\left[\sum_{i=1}^{m_i} \lambda_{cr_i} + \lambda_{th}\right]}{\mu_{s_i}}$. In [152], the relation between the latency bound and violation error rate of the M/M/1 queue is given in the following equation:

$$\varepsilon = e^{vc(1-\rho_{s_i})w} \tag{6.31}$$

For the multiple node case, the relation between the upper latency bound and violation error is given in [153],

$$P(W > w) = \left[\sum_{i=0}^{n-1} \frac{\mu_{s_i}(1-\rho_{s_i}w)^i}{i!} \right] e^{-\mu_{s_i}(1-\rho_{s_i})w} \tag{6.32}$$

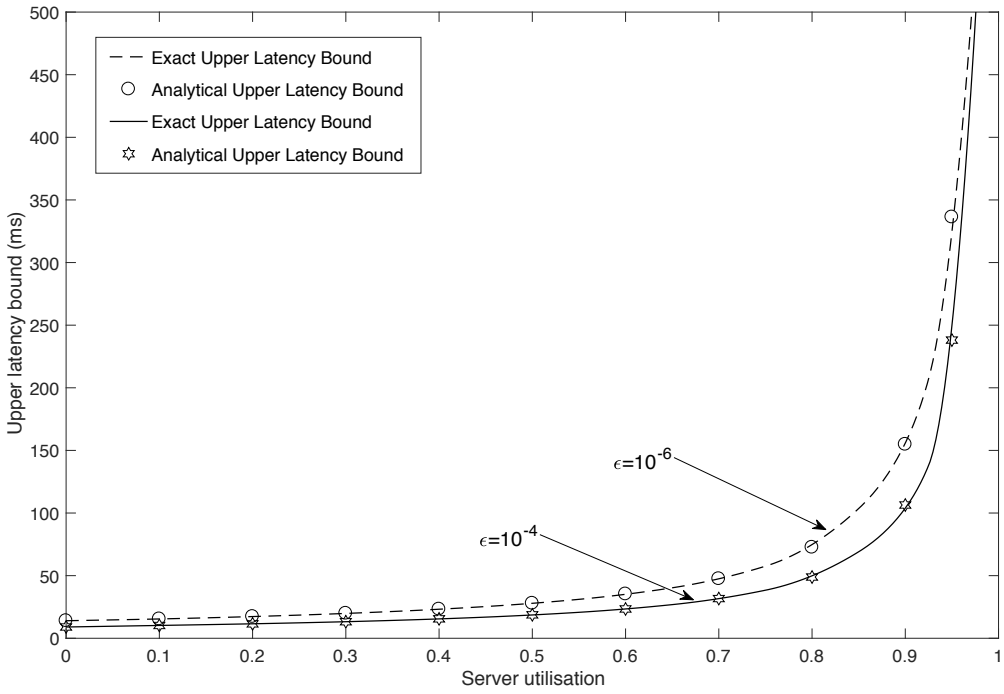

Figure 6.4: Comparison of Exact Theory Results with Those Obtained from the Analytical Model by Varying the Server Utilisation Rates

Next, we use the method in Section 6.4.5 to achieve the end-to-end latency bound for NFV networks and compare the results with those obtained from the exact bounds in Eq. (6.31) and Eq. (6.32). As shown in Fig. 6.4, the upper latency bounds are achieved from both the classical theory and analytical model by varying the server utilisation rates. In Fig. 6.4, service rate is set to be 1M bits/second; the arrival rates are set from 0 to 1M bits/second with an interval of 0.1M bits/second; two violation errors setting are adopted to reflect different SLA requirements: 10^{-6} and 10^{-4}; the packets size is set to be 1024 bits. NFV node is set to one as described in Eq. (6.31). From Fig. 6.4, the results of

the analytical model match well with those of the exact theory results. Furthermore, the smaller value of the violation error brings higher upper latency bound; this means that strict SLA requirement in terms of the violation error would push up the bound of the latency with given network resources.

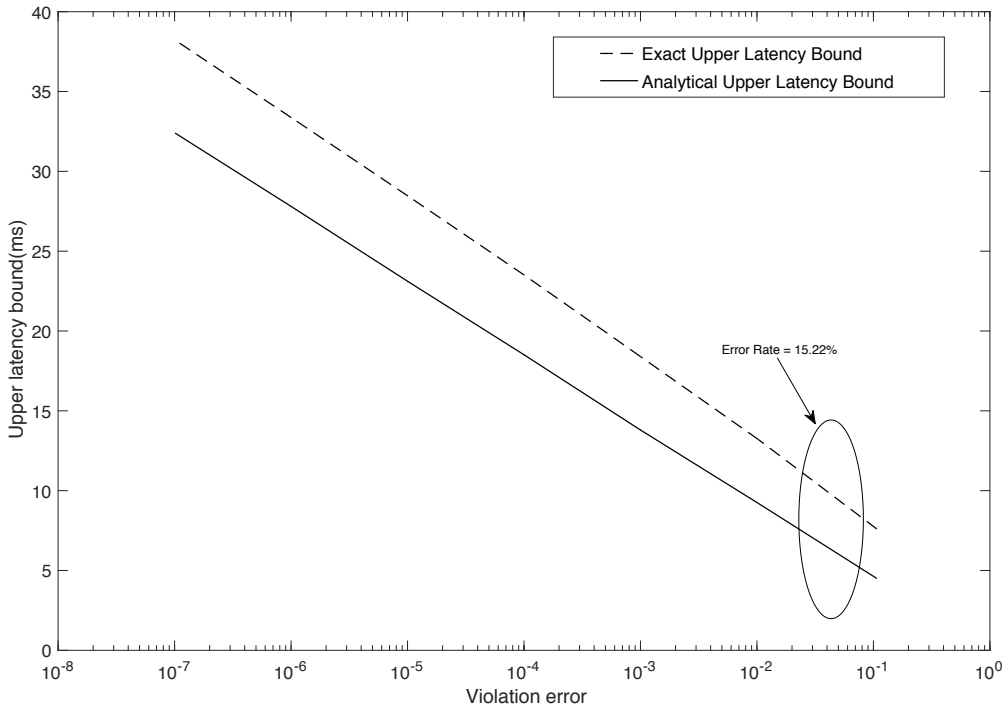

Figure 6.5: Comparison of Exact Theory Results with These Obtained from the Analytical Model by Varying the Violation Error

In order to evaluate the accuracy of the proposed analytical model under different violation error rates, Fig. 6.5 shows the upper latency bounds obtained from the Eq. (6.32) and analytical model. In Fig. 6.5, the arrival rate is fix at 0.5M bits/second; the service rate and packets sizes are set to be as same as those in Fig. 6.4; solid line shows the results obtained from the analytical model and dotted line shows the results of queue theory in Eq. (6.32). It can be seen that relative error of analytical model is around 15-20% compared with the exact result. The explanation of the relative error is as follows: to simplify the derivation process, the approach in Eq. (6.30) to derive the upper latency

Table 6.2: Network Configuration of OMNET++ Simulator

	μ_s	n	m_i	λ_{cr}	λ_{th_1}	λ_{th_2}	φ_1	φ_2	$1/v$	ε
Case I	1000	1	2	100	/	0	0.5	0.3	1024	$10^{(-4)}$
Case II	1000	3	0	100	/	0	0.09	0.06	1024	$10^{(-6)}$

bound adopts larger intervals than the intervals in Eq. (6.27); otherwise it is difficult to achieve a conservative and close-form upper latency bound. Compared with the results reported in the existing literatures [147]. 15-20% is acceptable for the least upper latency bound in stochastic network calculus. In chapter 7, the effort to tight the upper latency bound will be listed as the next step work.

6.5.1.2 Comparison of Analytical Model Results with Simulation Results

In order to comprehensively evaluate the performance of the proposed analytical model, a discrete-event simulator is developed in this research in OMNET++ simulation environment. The parameters that are used in this section are listed in Table 6.2. Two cases are designed in this section to evaluate the accuracy of the proposed model with multiple cross traffic and multiple NFV nodes. As shown in Figs. 6.6 and 6.7, the analytical model developed in this research matches well with the simulation results when the arrival rates of through traffic are moderate. From 6.7, it can be seen that the analytical model gradually reaches the saturation when arrival rate is approaching 1000 packets/second, while simulator could still get the results after saturation point. This is why the range of the horizontal axis is set as [0, 1100]. In addition, when the servers enter saturated mode, there are some discrepancies between the analytical model and simulation results. This is become some approximation are assumed during the derivation of the analytical model, which would cause the discrepancy when the server is high-loaded.

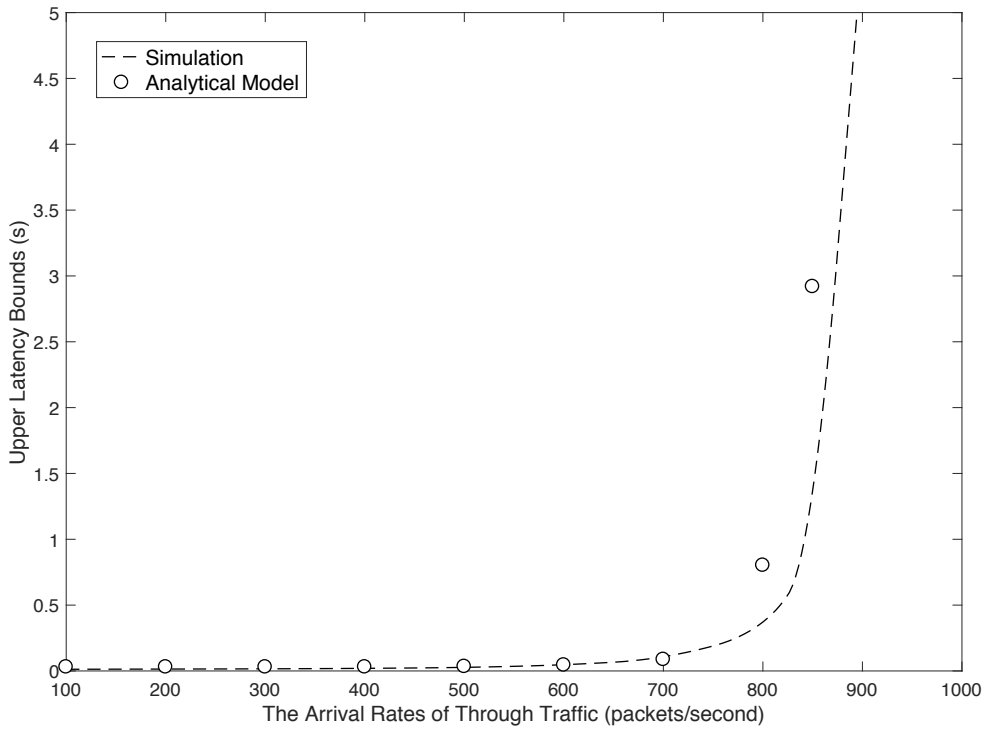

Figure 6.6: Comparison of Simulation Results with Those Obtained from the Analytical Model in Case I

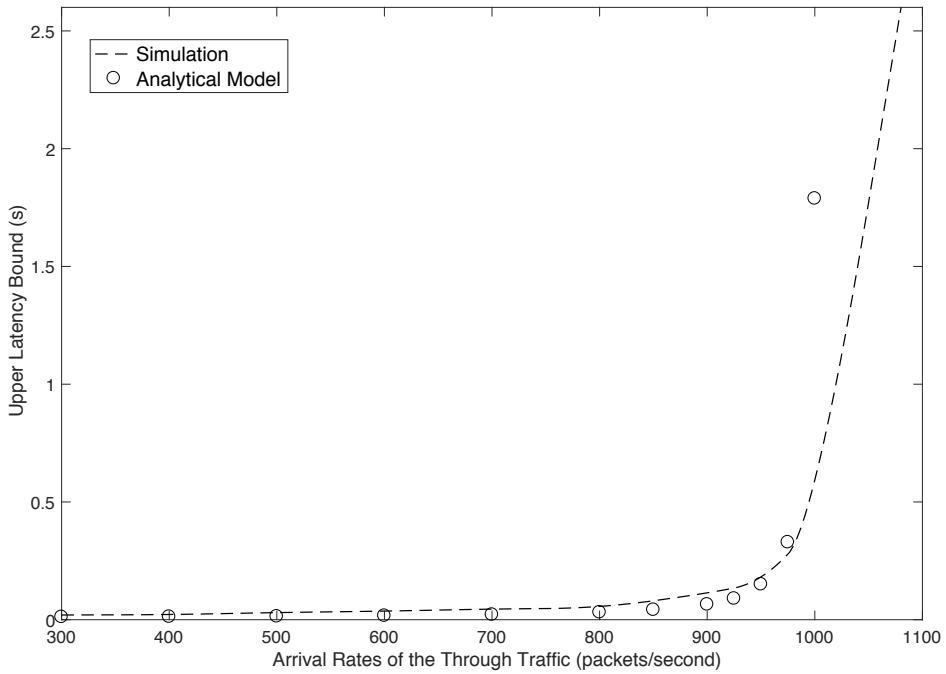

Figure 6.7: Comparison of Simulation Results with Those Obtained from the Analytical Model in Case II

6.5.2 Performance Analysis

In this section, the analytical model developed in Section 6.4 will be leveraged to investigate the impacts of the number of NFV nodes, the arrival rates of cross traffic and violation error probability on the performance of the through traffic. Different network configurations are exploited to achieve a comprehensive understanding of the performance of NFV chain in this section.

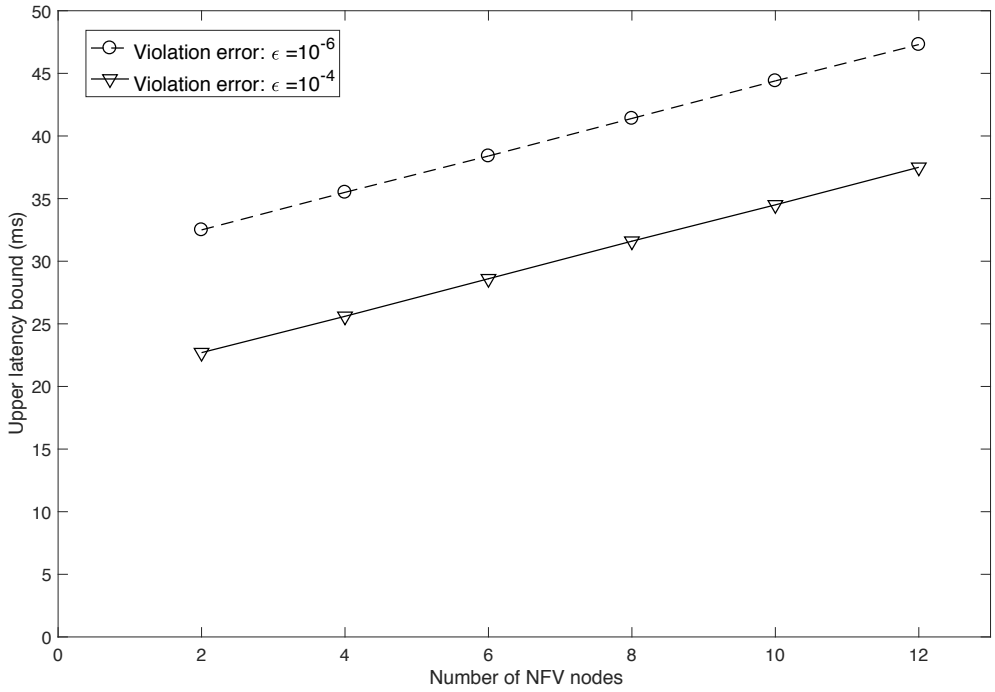

Figure 6.8: Impacts of the Number of the NFV Nodes on the Latency Performance of the Through Traffic

6.5.2.1 Impacts of the Number of NFV Nodes on the Upper Latency Bound

The number of NFV nodes is an important aspect for the deployment of NFV chain; adding NFV node to an existing NFV chain is able to introduce another network function for the end user, however, could result in additional processing latency and performance degradation. The aim of this section is to study the impact of the number of NFV nodes on

the upper latency bound with different violation error requirements. The network setting is described as follows: the arrival traffic is modelled as an Off-on Poisson process, which has two states (0 and 1); the transmission rate from state 0 to state 1 is set to be 0.5; from state 1 to state 0 is 0.3. When Markov chain is in state 0, there is no packet for through traffic. When Markov chain is in state 1, the arrival rate is set to be 0.3M bits/second; the service rate is fixed as 1M bits/second. The number of the cross traffic is set to be zero, to avoid the impact of cross traffic on the NFV nodes investigation of upper latency bound. Fig. 6.8 shows the relation between the number of the NFV nodes, n, and the least upper latency bound, w. It can be seen that with the increase of the number of NFV nodes, the least upper latency bound becomes higher. This can be explained from Eq. (6.30). The upper latency bound is described as a linear function of the number of the NFV nodes. Through the comparison of the solid line and dotted line, it can be seen that the increase of the violation error rate brings the drop of the upper latency bound. For instance, let us fix n as 6, when $\varepsilon = 10^{-6}$, the latency bound is equal to 38.4ms; when the ε increases from 10^{-6} to 10^{-4}, the upper bound latency bound drops from 38.4ms to 28.6ms. The explanation can be also found from Eq. (6.30); Within Eq. (6.30), it is easily observed that the upper bound latency bound is an increasing function of the violation error probability.

6.5.2.2 Impacts of Cross Traffic on the Latency Performance of Through Traffic

NFV brings network operator the benefits of flexible service deployment, scalable network architecture, and lower OPEX and CAPEX, while at the same time it struggles to provide end-to-end SLA-guaranteed services due to the co-existence feature of NFV chain deployment. The developed model in this work provides a cost-efficient approach to investigate the impacts of the cross traffic on the performance of the through traffic, such as

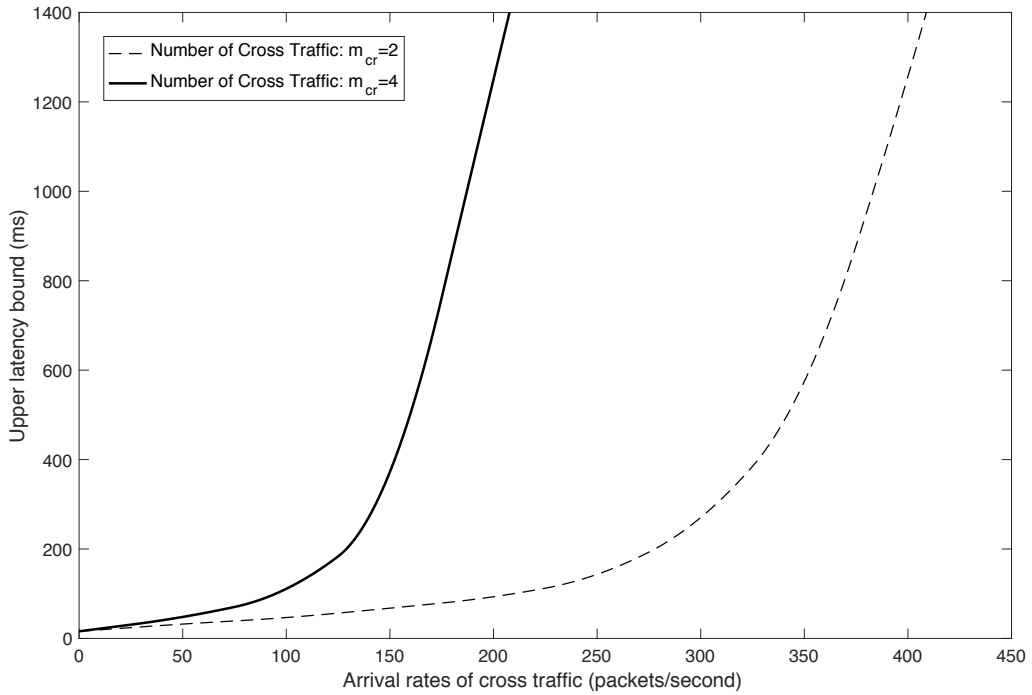

Figure 6.9: Impacts of the Arrival Rates of the Cross Traffic on the Latency Performance of the Through Traffic

in what degree the cross NFV traffic poses performance challenges for the through NFV traffic with given network resources. Network configuration is described as follows: the through traffic and server are set as same as that in the above subsection. The number of the NFV chain is set to be 2; the violation error rate is fix as 10^{-6}. The number of the cross traffic on the ith server, m_i is set to be 2 and 4; Fig. 6.9 shows the relationship between the arrival rates of the cross traffic and upper latency bound when m_i is equal to 2 and 4. Fig. 6.9 proves that cross traffic significantly impacts the performance of the NFV networks. Large number or higher volume of cross traffic brings higher upper latency bound for through traffic. Because under FIFO scheduling algorithm, the large number of cross traffic or high volume of cross traffic consumes significant amount of the server resources, leading to less resource available for through traffic and negative impacts on the service provisioning for through traffic.

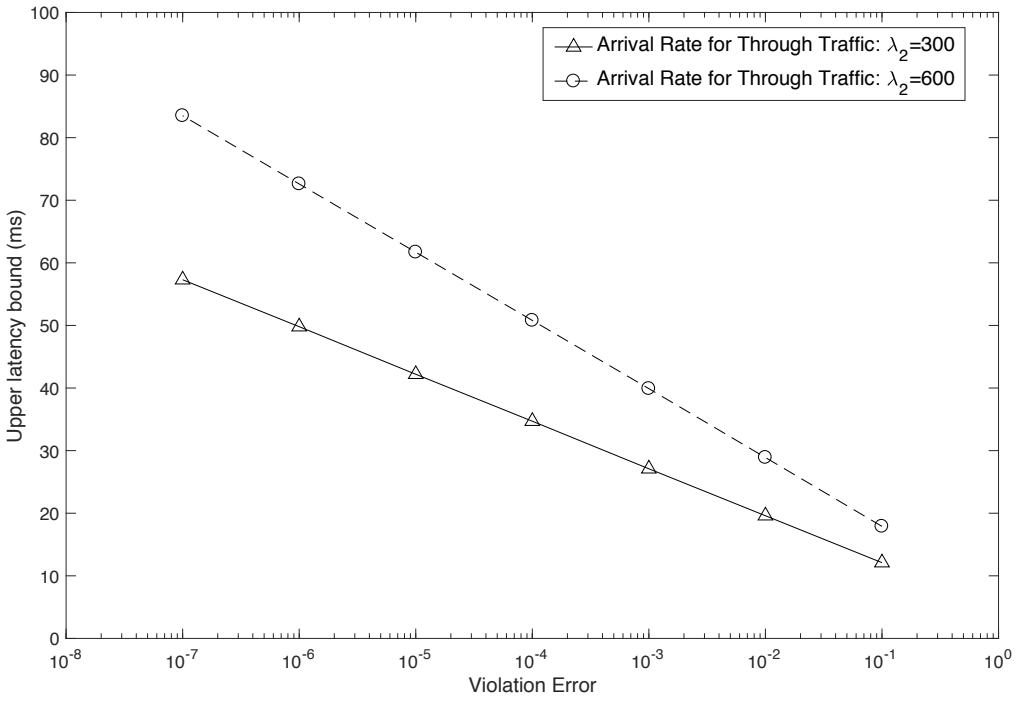

Figure 6.10: Impacts of Violation Error on the Latency Performance of the Through Traffic

6.5.2.3 Impacts of Violation Error Probability on the Latency Performance of Through Traffic

In NFV networks, network service is offered based on SLA agreements between network operator and service provider. The analytical model developed in this study is SLA-aware and is capable of providing the relationship between end-to-end latency bound and violation error probability. In this section, the service rate is set to be 1M bits/second; the number of the NFV node is set to be 2; the number and arrival rate for cross traffic are 2 and 0.1M bits/second; the arrival rate of the through traffic is set to be 0.3M and 0.5M bits/second. The transmission rates are set as same as previous sections. Fig. 6.10 gives the least upper latency bound by varying the violation error rates, ε, from 10^{-7} to 10^{-1}. It can be seen that the smaller value of ε significantly pushes up the upper latency bound; this means that with the strict violation (10^{-7}), the higher latency bound is needed to ensure that $(1-10^{-7})\%$ of the packets are delivered within the defined latency bound.

Furthermore, heavy volume of through traffic would also result in higher latency bound; it is not difficult to understand that with the given server resource, more arrivals would increase the server burden and result in the longer waiting time and the higher upper latency bound. Therefore, in order to reduce the upper latency bound, additional computing, storage and network resource would be needed once the upper latency bound can not meet the requirements of transmission latency. From the above analysis, the developed analytical model has practical value in the NFV service deployment and management.

6.6 Summary

NFV is regarded as a disruptive technology for telecommunication service provider to reduce CAPEX and OPEX through decoupling individual network services from the underlying hardware devices. In this chapter, a novel analytical model based on stochastic network calculus was proposed to investigate the upper latency bound of the NFV service chain. Instead of giving the average performance metrics, the developed model derives the worst-case of system performance with the aim of quantitatively achieving the network performance in term of SLA guarantee. During derivation of the upper latency bound, MGF and EBB are used to achieve the SACs and SSCs. In order to consider the cross traffic in the analytical model, leftover service technology was exploited to calculate the service available for through traffic. The end-to-end upper latency bound was calculated based on the achieved SACs, SSCs, violation error requirements and network topology settings. The exact theory results are used to validate the accuracy of the analytical models. The model is then used as practical and cost-effective tools to investigate the performance of NFV networks under various network configurations.

Chapter 7

Conclusions and Future Work

With the rapid developments of new emerging service and application, such as social media, Internet-of-Things, 3D immersive applications and High Definition 4K/8K videos, new network architectures are urgently needed to drive the evolution of the current network infrastructure to Future Internet to meet the requirements of these emerging applications and services. LTE-A, SDN and NFV have been regarded as the key technologies to achieve this ambition. The primary focus of this thesis is to investigate the resource allocation and analytical modelling technologies for LTE-A, SDN and NFV to enable the overall optimal operations of Future Internet. In the following, a summary of the research in this thesis is provided and some future directions are also discussed.

7.1 Conclusions

This thesis has presented new resource allocation algorithms and analytical tools for LTE-A, SDN and NFV architectures. In detail, we have studied the problems of QoS guaranteed radio resource allocation for LTE-A system with CA, the data-plane packet scheduling and performance modelling in SDN networks and the stochastic performance modelling for NFV networks. In order to achieve an improvement in real-time service provisioning and keep backward compatibility of LTE-A to LTE systems, we have pro-

posed a QoS-aware resource allocation algorithm in Chapter 3. In order to improve the forwarding capability and obtain the performance limitations of SDN network, a packet scheduling algorithm and two analytical models have been proposed in Sections 4 and 5. For capturing the dynamic and on-demand feature of NFV network in analytical modelling, Section 6 has presented a stochastic analytical model for NFV chain. The main contributions of this research are summarised as follows:

- A QoS-aware resource allocation algorithm has been proposed for LTE-A systems with CA, taking into account the system efficiency, user fairness and QoS requirements. The proposed resource allocation algorithm consists of three components, the higher level scheduler, the lower level scheduler and cross-cc user migration scheduler, which interact with each other to dynamically assign the radio resource to users. At the higher scheduler, an innovative resource allocation algorithm defines frame by frame the amount of data that each real-time source should transmit to satisfy its delay constraint. Once the higher level has accomplished its task, the lower scheduler, assigns resource blocks using the maximum throughput and proportional fair algorithms. The cross-cc user migration scheduler following the lower scheduler adjusts the user positions in CCs, with the aim of decreasing the unbalance degree among different CCs, improving the resource utilisation for CCs accomplishing their quotas in advance and reducing the flow loss rate for users in poor wireless channel. The simulation results have demonstrated that the proposed scheduling scheme outperformed the well-known Two-Level downlink scheduling scheme in terms of the packet loss probability, average queue length and throughput per user.

- A P^2S packet scheduling algorithm has been proposed to enhance the global fair-

ness index and reduce the packet loss probability. P^2S offers the high priority to the packets that fail to match any entry in the flow table in order to reduce the packet delay, increase the global fairness index, and reduce the packet loss probability. In addition, a new analytical model for predicting the packet latency has been developed to achieve quantitative performance evaluation of the P^2S scheme. Extensive simulation experiments have been conducted to validate the accuracy of the analytical model. The performance results can reveal the quantitative relationship between the given system resources and the achievable QoS and thus can be used in the stages of SDN network plan and deployment.

- A new analytical model has been developed for SDN architecture in the presence of MMPP arrivals, which is adopted capturing the traffic characteristics of multimedia applications. A PQ system has been adopted to model SDN data plane to capture the multi-queue nature of forwarding devices. A versatile method extending the EBA has been proposed to facilitate the decomposition of such a PQ system to two SSSQ systems in order to facilitate the derivation and improve the tractability of the analytical model. The key performance metrics including average latency and average network throughput have been derived by the model. The accuracy of the proposed model has been validated through extensive OMNeT++ simulation experiments. The validation results have revealed that the average latency and the average throughput predicted by the developed analytical model reasonably match those obtained from the simulation experiments. Furthermore, the analytical model has been adopted as a cost-effective tool to study the impact of flow table hit probability and the service resource allocation in the SDN controller and the switch on the system performance.

- A novel dynamic analytical model has been proposed for NFV networks, which focused on the dynamic and on-demand feature of the service provision and achieved the relationship between packet loss probability and delay bound. Two kind of the dynamics were considered in the proposed analytical model: service capability of individual VNF and number of the NFVs in service chain. Technical contributions of the proposed analytical models include 1) characterising and modelling the traffic process and service process of NFV networks to capture the dynamic and on-demand features; (2) deriving the performance bounds for the end-to-end service with the input of the required SLAs in terms of the packet loss probability; and (3) investigating the impacts of the different resource allocations strategies on the end-to-end performances. The proposed model jointly exploited the EBB and MGF to achieve the SAC and SSC for different arrival traffic and service models. In addition, in order to achieve a non-complex analytical model, the leftover service, statistical multiplexing technologies were adopted in this research. In order to show the accuracy of the proposed analytical model, the results of the analytical model with different parameter settings were compared with these obtained from accurate queueing results.

7.2 Future Work

In this section, we discuss the open issues and problems that require further investigations in the areas of the resource allocation and performance modelling of LTE-A, SDN and NFV networks.

- Optimal CC allocation algorithm in LTE-A systems: most of the existing work assumed that LTE-A users are always assigned to access all CCs regardless of their QoS requirements, channel quality and buffer states, which results in lower system

performance and unsatisfied service provisioning. To alleviate the performance lost, more work is needed to investigate the optimal CC allocation strategy to allocation LTE-A user to different CCs, taking into considerations of QoS parameters such as the QoS Class Identifier (QCI), Guaranteed Bit Rate (GBR), and the Aggregated Maximum Bit Rate (AMBR) for non-GBR bearers to provide useful information for determining the number of required CCs for the user. As an example, users only having a voice over IP call or a streaming connection with moderate GBR can be assigned a single CC, while still being able to fulfil the users QoS requirements. Assigning a single CC to such user has the advantage that terminal power consumption is kept lower, as compared to cases where the user is configured with a CC set larger than one. Secondly, corresponding control signalling overhead is also reduced by configuring a smaller number of CCs for the user.

- Analytical models of LTE-A systems with least queue length strategy: most of the scheduling work in LTE-A system adapts least load balancing method to allocate the new arrival LTE users or new arrival packets; this can achieve better balance load among different CCs. However, least load strategy would result in serious problem for analytical work, especially in the case of more than 2 CCs existing in LTE-A system. Most of the existing analytical work on LTE-A with CC simply addressed this issue by assuming round robin as the carrier load balancing methods, and did not capture the key features of the least load allocation algorithms. In this area, we will investigate how to use least queue length theory in the analytical model to address the above problem for LTE-A systems.

- Analytical modelling of SDN networks with multi-hop method: most of the existing research work on SDN network analytical models simply assume that the

underlying network devices are directly connected with the SDN controller even in large scale network scenario. However, this assumption does not consider the case of multi-hop communication between SDN controller and network devices, as building connections between SDN controller and individual forwarding devices is neither OPEX-saving for network operators nor practical for network plan and deployment. Therefore, how to investigate the performance of SDN network with multi-hop control communications needs further research investigation. Herein, the topology of the SDN network should be as practical as possible, for instance, in the data centre, network infrastructure topology including fat-tree, DCell, BCube, Camcube, FiConn, Jelly fish, and Scafida should be modelled separately for different routing and switch strategies.

- Analytical modelling of SDN networks with in-band control: the second research issue in SDN analytical model that needs further research is how to model the network performance in-band control scheme. The messages between SDN controller and the switches need to be forwarded by the underlying switches to SDN controller in the manner of hop-by-hop. Therefore, whether the control messages consume the data-plane bandwidth generates two communications strategies, in-band control and out-band control. In-band control refers to that the control message and data message use the same transmission channel for information delivery. While out-band control refers to that the control messages are allocated with specific transmission channel. Most of the existing research only considers the out-band control in their analytical model, while in-band control has been appeared in some of the industry products, such as HP 5200 SDN switch. In-band control can benefit for the resource utilisation and non-real-time application and services. In this area, the research to investigate the SDN network performance with in-band control has not

been reported in the literature and need more research focus and efforts.

- Optimising the performance bounds for analytical models of NFV networks: compared with the queueing theory, stochastic network calculus is capable of investigating the dynamic features of the network architecture, which makes it suitable for NFV service chain scenario. Stochastic network calculus provides a series of the techniques to derive the the end-to-end performance bounds. However, the accuracy of the the performance bounds is restricted to the selection of the free parameters. A low-complex multiple objective optimisation algorithm that can efficiently tight the performance bounds for NFV network is urgently needed in NFV stochastic performance study.

Bibliography

[1] Kan Zheng, Fanglong Hu, Wenbo Wang, Wei Xiang, and Mischa Dohler. Radio resource allocation in lte-advanced cellular networks with m2m communications. *IEEE Communications Magazine*, 50(7):184–192, 2012.

[2] Francesco Capozzi, Giuseppe Piro, Luigi Alfredo Grieco, Gennaro Boggia, and Pietro Camarda. Downlink packet scheduling in lte cellular networks: Key design issues and a survey. *IEEE Communications Surveys & Tutorials*, 15(2):678–700, 2013.

[3] Monowar Hasan, Ekram Hossain, and Dong In Kim. Resource allocation under channel uncertainties for relay-aided device-to-device communication underlaying lte-a cellular networks. *IEEE Transactions on Wireless Communications*, 13(4):2322–2338, 2014.

[4] Shahid Mumtaz, Kazi Mohammed Saidul Huq, Ayman Radwan, Jonathan Rodriguez, and Rui L Aguiar. Energy efficient interference-aware resource allocation in lte-d2d communication. In *2014 IEEE International Conference on Communications (ICC)*, pages 282–287. IEEE, 2014.

[5] Siamak Azodolmolky, Reza Nejabati, Maryam Pazouki, Philipp Wieder, Ramin Yahyapour, and Dimitra Simeonidou. An analytical model for software defined networking: A network calculus-based approach. In *Proceedings of the 2013 IEEE*

Global Communications Conference (GLOBECOM), pages 1397–1402, December 2013.

[6] Alfio Lombardo, Antonio Manzalini, Vincenzo Riccobene, and Giovanni Schembra. An analytical tool for performance evaluation of software defined networking services. In *2014 IEEE Network Operations and Management Symposium (NOMS)*, pages 1–7. IEEE, 2014.

[7] Xiangxin Kong, Zhiliang Wang, Xingang Shi, Xia Yin, and Dan Li. Performance evaluation of software-defined networking with real-life isp traffic. In *2013 IEEE Symposium on Computers and Communications (ISCC)*, pages 000541–000547. IEEE, 2013.

[8] Siamak Azodolmolky, Philipp Wieder, and Ramin Yahyapour. Performance evaluation of a scalable software-defined networking deployment. In *2013 Second European Workshop on Software Defined Networks*, pages 68–74. IEEE, 2013.

[9] Bo Han, Vijay Gopalakrishnan, Lusheng Ji, and Seungjoon Lee. Network function virtualization: Challenges and opportunities for innovations. *IEEE Communications Magazine*, 53(2):90–97, 2015.

[10] Rashid Mijumbi, Joan Serrat, Juan-Luis Gorricho, Niels Bouten, Filip De Turck, and Raouf Boutaba. Network function virtualization: State-of-the-art and research challenges. *IEEE Communications Surveys & Tutorials*, 18(1):236–262, 2015.

[11] Timothy Wood, KK Ramakrishnan, Jinho Hwang, Grace Liu, and Wei Zhang. Toward a software-based network: integrating software defined networking and network function virtualization. *IEEE Network*, 29(3):36–41, 2015.

[12] Jemal H Abawajy. An efficient adaptive scheduling policy for high-performance computing. *Future Generation Computer Systems*, 25(3):364–370, March 2009.

[13] Dazhi Chen and Pramod K Varshney. Qos support in wireless sensor networks: A survey. In *International conference on wireless networks*, volume 233, pages 1–7, 2004.

[14] Yuanye Wang, Klaus I Pedersen, Troels B Sorensen, and Preben E Mogensen. Carrier load balancing and packet scheduling for multi-carrier systems. *IEEE Transactions on Wireless Communications*, 9(5):1780–1789, 2010.

[15] Yunzhi Qian, Canjun Ren, Suwen Tang, and Ming Chen. Multi-service qos guaranteed based downlink cross-layer resource block allocation algorithm in lte systems. In *Wireless Communications & Signal Processing, 2009. WCSP 2009. International Conference on*, pages 1–4. IEEE, 2009.

[16] Wen-Ching Chung, Chung-Ju Chang, and Li-Chun Wang. An intelligent priority resource allocation scheme for lte-a downlink systems. *IEEE Wireless Communications Letters*, 1(3):241–244, 2012.

[17] Md Shamsul Alam, Jon W Mark, and Xuemin Sherman Shen. Relay selection and resource allocation for multi-user cooperative ofdma networks. *IEEE Transactions on Wireless Communications*, 12(5):2193–2205, 2013.

[18] Cheng-Shang Chang, Duan-Shin Lee, and Chao-Kai Tu. Using switched delay lines for exact emulation of fifo multiplexers with variable length bursts. *IEEE Journal on Selected Areas in Communications*, 24(4):108–117, 2006.

[19] Yulei Wu, Geyong Min, and Laurence T Yang. Performance analysis of hybrid wireless networks under bursty and correlated traffic. *IEEE Transactions on Vehicular Technology*, 62(1):449–454, 2013.

[20] Geyong Min, Yulei Wu, and Ahmed Yassin Al-Dubai. Performance modelling and analysis of cognitive mesh networks. *IEEE Transactions on Communications*, 60(6):1474–1478, 2012.

[21] Jia Hu, Geyong Min, and Mike E Woodward. Performance analysis of a threshold-based dynamic txop scheme for intra-ac qos in wireless lans. *Future Generation Computer Systems*, 38:69–74, 2014.

[22] Xiaolong Jin and Geyong Min. Modelling and analysis of priority queueing systems with multi-class self-similar network traffic: A novel and efficient queue-decomposition approach. *IEEE Transactions on Communications*, 57(5):1444–1452, May 2009.

[23] Geyong Min, Jia Hu, and Mike E. Woodward. Performance modelling and analysis of the txop scheme in wireless multimedia networks with heterogeneous stations. *IEEE Transactions on Wireless Communications*, 10(12):4130–4139, December 2011.

[24] Lei Liu, Xiaolong Jin, and Geyong Min. Modelling an integrated scheduling scheme under bursty mmpp traffic. In *Proceedings of the 23rd IEEE International Conference on Advanced Information Networking and Applications Workshops/Symposia*, pages 212–217, May 2009.

[25] Michael Jarschel, Simon Oechsner, Daniel Schlosser, Rastin Pries, Sebastian Goll, and Phuoc Tran-Gia. Modeling and performance evaluation of an openflow archi-

tecture. In *Proceedings of the 23rd International Teletraffic Congress (ITC)*, pages 1–7, September 2011.

[26] Kashif Mahmood, Ameen Chilwan, Olav Østerbø, and Michael Jarschel. Modelling of openflow-based software-defined networks: the multiple node case. *IET Networks*, 4(5):278–284, 2015.

[27] Rishi Kapoor, Alex C. Snoeren, Geoffrey M. Voelker, and George Porter. Bullet trains: A study of nic burst behavior at microsecond timescales. In *Proceedings of the 9th ACM Conference on Emerging Networking Experiments and Technologies*, CoNEXT '13, pages 133–138, 2013.

[28] Pall Beck, Peter Clemens, Santiago Freitas, Jeff Gatz, Michele Girola, Jason Gmitter, Holger Mueller, Ray O'Hanlon, Veerendra Para, Joe Robinson, Andy Sholomon, Jason Walker, and Jon Tate. *IBM and Cisco: Together for a World Class Data Center*. IBM Redbooks publication, July 2013.

[29] Pethuru Raj, Anupama Raman, Dhivya Nagaraj, and Siddhartha Duggirala. *High-Performance Big-Data Analytics*. 1617-7975. Springer International Publishing, 2015.

[30] Zhi Liu, Xiang Wang, Weishen Pan, Baohua Yang, Xiaohe Hu, and Jun Li. Towards efficient load distribution in big data cloud. In *Proceedings of the 2015 International Conference on Computing, Networking and Communications (ICNC)*, pages 117–122, Feb 2015.

[31] Yulei Wu, Geyong Min, Mohamed Ould-Khaoua, and Hao Yin. Modelling and analysis of pipelined circuit switching in interconnection networks with bursty traf-

fic and hot-spot destinations. *Journal of Systems and Software*, 84(12):2097–2106, 2011.

[32] Ming Xia, Meral Shirazipour, Ying Zhang, Howard Green, and Attila Takacs. Network function placement for nfv chaining in packet/optical datacenters. *Journal of Lightwave Technology*, 33(8):1565–1570, 2015.

[33] Hendrik Moens and Filip De Turck. Vnf-p: A model for efficient placement of virtualized network functions. In *10th International Conference on Network and Service Management (CNSM) and Workshop*, pages 418–423. IEEE, 2014.

[34] Aleksandar Damnjanovic, Juan Montojo, Yongbin Wei, Tingfang Ji, Tao Luo, Madhavan Vajapeyam, Taesang Yoo, Osok Song, and Durga Malladi. A survey on 3gpp heterogeneous networks. *IEEE Wireless Communications*, 18(3):10–21, 2011.

[35] Stefan Schwarz, Josep Colom Ikuno, Michal Šimko, Martin Taranetz, Qi Wang, and Markus Rupp. Pushing the limits of lte: A survey on research enhancing the standard. *IEEE Access*, 1:51–62, 2013.

[36] S Srikanth, PA Murugesa Pandian, and Xavier Fernando. Orthogonal frequency division multiple access in wimax and lte: a comparison. *IEEE Communications Magazine*, 50(9):153–161, 2012.

[37] Qinghua Li, Guangjie Li, Wookbong Lee, Moon-il Lee, David Mazzarese, Bruno Clerckx, and Zexian Li. Mimo techniques in wimax and lte: a feature overview. *IEEE Communications magazine*, 48(5):86–92, 2010.

[38] Mamoru Sawahashi, Yoshihisa Kishiyama, Akihito Morimoto, Daisuke Nishikawa, and Motohiro Tanno. Coordinated multipoint transmission/reception

techniques for lte-advanced [coordinated and distributed mimo]. *IEEE Wireless Communications*, 17(3):26–34, 2010.

[39] Amitava Ghosh, Rapeepat Ratasuk, Bishwarup Mondal, Nitin Mangalvedhe, and Tim Thomas. Lte-advanced: next-generation wireless broadband technology [invited paper]. *IEEE Wireless Communications*, 17(3):10–22, 2010.

[40] Michel Mouly, Marie-Bernadette Pautet, and Thomas Foreword By-Haug. *The GSM system for mobile communications*. Telecom publishing, 1992.

[41] Andrew J Viterbi. *CDMA: principles of spread spectrum communication*. Addison Wesley Longman Publishing Co., Inc., 1995.

[42] 3GPP. Group radio access network; physical channel and modulation (release 8). *Tech. Spec. 36.211 V8.7.0*, May 2009.

[43] Hyojoon Kim and Nick Feamster. Improving network management with software defined networking. *IEEE Communications Magazine*, 51(2):114–119, 2013.

[44] Bruno Astuto A Nunes, Marc Mendonca, Xuan-Nam Nguyen, Katia Obraczka, and Thierry Turletti. A survey of software-defined networking: Past, present, and future of programmable networks. *IEEE Communications Surveys & Tutorials*, 16(3):1617–1634, 2014.

[45] Open Networking Fundation. Software-defined networking: The new norm for networks. *ONF White Paper*, 2012.

[46] Li Erran Li, Z Morley Mao, and Jennifer Rexford. Toward software-defined cellular networks. In *2012 European Workshop on Software Defined Networking*, pages 7–12. IEEE, 2012.

[47] Saurav Das, Guru Parulkar, and Nick McKeown. Why openflow/sdn can succeed where gmpls failed. In *European Conference and Exhibition on Optical Communication*, pages Tu–1. Optical Society of America, 2012.

[48] Siamak Azodolmolky, Philipp Wieder, and Ramin Yahyapour. Sdn-based cloud computing networking. In *2013 15th International Conference on Transparent Optical Networks (ICTON)*, pages 1–4. IEEE, 2013.

[49] Antoine Feghali, Rima Kilany, and Maroun Chamoun. Sdn security problems and solutions analysis. In *2015 International Conference on Protocol Engineering (ICPE) and International Conference on New Technologies of Distributed Systems (NTDS)*, pages 1–5. IEEE, 2015.

[50] Sakir Sezer, Sandra Scott-Hayward, Pushpinder Kaur Chouhan, Barbara Fraser, David Lake, Jim Finnegan, Niel Viljoen, Marc Miller, and Navneet Rao. Are we ready for sdn? implementation challenges for software-defined networks. *IEEE Communications Magazine*, 51(7):36–43, 2013.

[51] Nick McKeown, Tom Anderson, Hari Balakrishnan, Guru Parulkar, Larry Peterson, Jennifer Rexford, Scott Shenker, and Jonathan Turner. Openflow: enabling innovation in campus networks. *ACM SIGCOMM Computer Communication Review*, 38(2):69–74, 2008.

[52] George Tsirtsis and Pyda Srisuresh. Network address translation-protocol translation (nat-pt). Technical report, 2000.

[53] John Barkley. Comparing simple role based access control models and access control lists. In *Proceedings of the second ACM workshop on Role-based access control*, pages 127–132. ACM, 1997.

[54] Peter Newman, Greg Minshall, Tom Lyon, and Larry Huston. Ip switching and gigabit routers. *IEEE Communications magazine*, 35(1):64–69, 1997.

[55] Karen Scarfone and Peter Mell. Guide to intrusion detection and prevention systems (idps). *NIST special publication*, 800(2007):94, 2007.

[56] Zvika Bronstein, Evelyne Roch, Jinwei Xia, and Adi Molkho. Uniform handling and abstraction of nfv hardware accelerators. *IEEE Network*, 29(3):22–29, 2015.

[57] Hassan Hawilo, Abdallah Shami, Maysam Mirahmadi, and Rasool Asal. Nfv: state of the art, challenges, and implementation in next generation mobile networks (vepc). *IEEE Network*, 28(6):18–26, 2014.

[58] European Telecommunication Standards Institute Fundation. Network functions virtualisation: An introduction, benefits, enablers, challenges & call for action. *ETSI NFV Whitepaper*, 2012.

[59] ISG ETSI. on network functions virtualization (nfv). *Virtualization Requirements*, 2013.

[60] John Frank Charles Kingman. *Poisson processes*. Wiley Online Library, 1993.

[61] Carey Williamson. Internet traffic measurement. *IEEE Internet Computing*, 5(6):70–74, 2001.

[62] Wolfgang Fischer and Kathleen Meier-Hellstern. The markov-modulated poisson process (mmpp) cookbook. *Performance evaluation*, 18(2):149–171, 1993.

[63] Luca Muscariello, Marco Mellia, Michela Meo, M Ajmone Marsan, and R Lo Cigno. Markov models of internet traffic and a new hierarchical mmpp model. *Computer Communications*, 28(16):1835–1851, 2005.

[64] Harry Heffes and David Lucantoni. A markov modulated characterization of packetized voice and data traffic and related statistical multiplexer performance. *IEEE Journal on selected areas in communications*, 4(6):856–868, 1986.

[65] Tadafumi Yoshihara, Shoji Kasahara, and Yutaka Takahashi. Practical time-scale fitting of self-similar traffic with markov-modulated poisson process. *Telecommunication Systems*, 17(1-2):185–211, 2001.

[66] Wolfgang Fischer and Kathleen Meier-Hellstern. The markov-modulated poisson process (mmpp) cookbook. *Performance Evaluation*, 18(2):149 – 171, 1993.

[67] Howon Lee and DongHo Cho. Capacity improvement and analysis of voip service in a cognitive radio system. *IEEE Transactions on Vehicular Technology*, 59(4):1646–1651, May 2010.

[68] Brian L. Mark and Yariv Ephraim. Explicit causal recursive estimators for continuous-time bivariate markov chains. *IEEE Transactions on Signal Processing*, 62(10):2709–2718, May 2014.

[69] Kuanghao Liu, Xinhua Ling, Xuemin Shen, and Jon W.Mark. Performance analysis of prioritized mac in uwb wpan with bursty multimedia traffic. *IEEE Transactions on Vehicular Technology*, 57(4):2462–2473, July 2008.

[70] Donald Gross. *Fundamentals of queueing theory*. John Wiley & Sons, 2008.

[71] Yuming Jiang. A basic stochastic network calculus. *ACM SIGCOMM Computer Communication Review*, 36(4):123–134, 2006.

[72] Yuming Jiang. A note on applying stochastic network calculus. In *Proceedings of SIGCOMM*, volume 10, pages 16–20. Citeseer, 2010.

[73] Markus Fidler and Amr Rizk. A guide to the stochastic network calculus. *IEEE Communications Surveys & Tutorials*, 17(1):92–105, 2015.

[74] Markus Fidler. Survey of deterministic and stochastic service curve models in the network calculus. *IEEE Communications Surveys & Tutorials*, 12(1):59–86, 2010.

[75] Petteri Kela, Jani Puttonen, Niko Kolehmainen, Tapani Ristaniemi, Tero Henttonen, and Martti Moisio. Dynamic packet scheduling performance in utra long term evolution downlink. In *Wireless Pervasive Computing, 2008. ISWPC 2008. 3rd International Symposium on*, pages 308–313. IEEE, 2008.

[76] Guillaume Monghal, Klaus I Pedersen, Istvan Z Kovacs, and Preben E Mogensen. Qos oriented time and frequency domain packet schedulers for the utran long term evolution. In *Vehicular Technology Conference, 2008. VTC Spring 2008. IEEE*, pages 2532–2536. IEEE, 2008.

[77] Raymond Kwan, Cyril Leung, and Jie Zhang. Proportional fair multiuser scheduling in lte. *IEEE Signal Processing Letters*, 16(6):461–464, 2009.

[78] Achankeng Leke and John M Cioffi. A maximum rate loading algorithm for discrete multitone modulation systems. In *Global Telecommunications Conference, 1997. GLOBECOM'97., IEEE*, volume 3, pages 1514–1518. IEEE, 1997.

[79] Jeongsik Park, Sungho Hwang, and Ho-Shin Cho. A packet scheduling scheme to support real-time traffic in ofdma systems. In *2007 IEEE 65th Vehicular Technology Conference-VTC2007-Spring*, pages 2766–2770. IEEE, 2007.

[80] Ahmed Abdel-Hadi and Charles Clancy. A utility proportional fairness approach for resource allocation in 4g-lte. In *Computing, Networking and Communications (ICNC), 2014 International Conference on*, pages 1034–1040. IEEE, 2014.

[81] Giuseppe Piro, Luigi Alfredo Grieco, Gennaro Boggia, Rossella Fortuna, and Pietro Camarda. Two-level downlink scheduling for real-time multimedia services in lte networks. *IEEE Transactions on Multimedia*, 13(5):1052–1065, 2011.

[82] Mohamad Assaad. Frequency-time scheduling for streaming services in ofdma systems. In *2008 1st IFIP Wireless Days*, pages 1–5. IEEE, 2008.

[83] Y. Qian, C. Ren, S. Tang, and M. Chen. Multi-service qos guaranteed based downlink cross-layer resource block allocation algorithm in lte systems. In *2009 International Conference on Wireless Communications Signal Processing*, pages 1–4, Nov 2009.

[84] X. Wang, G. B. Giannakis, and A. G. Marques. A unified approach to qos-guaranteed scheduling for channel-adaptive wireless networks. *Proceedings of the IEEE*, 95(12):2410–2431, Dec 2007.

[85] Xiang Zhang and Wenbo Wang. Carrier aggregation for lte-advanced mobile communication systems. *IEEE Communications Magazine*, page 89, 2010.

[86] Guohui Wang, T.S. Eugene Ng, and Anees Shaikh. Programming your network at run-time for big data applications. In *Proceedings of the First Workshop on Hot Topics in Software Defined Networks*, pages 103–108, 2012.

[87] Mianxiong Dong, He Li, Kaoru Ota, and Jiang Xiao. Rule caching in sdn-enabled mobile access networks. *IEEE Network*, 29(4):40–45, July 2015.

[88] He Li, Mianxiong Dong, and Kaoru Ota. Radio access network virtualization for the social internet of things. *IEEE Cloud Computing*, 2(6):42–50, November 2015.

[89] Abhinava Sadasivarao, Sharfuddin Syed, Ping Pan, Chris Liou, Inder Monga, Chin Guok, and Andrew Lake. Bursting data between data centers: Case for transport

sdn. In *Proceedings of the 2013 IEEE Annual Symposium on High-Performance Interconnects (HOTI)*, pages 87–90, August 2013.

[90] Zhao Li, Yao Shen, Bin Yao, and Minyi Guo. Ofscheduler: A dynamic network optimizer for mapreduce in heterogeneous cluster. *International Journal of Parallel Programming*, 43(3):472–488, 2015.

[91] Peng Qin, Bin Dai, Benxiong Huang, and Guan Xu. Bandwidth-aware scheduling with sdn in hadoop: A new trend for big data. *IEEE Systems Journal*, pages 1–8, 2015.

[92] He Li, Mianxiong Dong, Xiaofei Liao, and Hai Jin. Deduplication-based energy efficient deduplication-based energy efficient storage system in cloud environment. *Computer Journal*, pages 1–11, December 2014.

[93] Jad Naous, David Erickson, G. Adam Covington, Guido Appenzeller, and Nick McKeown. Implementing an openflow switch on the netfpga platform. In *Proceedings of the 4th ACM/IEEE Symposium on Architectures for Networking and Communications Systems*, pages 1–9, 2008.

[94] Gianni Antichi, Andrea Di Pietro, Stefano Giordano, Gregorio Procissi, and Domenico Ficara. Design and development of an openflow compliant smart gigabit switch. In *Proceedings of the 2011 IEEE Global Telecommunications Conference (GLOBECOM)*, pages 1–5, December 2011.

[95] Andrea Bianco, Robert Birke, Luca Giraudo, and Manuel Palacin. Openflow switching: Data plane performance. In *Proceedings of the 2010 IEEE International Conference on Communications (ICC)*, pages 1–5, May 2010.

[96] Asif Khan and Nirav Dave. Enabling hardware exploration in software-defined networking: A flexible, portable openflow switch. In *Proceedings of the 2013 IEEE Annual International Symposium on Field-Programmable Custom Computing Machines (FCCM)*, pages 145–148. IEEE, April 2013.

[97] Yulei Wu, Geyong Min, Keqiu Li, and Bahman Javadi. Modeling and analysis of communication networks in multicluster systems under spatio-temporal bursty traffic. *IEEE Transactions on Parallel and Distributed Systems*, 23(5):902–912, 2012.

[98] Geyong Min, Yulei Wu, Keqiu Li, and Ahmed Y Al-Dubai. Performance modelling and optimization of integrated wireless lans and multi-hop mesh networks. *International Journal of Communication Systems*, 23(9-10):1111–1126, 2010.

[99] Yulei Wu, Geyong Min, Mohamed Ould-Khaoua, Hao Yin, and Lan Wang. Analytical modelling of networks in multicomputer systems under bursty and batch arrival traffic. *The Journal of Supercomputing*, 51(2):115–130, 2010.

[100] Jia Hu, Geyong Min, Michael E Woodward, and Weijia Jia. A comprehensive analytical model for ieee 802.11 e qos differentiation schemes under unsaturated traffic loads. In *2008 IEEE International Conference on Communications*, pages 241–245. IEEE, 2008.

[101] Xiongzi Ge, Yi Liu, David HC Du, Liang Zhang, Hongguang Guan, Jian Chen, Yuping Zhao, and Xinyu Hu. Openanfv: accelerating network function virtualization with a consolidated framework in openstack. *ACM SIGCOMM Computer Communication Review*, 44(4):353–354, 2015.

[102] Raj Jain and Subharthi Paul. Network virtualization and software defined networking for cloud computing: a survey. *IEEE Communications Magazine*, 51(11):24–31, 2013.

[103] Panagiotis Demestichas, Andreas Georgakopoulos, Dimitrios Karvounas, Kostas Tsagkaris, Vera Stavroulaki, Jianmin Lu, Chunshan Xiong, and Jing Yao. 5g on the horizon: key challenges for the radio-access network. *IEEE Vehicular Technology Magazine*, 8(3):47–53, 2013.

[104] Koji Yamazaki, Takeshi Osaka, Sadayuki Yasuda, Shoko Ohteru, and Akihiko Miyazaki. Accelerating sdn/nfv with transparent offloading architecture. In *Presented as part of the Open Networking Summit 2014 (ONS 2014)*, 2014.

[105] DPDK Intel. Data plane development kit. *URL http://dpdk. org*, 2014.

[106] Network Functions Virtualisation. Nfv performance & portability best practises. *ETSI Standard GS NFV-PER*, 1, 2014.

[107] C. L. I, J. Huang, R. Duan, C. Cui, J. (. Jiang, and L. Li. Recent progress on c-ran centralization and cloudification. *IEEE Access*, 2:1030–1039, 2014.

[108] Ralf Lübben, Markus Fidler, and Jörg Liebeherr. Stochastic bandwidth estimation in networks with random service. *IEEE/ACM Transactions on Networking*, 22(2):484–497, 2014.

[109] Qiang Duan. Modeling and analysis for end-to-end service performance in virtualization-based next generation internet. In *Global Telecommunications Conference (GLOBECOM 2010), 2010 IEEE*, pages 1–6. IEEE, 2010.

[110] Open Networking Fundation. Openflow switch specification version 1.3.3. *ONF Specification*, 2013.

[111] Mikio Iwamura, Kamran Etemad, Mo-Han Fong, Ravi Nory, and Robert Love. Carrier aggregation framework in 3gpp lte-advanced [wimax/lte update]. *IEEE Communications Magazine*, 48(8):60–67, 2010.

[112] 3GPP. Proposal for candidate radio interface technologies for imt advanced based on lte release 10 and beyond. *Tech. Spec.*, Oct 2009.

[113] 3GPP. Evolved universal terrestrial radio access (e-utra) and evolved universal terrestrial radio access network (e-utran). *Tech. Spec. 36.300 v8.0.0*, Mar 2007.

[114] Hui Tian, Songtao Gao, Jianchi Zhu, and Lan Chen. Improved component carrier selection method for non-continuous carrier aggregation in lte-advanced systems. In *Vehicular Technology Conference (VTC Fall), 2011 IEEE*, pages 1–5. IEEE, 2011.

[115] Dongwoon Bai, Cheolhee Park, Jungwon Lee, Hoang Nguyen, Jaspreet Singh, Ankit Gupta, Zhouyue Pi, Taeyoon Kim, Chaiman Lim, Min-Goo Kim, et al. Lte-advanced modem design: challenges and perspectives. *IEEE Communications Magazine*, 50(2):178–186, 2012.

[116] X. Liu and H. Zhu. Resource allocation in ofdma systems in the presence of packet retransmission. In *2010 IEEE 71st Vehicular Technology Conference*, pages 1–5, May 2010.

[117] Piyush Agrawal and Neal Patwari. Correlated link shadow fading in multi-hop wireless networks. *IEEE Transactions on Wireless Communications*, 8(8):4024–4036, 2009.

[118] Bernard Sklar. Rayleigh fading channels in mobile digital communication systems. i. characterization. *IEEE Communications magazine*, 35(9):136–146, 1997.

[119] Vinko Erceg, Larry J Greenstein, Sony Y Tjandra, Seth R Parkoff, Ajay Gupta, Boris Kulic, Arthur A Julius, and Renee Bianchi. An empirically based path loss model for wireless channels in suburban environments. *IEEE Journal on selected areas in communications*, 17(7):1205–1211, 1999.

[120] Theodore S Rappaport et al. *Wireless communications: principles and practice*, volume 2. Prentice Hall PTR New Jersey, 1996.

[121] Thomas Schwengler. Wireless and cellular communications. *class notes for TLEN*, 5510, 2011.

[122] Baoguo Yang, Khaled Ben Letaief, Roger S Cheng, and Zhigang Cao. Channel estimation for ofdm transmission in multipath fading channels based on parametric channel modeling. *IEEE transactions on communications*, 49(3):467–479, 2001.

[123] William C Jakes and Donald C Cox. *Microwave mobile communications*. Wiley-IEEE Press, 1994.

[124] Yingbo Li and YL Guan. Modified jakes model for simulating multiple uncorrelated fading waveforms. In *IEEE International Conference on Communications*, 2000.

[125] Lawrence Joel Greenstein and Nelson Ray Sollenberger. Method and apparatus for enhancing communication reception at a wireless communication terminal, October 10 2000. US Patent 6,131,016.

[126] Christian Esteve Rothenberg, Marcelo Ribeiro Nascimento, Marcos Rogerio Salvador, Carlos Nilton Araujo Corrêa, Sidney Cunha de Lucena, and Robert Raszuk. Revisiting routing control platforms with the eyes and muscles of software-defined

networking. In *Proceedings of the first workshop on Hot topics in software defined networks*, pages 13–18. ACM, 2012.

[127] Michael E Woodward. *Communication and computer networks: modelling with discrete-time queues*. Wiley-IEEE Computer Society Pr, 1994.

[128] Kleinrock Leonard. *Queueing Systems Volume 1: Theory*. John Wiley & Sons, 1975.

[129] OMNet++. *OMNeT++ Network Simulator*, 2011.

[130] Raj Jain, Dah-Ming Chiu, and William R Hawe. *A quantitative measure of fairness and discrimination for resource allocation in shared computer system*, volume 38. Eastern Research Laboratory, Digital Equipment Corporation Hudson, MA, 1984.

[131] Soheil Yeganeh, Amin Tootoonchian, and Yashar Ganjali. On scalability of software-defined networking. *IEEE Communications Magazine*, 2(51):136–141, 2013.

[132] Arthur W Berger and Ward Whitt. Effective bandwidths with priorities. *IEEE/ACM Transactions on networking*, 6(4):447–460, 1998.

[133] Xiangxin Kong, Zhiliang Wang, Xingang Shi, and Xia Yin. Performance evaluation of software-defined networking with real-life isp traffic. In *Proceedings of the 2013 IEEE Symposium on Computers and Communications (ISCC)*, pages 541–547, July 2013.

[134] ONF. Software-defined networking: The new norm for networks. Technical report, Open Network Foundation, 2012.

[135] Xiaolong Jin and Geyong Min. Modelling and analysis of priority queueing systems with multi-class self-similar network traffic: a novel and efficient queue-decomposition approach. *IEEE Transactions on Communications*, 57(5):1444–1452, 2009.

[136] Petteri Mannersalo and Ilkka Norros. A most probable path approach to queueing systems with general gaussian input. *Computer Networks*, 40(3):399 – 412, 2002.

[137] Peixia Gao, Sabine Wittevrongel, Koenraad Laevens, Danny Vleeschauwer, and Herwig Bruneel. Distributional little's law for queues with heterogeneous server interruptions. *Electronics Letters*, 46(11):763–764, May 2010.

[138] Shahram Shah-Heydari and Tho Le-Ngoc. Mmpp models for multimedia traffic. *Telecommunication Systems*, 15(3-4):273–293, 2000.

[139] Yulei Wu, Geyong Min, and Laurence T. Yang. Performance analysis of hybrid wireless networks under bursty and correlated traffic. *IEEE Transactions on Vehicular Technology*, 62(1):449–454, January 2013.

[140] Huei-Wen Ferng and Jin-Fu Chang. Connection-wise end-to-end delay analysis in atm networks. *IEICE Transactions on Communications*, 83(3):659–671, March 2000.

[141] Huei-Wen Ferng and Jin-Fu Chang. Departure processes of bmap/g/1 queues. *Queueing Systems Theory and Applications*, 39(2/3):109–135, Octomber 2001.

[142] H. Heffes. A class of data traffic processes-covariance function characterization and related queuing results. *Bell System Technical Journal*, 59(6):897–929, July 1980.

[143] Chengchao Liang, F Richard Yu, and Xi Zhang. Information-centric network function virtualization over 5g mobile wireless networks. *IEEE Network*, 29(3):68–74, 2015.

[144] Aaron Gember-Jacobson, Raajay Viswanathan, Chaithan Prakash, Robert Grandl, Junaid Khalid, Sourav Das, and Aditya Akella. Opennf: Enabling innovation in network function control. *ACM SIGCOMM Computer Communication Review*, 44(4):163–174, 2015.

[145] Michael George Bulmer. *Principles of statistics*. Courier Corporation, 2012.

[146] Ahmed M Mohammed and Adel F Agamy. A survey on the common network traffic sources models. *International Journal of Computer Networks*, 3(2), 2011.

[147] Markus Fidler. A network calculus approach to probabilistic quality of service analysis of fading channels. In *IEEE Globecom 2006*, pages 1–6. IEEE, 2006.

[148] Giuseppe Faraci, Alfio Lombardo, and Giovanni Schembra. A processor-sharing scheduling strategy for nfv nodes. *Journal of Electrical and Computer Engineering*, 2016:1, 2016.

[149] Cheng-Shang Chang. *Performance guarantees in communication networks*. Springer Science & Business Media, 2012.

[150] Markus Fidler. An end-to-end probabilistic network calculus with moment generating functions. In *200614th IEEE International Workshop on Quality of Service*, pages 261–270. IEEE, 2006.

[151] Jörg Liebeherr, Markus Fidler, and Shahrokh Valaee. A system-theoretic approach to bandwidth estimation. *IEEE/ACM Transactions on Networking (TON)*, 18(4):1040–1053, 2010.

[152] Gunter Bolch, Stefan Greiner, Hermann de Meer, and Kishor S Trivedi. *Queueing networks and Markov chains: modeling and performance evaluation with computer science applications*. John Wiley & Sons, 2006.

[153] Leonard Kleinrock. Queueing systems, volume i: theory. 1975.